Advances in Predictive, Preventive and Personalised Medicine
Series Editor: Olga Golubnitschaja

Lotfi Chaari *Editor*

Digital Health in Focus of Predictive, Preventive and Personalised Medicine

EPMA
European Association for Predictive Preventive & Personalised Medicine

Springer

Digital Health in Focus of Predictive, Preventive and Personalised Medicine

Advances in Predictive, Preventive and Personalised Medicine

Volume 12

More information about this series at http://www.springer.com/series/10051

Lotfi Chaari
Editor

Digital Health in Focus of Predictive, Preventive and Personalised Medicine

Springer

Editor
Lotfi Chaari
IRIT-ENSEEIHT (UMR 5505)
University of Toulouse
TOULOUSE CEDEX 7, France

ISSN 2211-3495 ISSN 2211-3509 (electronic)
Advances in Predictive, Preventive and Personalised Medicine
ISBN 978-3-030-49814-6 ISBN 978-3-030-49815-3 (eBook)
https://doi.org/10.1007/978-3-030-49815-3

This Springer imprint is published by the registered company Springer Nature Switzerland AG.
The registered company address is: Gewerbestrasse 11, 6330 Cham, Switzerland

What This Book Series Is About

Current Healthcare: What Is Behind the Issue?

For many acute and chronic disorders, the current healthcare outcomes are considered as being inadequate: global figures cry for preventive measures and personalised treatments. In fact, severe chronic pathologies, such as cardiovascular disorders, diabetes and cancer, are treated after onset of the disease, frequently at near end stages. Pessimistic prognosis considers pandemic scenario for type 2 diabetes mellitus, neurodegenerative disorders and some types of cancer over the next 10–20 years followed by the economic disaster of healthcare systems in a global scale.

Advanced Healthcare Tailored to the Person: What Is Beyond the Issue?

Advanced healthcare promotes the paradigm change from delayed interventional to predictive medicine tailored to the person, from reactive to preventive medicine and from disease to wellness. The innovative Predictive, Preventive and Personalised Medicine (PPPM) is emerging as the focal point of efforts in healthcare aimed at curbing the prevalence of both communicable and non-communicable diseases, such as diabetes, cardiovascular diseases, chronic respiratory diseases, cancer and dental pathologies. The cost-effective management of diseases and the critical role of PPPM in modernisation of healthcare have been acknowledged as priorities by global and regional organisations and health-related institutions, such as the United Nations Organisation, the European Union and the National Institutes of Health.

Why Integrative Medical Approach by PPPM as the Medicine of the Future?

PPPM is the new integrative concept in healthcare sector that enables to predict individual predisposition before onset of the disease, to provide targeted preventive measures and to create personalised treatment algorithms tailored to the person. The expected outcomes are conducive to more effective population screening, prevention early in childhood, identification of persons at risk, stratification of patients for the optimal therapy planning, prediction and reduction of adverse drug-drug or drugdisease interactions relying on emerging technologies, such as pharmacogenetics, pathology-specific molecular patters, subcellular imaging, disease modelling, individual patient profiles, etc. Integrative approach by PPPM is considered as the medicine of the future. Being at the forefront of the global efforts, the European Association for Predictive, Preventive and Personalised Medicine (EPMA, http://www.epmanet.eu/) promotes the integrative concept of PPPM among healthcare stakeholders, governmental institutions, educators, funding bodies, patient organisations and public domain.

Current book series, published by Springer in collaboration with EPMA, overview multidisciplinary aspects of advanced biomedical approaches and innovative technologies. The integration of individual professional groups into the overall concept of PPPM is a particular advantage of this book series. Expert recommendations focus on the cost-effective management tailored to the person in health and disease. Innovative strategies are considered for standardisation of healthcare services. New guidelines are proposed for medical ethics, treatment of rare diseases, innovative approaches to early and predictive diagnostics, patient stratification and targeted prevention in healthy individuals, persons at risk, individual patient groups, subpopulations, institutions, healthcare economy and marketing.

About the Book Series Editor

Prof. Dr. Olga Golubnitschaja

Dr. Olga Golubnitschaja Department of Radiology, Medical Faculty, Rheinische Friedrich-Wilhelms-Universität, Bonn, Germany, has studied journalism, biotechnology and medicine and has been awarded research fellowships in Austria, Russia, the UK, Germany, the Netherlands and Switzerland (early and predictive diagnostics in paediatrics, neurosciences and cancer). She is the author of more than 400 well-cited international publications (research and review articles, position papers, books and book contributions) in the innovative field of predictive, preventive and personalised medicine (PPPM) with the main research focus on pre- and perinatal diagnostics, diagnostics of cardiovascular disease and neurodegenerative pathologies, predictive diagnostics in cancer and diabetes.

She has been awarded National and International Fellowship of the Alexander von Humboldt Foundation and Highest Prize in Medicine and Eiselsberg Prize in Austria.

Since 2009, Dr. Golubnitschaja is the *Secretary General* of the European Association for Predictive, Preventive and Personalised Medicine (EPMA, Brussels) networking over 50 countries worldwide (www.epmanet.eu), *Series Editor* of *Advances in Predictive, Preventive and Personalised Medicine* (**Springer Nature**),

Editor of *Predictive Diagnostics and Personalised Treatment: Dream or Reality* (Nova Science Publishers, New York 2009) and Co-editor of *Personalisierte Medizin* (Health Academy, Dresden 2010).

She is the European Representative in the EDR Network at the National Institutes of Health, USA (http://edrn.nci.nih.gov/).

She is a regular reviewer for over 30 clinical and scientific journals and serves as a grant reviewer for national (ministries of health in several European countries) and international funding bodies.

Since 2007 until now, she has been working as the European Commission evaluation expert for FP7, Horizon 2020, IMI-1 (Innovative Medical Initiatives) and IMI-2. From 2010 to 2013, she was involved in creating the PPPM-related contents for the European Programme 'Horizon 2020'.

Currently, Dr. Golubnitschaja is Vice-Chair of the Evaluation Panel for Marie Curie Mobility Actions at the European Commission in Brussels.

Preface

Predictive, Preventive and Personalised Medicine (3PM) is a new paradigm for both bio/medical sciences and management of medical services created and promoted by the expert groups of EPMA in early twenty-first century.

On the other hand, Information Technology (IT) comprises essential tools for many aspects of societal organisation at individual and population levels, being therefore instrumental for the development and implementation of advanced 3PM concepts benefiting healthy individuals, patients, healthcare system, and the society as a whole.

Potential IT/3PM benefits could be well exemplified by the current Covid-19 Pandemic challenge, when optimal policy-making decisions could be made only by application of predictive IT algorithms for cost-effective targeted preventive measures saving lives and considering the entire spectrum of socio-economical issues related to this complex situation.

Contextually, this book addresses the IT-generated solutions for practical implementation of 3PM concepts. It presents innovative methods, algorithms and approaches which synergistically demonstrate a potential to advance 3PM concepts and implementation. A spectrum of relevant IT solutions is considered such as predictive and prognostic tools, health monitoring for targeted prevention, Internet of Things (IoT), Artificial Intelligence (AI), big data analysis and personalisation of treatment algorithms.

Toulouse, France — Lotfi Chaari

Introduction

Keywords: Predictive Preventive Personalised Medicine (PPPM, 3PM); eHealth; IoT for Health; Artificial Intelligence; Big Data Analysis; Deep Learning; Health Monitoring; 3D Visualization; Covid-19 Pandemic Monitoring

Introducing Information Technology (IT) tools in today's and future medicine is being increasingly considered all over the world, especially in developed countries. Indeed, these countries are suffering the most from population aging and chronic diseases. This induces original challenges not only for healthcare but also for well-being. In this sense, Predictive, Preventive and Personalised Medicine (3PM) has been identified since more than a decade as a research avenue having huge potential for developed societies.

From Traditional to 3PM

The history of medicine[1] is rich in important events and discoveries. For centuries, medicine has regularly faced important challenges. Evolution has therefore happened relatively to historical events, but also with respect to the practice methodology. Regarding events, there is no better example than the current Coronavirus Pandemic, which is demonstrating that healthcare systems in both developed and developing countries are not adapted to such situations.

In terms of practice methodology, medicine moved from Traditional (T) practice to Complementary and Alternative Medicine (CAM) and then to Person-Centred Medicine (PCM), Individualised Medicine (IM), Stratified Medicine (SM), Personalised Medicine (PM), and more recently Predictive, Preventive and Personalised Medicine (3PM). 3PM is becoming today one of the main priorities of the European Commission (EC) to solve current health challenges [2]. Although these challenges are to a large extent due to population aging trends, chronic and severe diseases, earlier considered as being linked to the elderly, nowadays occur more and more frequently to younger generations, such as diabetes mellitus type 2, some types of aggressive cancers and 'young' stroke, among others [3,4,5,6]. Contextually, inno-

vative population screening programmes based on advanced concepts of prediction, targeted prevention and personalisation of medical services have to be investigated.

3PM Meeting IT

Today, the paradigm of handling chronic diseases is facing a shift from reactive to Predictive, Preventive and Personalised. Recent studies clearly established this evidence in general [7] and specific chronic diseases such as heart failure [8].

This paradigm shift has been conducted by handling more patient-related data. As most of today's applications, these data may be of very large volumes. It is mostly collected from sensors either related to people's physiological state or environment.

To analyse the generated data volumes, it is not possible any more to rely on manual or operator-based tools. Hopefully, research during the last two decades in the field of IT has led to the development of many automatic and efficient tools to collect, process and analyse data. The 3PM community has therefore managed to formulate unsolved problems to be investigated using IT tools [9, 10].

IT Meeting 3PM

On the other hand, IT has completely changed our lives. Starting from homes, vehicles or even work and restaurants, we use IT tools throughout the day. On the other hand, IT today is contributing to the understanding and monitoring of the current Covid-19 Pandemic [11]. This allowed countries to adapt their prediction and prevention strategies either through non-pharmacological interventions (NPI) or personalised imagery-based testing [12]. 3PM is therefore being adopted as a paradigm to handle both the pandemic and post-pandemic phases.

In the context of healthcare, IT has a lot offer, such as patients management at hospitals, exploration tools like imagery, telemedicine, and data-driven clinical decision systems (CDS). More recently, Artificial Intelligence (AI) is being investigated deeper despite the sensitivity of the medical field [13]. Specifically, the AI community [8] has investigated solving 3PM problems. In parallel, similar contributions in the field of 3PM have been made by other scientific communities such as Internet of Things (IoT) [14].

This book addresses new contributions in the field of IT regarding 3PM. It therefore contributes to document how IT is meeting 3PM to solve current problems and give new perspectives for the future. The book's content covers tools serving personalised prediction, tools for diagnosis and prevention, monitoring, visualisation, data analytics, AI and personalized medical systems.

The reported original contributions have been presented to the second International Conference on Digital Health Technologies (ICDHT 2019). This book therefore provides one with a technical idea about future trends using IT tools for 3PM.

References

[1] Golubnitschaja, O., Baban, B., Boniolo, G., Wang, W., Bubnov, R., Kapalla, M., Krapfenbauer, K., Mozaffari, M.S., Costigliola, V: Medicine in the early twenty-first century: paradigm and anticipation - EPMA position paper 2016. EPMA J. **7**(23), (2016)

[2] Lemke, H.U., Golubnitschaja, O.: Towards personal health care with model-guided medicine: long-term PPPM-related strategies and realisation opportunities within 'Horizon 2020'. EPMA J. **5**(1), 8 (2014)

[3] Duarte, A.A., Mohsin, S., Golubnitschaja, O.: Diabetes care in figures: current pitfalls and future scenario. EPMA J. **9**(2), (2018)

[4] Kunin, A., Polivka, J. Jr., Moiseeva, N., Golubnitschaja, O.: "Dry Mouth" and "Flammer" syndromes – neglected risks in adolescents and new concepts by predictive, preventive and personalised approach. EPMA J. **9**(3), 307–317 (2018)

[5] Golubnitschaja, O., Flammer, J.: Individualised patient profile: Clinical utility of Flammer syndrome phenotype and general lessons for predictive, preventive and personalised medicine. EPMA J. **9**(1), 15–20 (2018)

[6] Polivka, J. Jr., Polivka, J., Pesta, M., Rohan, V., Celedova, L., Mahajani, S., Topolcan, O., Golubnitschaja, O.: Risks associated with the stroke predisposition at young age: facts and hypotheses in light of individualized predictive and preventive approach. EPMA J. **10**(1), 81–99 (2019)

[7] Seifirad, S., Haghpanah, V.: Inappropriate modeling of chronic and complex disorders: How to reconsider the approach in the context of predictive, preventive and personalized medicine, and translational medicine. EPMA J. **10**(3), 195–209 (2019)

[8] Barrett, M., Boyne, J., Brandts, J., Brunner-La Rocca, H.P., De Maesschalck, L., De Wit, K., Dixon, L., Eurlings, C., Fitzsimons, D., Golubnitschaja, O., Hageman, A., Heemskerk, F., Hintzen, A., Helms, T.M., Hill, L., Hoedemakers, T., Marx, N., McDonald, K., Mertens, M., Müller-Wieland, D., Palant, A., Piesk, J., Pomazanskyi, A., Ramaekers, J., Ruff, P., Schütt, K., Shekhawat, Y., Ski, C.F., Thompson, D.R., Tsirkin, A., van der Mierden, K., Watson, C., Zippel-Schultz, B.: Artificial intelligence supported patient self-care in chronic heart failure: a paradigm shift from reactive to predictive, preventive and personalised care. EPMA J. **10**(4), 445–464 (2019)

[9] Fröhlich, H., Patjoshi, S., Yeghiazaryan, K., Kehrer, C., Kuhn, W., Golubnitschaja, O.: Premenopausal breast cancer: potential clinical utility of the multi-omic based machine learning approach for patient stratification. EPMA J. **9**(2), (2018)

[10] Gerner, C., Costigliola, V., Golubnitschaja, O.: Multiomic patterns in body fluids: Technological Challenge with a Great Potential to Implement the Advanced Paradigm of 3P Medicine. Mass Spectrometry Rev. 195–209 (2019)

[11] Chaari, L., Golubnitschaja, O.: Covid-19 pandemic by the "real-time" monitoring: the Tunisian case and lessons for global epidemics in the context 3PM strategies. EPMA J. (2020) https://doi.org/10.1007/s13167-020-00207-0

[12] Xiaowei, X., Xiangao, J., Chunlian, M., Peng, D., Xukun, L., Shuangzhi, L., Liang, Y., Yanfei, C., Junwei, S., Guanjing, L., Yongtao, L., Hong, Z., Kaijin, X., Lingxiang, R., Wei, W.: Deep learning system to screen coronavirus disease 2019 pneumonia. In: arXive. 2020. https://arxiv.org/ftp/arxiv/papers/2002/2002.09334.pdf. Accessed 21 Feb 2020
[13] Davenport, T., Ravi, K.: The potential for artificial intelligence in healthcare. Future Healthcare J. **6**(2), 94–98 (2019)
[14] Schreier, G.: The internet of things for personalized health. Stud. Health Technol. Inform. **200**, 22–31 (2014)

Contents

About the Editor

Lotfi Chaari received his PhD degree from the University of Paris-Est in France. He prepared for his PhD with the Signal and Communication Group of the Laboratoire d'Informatique Gaspard Monge (LIGM), in collaboration with NeuroSpin-CEA, the first centre in Europe dedicated to ultra-high field MRI and applications in cognitive neurosciences. He then moved to Grenoble as a Postdoctoral Fellow at INRIA with the Mistis team. In 2012, he joined the Institut National Polytechnique de Toulouse as an Associate Professor. He is also member of the IRIT laboratory. In 2017, he received the HDR dissertation from the University of Toulouse. Lotfi Chaari's research is focused on medical signal and image processing with various applications and imaging modalities. He is an expert for a number of journals of the signal and image processing as well as the medical imaging communities. He also worked as an expert for institutions like the French National Research Agency and European Commission.
Prof. Lotfi Chaari has participated in the organization of several special sessions for international conferences, is a regular member of various technical programme committees, and was the Co-founder and General Chair of the two first editions of the International Conference on Digital Health Technologies.

A New Scalable and Comprehensive Real-Time Evaluation System of Dependence

Marie-Claude Mendo, Julien Mistrzak, Vincent Peirolo, and Laurent Billonnet

1 Context

According to the latest projections of the French population, in 2050, one in three inhabitants should be more than 60 years old in France. Every country in Europe is concerned with 2.3 million of dependent elderly. In 2016, 7500 nursing homes hosted about 600,000 seniors. Other seniors have chosen or not to stay at home [1].

The French caregiver Association counts 8.3 million caregivers. To improve the daily life and the accompaniment of people in loss of autonomy, the French government has developed several plans (old age, Alzheimer's) and laws, the most recent of which is the law ASV (adaptation of society to ageing). This includes the physical environment (habitat), the social environment (family caregivers) and the traditional AGGIR grid (gerontological autonomy iso-resource groups) [2].

The AGGIR grid evaluates the level of dependence of people over 60. The GIR index found is used to adapt the Personalized Autonomy Allowance. This index goes from 1 to 6 and one is the highest level of dependence. GIR 1–4 indices allow to benefit for an assistance plan funded by the county council, including human, financial, technical (home automation for example) for the seniors and their families.

However, this tool do not take into account several parameters; such as caregivers (while they are essential for efficient home support and to maintain social link), neurodegenerative diseases (such as Parkinson and Alzheimer) or emotions and affects of the people with loss of autonomy [3].

There is also a problem of temporality between evaluations. In the current model, the AGGIR grid is evaluated only once every 2 years. The medical status and the

M.-C. Mendo · J. Mistrzak · V. Peirolo · L. Billonnet (✉)
University of Limoges, Limoges, France
e-mail: laurent.billonnet@unilim.fr

L. Chaari (ed.), *Digital Health in Focus of Predictive, Preventive and Personalised Medicine*, Advances in Predictive, Preventive and Personalised Medicine 12,
https://doi.org/10.1007/978-3-030-49815-3_1

dependence level of the user can decline in a few days, which should rationally require a new immediate evaluation.

2 How to Overcome All of These Shortcomings?

To solve all these weaknesses, we propose a global scalable system for evaluation of the people with loss of autonomy without age restriction. Based upon activity monitoring, the goal is to set up an intelligent system with sensors that can detect in real-time changes that occur after the initial evaluation using standard grids [4]. Parameters referred by the process are: transfers, movement inside and outside the house, urinary and faecal elimination, feeding, tracking and orientation in living space and time, communication, dressing and undressing. It is also possible to rate the evolution of pathologies, emotions of the user and the people around him (family, caregivers), falls and global physical activity.

According to the literature, there are different means of fall detection and activity monitoring for the elderly. One concerns "direct detection" [5] solutions, which detect a sudden change in the position of the body (drop) thanks to the accelerometers or equivalent sensors. The second refers to environmental sensors to monitor and analyse the activities (or absence of activity also called "peripheral sensing") of the person [6].

The RE-AGGIR (react) system aims to integrate the AGGIR grid and its multi-dimensional assessment into the habitat [7]:

- Feeding is one of the primary needs of life. Appetite reduction is one of the main factors in the loss of autonomy. Therefore, monitoring the diet on a daily basis can detect when the persons are no longer able to feed themselves.
- Approximately 78% of incidents and accidents usually occur overnight in seniors. So monitoring night activities must be part of our system.
- Falls are among the causes of hospitalization and mortality in the elderly. The post-fall syndrome leads to a reduction in the activities of the elder and the latter will adopt other postures to avoid falling again.
- Monitoring the grasping abilities enables to monitor the dressing and the onset of neurodegenerative diseases.
- Monitoring the outward comings and goings will allow us to know if the persons in loss of autonomy continue to have relations and/or activities outside their home thus maintaining a reasonable level of social link.
- Monitoring the attendance of the bathroom and the toilets allows having information on the hygiene of the elderly person (it is also one of the items of the AGGIR grid). Natural elimination is one of the items evaluated by the Aggir grid.

In terms of ethics and privacy respect, the system has to be practically invisible to the inhabitants since the success of our system is based first on its acceptance by the

users. The data collected by the sensors will be analysed and processed intelligently by a central system. This will be connected to a monitoring interface that can issue alerts autonomously in case of emergency. The system will stay connected to the AGGIR grid's algorithm so that the GIR index can be automatically refreshed in real-time and transmitted to care services, prescribers and caregivers.

3 A Real-Time Evaluation System

3.1 Expected Benefits

Our goal is to consider the actual AGGIR grid, adding social and family environment parameters.

The re-AGGIR system has several advantages such as the daily monitoring of the evolution of pathologies in real time. It helps to reduce the delays in the intervention of professionals and prevent the loss of autonomy. It complements the remote assistance services and operates in autonomy without interaction.

RÉ-AGGIR makes it possible to re-adapt services and home support according to needs while monitoring the parameters that are part of the primary needs of the people.

Our proposal therefore consists of a panel of four types of sensors. We describe the role and implementation strategy of the different sensor types (see Fig. 1) further.

3.2 Central Unit

Pure and discrete, the design of this central unit (see Fig. 2) allows it to be placed anywhere in the house without being imposing or too intrusive. This unit collects the data of all sensors and processes it to send alerts to caregivers and professionals.

3.3 Presence Sensors

In general, a motion detector is a sensor placed at a strategic location to detect intrusions into a house. On the one hand, we use its ability to detect a presence, help daily lighting of the lamps in case of motion detection. This is essential for night walking. On the other hand, it allows monitoring the frequency of these movements.

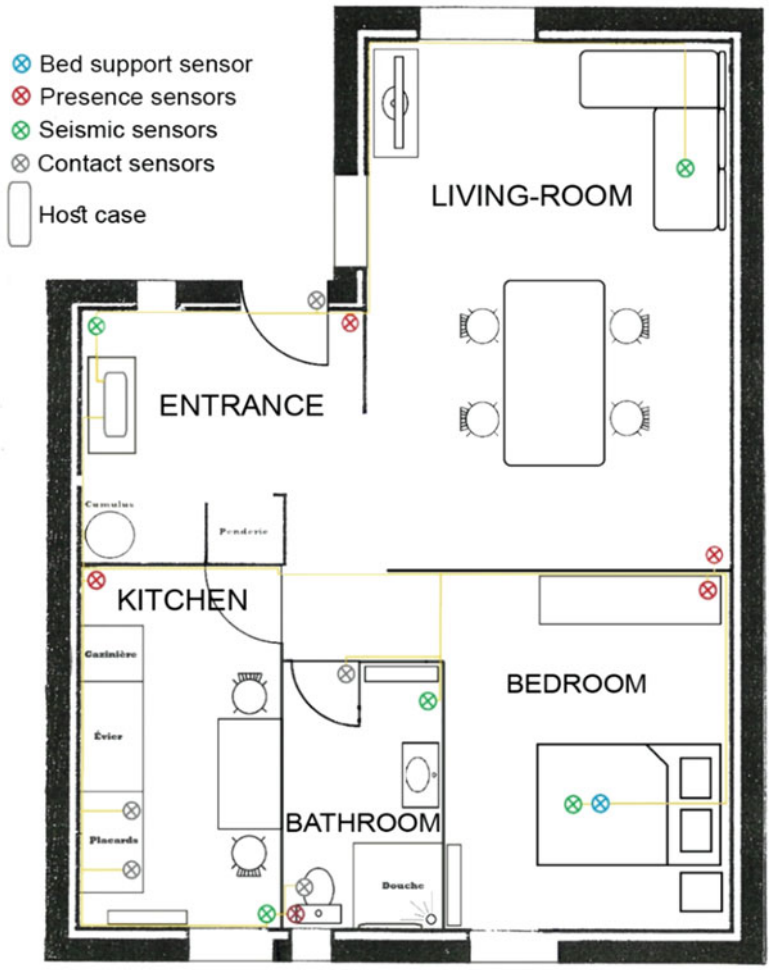

Fig. 1 Example of sensors implantation into a house

3.4 Contact Sensors

A contact sensor is a simple and effective solution for detecting for example opening of household appliances or doors/windows. In our system, it will be used to monitor three parameters: eating habits, natural elimination and hygiene, outside activities.

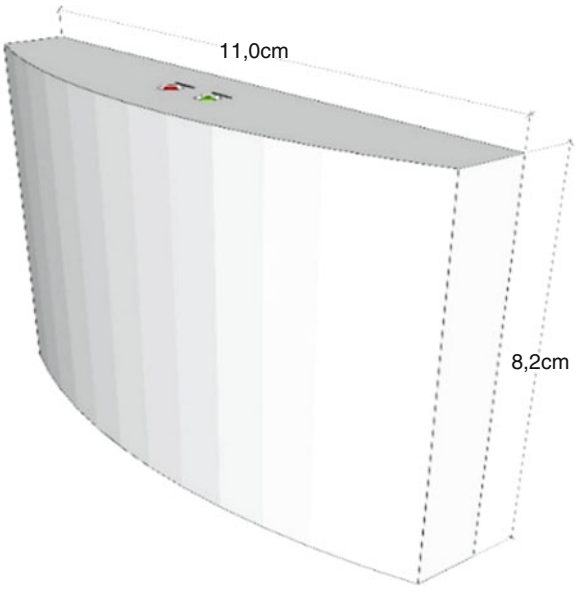

Fig. 2 Design of the central unit

3.5 Bed Support Sensor

Sleep cycle changes during normal aging of people. However, for the elderly, the night is the time when the risk is important. As nocturnal ambulation is a precursor to Alzheimer's disease and needs to be monitored. In this case, the contact sensors placed in the kitchen, coupled with the bed sensor, will detect and signal the action. The contact sensor will also be installed in the toilet.

The support sensor is a plate with sensors that slides under the mattress. It can detect a presence by contact with the person. Equipped with an intelligent system, He is able to differentiate the sitting position from the lying position. What makes the sleep measurement readings of the person more reliable.

3.6 Seismic Sensor

This sensor is the size of a two-euro coin and is placed directly on the floor of each room and in the centre. Thanks to its extreme thinness, it does not feel almost under foot when walking on it. This apparel records and analyses in real time the slightest vibrations that the soil propagates. Thanks to its precise parameterization, it is able to analyse the weight of an impact and thus to diagnose if the vibration is due to an object fallen to the ground or a person falling.

3.7 Limits of the System

Like any human work, the re-AGGIR system has some limitations, such as the grasping measurement that is part of the AGGIR grid. RE-AGGIR is going to need human help to monitor these settings. The system is not also able to identify the person who is the victim of a fall when there are several inhabitants in the house. Actually, only people who reside in areas covered by an internet network can use RE-AGGIR. The others will have to wait for network coverage throughout the territory. Finally, the affects cannot be evaluated without human aid.

4 Conclusion

Our system not only complements tele assistance services, but also secures the elderly, prevents loss of autonomy by monitoring daily changes in pathologies and facilitates the intervention of professionals. RE-AGGIR is a global evaluation system that combines discretion, comfort and technology. RE-AGGIR accompanies seniors as well as anyone without age distinction. However, for some parameters like affects, dressing / undressing, grasping, RE-AGGIR will need to use intrusive devices such as the cameras to work efficiently. It will also need a human interaction to estimate and accompany the seniors at best.

The system estimates the dependence in real time and makes it possible to adapt the different supports according to the evolution of the needs of the people with loss of autonomy. RE-AGGIR presents several advantages: the safety of the aidant, the prevention of the loss of autonomy, the serenity of the caregiver and the relatives. It is a comprehensive complement to the tele assistance services. With the increasing impact of IoT in several domains, possibilities of application extensions seems infinite.

References

1. Insee.fr https://www.insee.fr/fr/statistiques/1280826. Retrieved October 21 2018
2. Lalive d'Epinay, C., & Spini, D.: Années fragiles. Quebec University of Laval press edition, p. 146 (2008)
3. Quentin, B.: Gérontologie et société. Fondation nationale de gérontologie, 141, pp 171 (2012)
4. Guyonnet, S., & Raynaud-Simon, A.: Fragilité et nutrition, Repérage et maintien de l'autonomie des personnes âgées fragiles, (en ligne) Livre blanc.org décembre 2013, https://fragilite.org/livre-blanc.php ; reached on 10th of December 2018
5. Silvereco, Chute de la personne âgée : causes, conséquences et prévention (en ligne), octobre 2017, available on https://www.silvereco.fr/chute-de-la-personne-agee-causes-consequences-et-prevention/3187245, booked on 3rd of January 2019

6. Nexecur, Quelles sont les signes de la perte d'autonomie ? (En ligne), Enquête Santé handicap 2009, available on https://www.nexecur.fr/comment-detecter-perte-d-autonomie, reached on 25th of January 2019
7. Leduc Florence, Notre projet politique, (en ligne) Association française des aidants, available on sur https://www.aidants.fr/lassociation/notre-projet-politique, reached 28th of January 2019

An Ontology Based Authentication Framework for Healthcare Monitoring

Amira Henaien and Hadda BelHadj

1 Introduction

Nowadays, the widespread use of smart devices is producing a radical changes in our daily life activities. As one of the fields the most affected is healthcare attending more than 40% from the hole investments of the market of WoT [2, 4]. Several successful industrial or research works are developed with a very efficient design to track and monitor the health of a patient continuously and ubiquitously. The principle idea of WoT Healthcare Applications consists in involving a set of smart devices connected to daily life objects in the body of the patient or its environment. The main job of those devices is to collect the necessary data for an ubiquitous healthcare monitoring. And it may includes any sensing data about the user's health situation and the environment situation, the medical history of a patient, a device information and any health domain-specific data. It is very necessary and challenging to create new standardization and develop good practices to improve the usability, the maintainability, and the security of healthcare applications. As it is discussed in [3, 4], form this list, security is a priority. Any lost or fake information can leads to a dangerous situation and even to the death of human being. For a cardiology patient in a critical situation, any missing vital sign, as its heart beat, can delay an alert or completely loose it and deprive him from getting any aids. The wrong information or the missing data are not always technical bugs. It is absolutely possible that they are a willfully human being made errors spontaneously

A. Henaien (✉)
King Khalid University, Abha, Saudi Arabia
e-mail: aheniaen@kku.edu.sa

H. BelHadj
Laboratory of Technology and Smart Systems, Digital Research Center of Sfax, Sfax, Tunisia
e-mail: Hadda.lBnelhadj@esti.rnu.tn

L. Chaari (ed.), *Digital Health in Focus of Predictive, Preventive and Personalised Medicine*, Advances in Predictive, Preventive and Personalised Medicine 12,
https://doi.org/10.1007/978-3-030-49815-3_2

or deliberately. For this reasons, the system should be enhanced enough to protect its data. As the most first action that can be taken is a strong authentication system to limited the access using a powerful authentication methods.

Different authentication solutions are efficiently used and approved for information systems in general and medical systems in particular. However, new ubiquitous and continuous healthcare monitoring applications have a very particular type of users like: people with special needs, handicaps, old persons, new born babies. For this reason, common methods, viz, knowledge-based or possession-based methods are no more feasible. An old person with Alzaheimer probably is never able to remember the password. It is becoming necessary to create a standardized authentication technique supporting the variety of health situation of users and providing the highest guaranty of protection for the data. A technique taking on consideration the health and mental situation of a user should specify for each user his situations, specify the different possible means of authentication and associate a semantic interpretation to each one. Finally, this technique should be able to reason and interpret the best authentication technique for each user.

This paper presents a new ontology based authentication methodology for healthcare monitoring in a predictive, preventive and personalized medicine system. The main idea consists on allowing different and adapted methods of authentication depending in the health and mental situation of the user. The system allow for a caregiver or a doctor to define the different abilities and capabilities of a patient. Based on those information, the system is able to define the appropriate method to be used for the user to authenticate and is able to provide this method ubiquitously to be identified. This paper is organized as the following: Sect. 2 is a presentation of the background of this work. Section 3 is an overview of this framework. In Sect. 4 we present the main component of this framework, the knowledge management system. Finally, Sect. 5 is a conclusions and perspectives.

2 Related Work and Background

Context and Rules Based Authentication In a very general way, the process of the authentication is confirming that a specific attribute claimed by an entity in a system. This confirmation is in many cases an identification of an entity that claims using credentials. Usual identification methods are knowledge-based methods, i.e. a password, answer question, generated code, etc. Traditional authentication methods have been enhanced with different techniques, viz, location based authentication [1], bio-metric information based authentication [11], context-awareness based authentication [1, 5, 13, 14], shared authorization and authentication rules across network based authentication [17].

Security and Medicine Ontologies Ontologies are becoming a powerful tool in the development of interdisciplinary systems as e-healthcare systems since their are able to represent and interrelate many types of knowledge.

Based Context Modeling for Healthcare Applications During the last years, different medical ontologies have been proposed to summarize medicine terms and concepts, viz, Systematized Nomenclature of Medicine Clinical Terms (SNOMED CT) [15], International Classification of Diseases (ICD)-10 [9] and International Classification Nursing Practice ICNP [10]. The ontology ICNP is a formal structure containing terms and definitions providing a formal nursing terminology for the construction of nursing diagnoses, interventions, and results. Ontology is not only used for terminology, it is also involved in different healthcare applications, viz, [6] proposing a context-aware system for antihypertensive drug recommendations or [8] designing a diabetes diagnosis framework.

Ontology Based Security Approaches Besides to medicine ontologies, some security approaches have been proposed based on ontologies viz, [12] an ontology base authorization enabling semantically matching diverse authorization requests and semantic rule reasoning on requested access; [7] an ontology-based interoperation service translating security attributes from local security vocabularies into the attributes recognized by the central vocabulary. Souad et al. in [16] propose a classification into eight families of existing security ontologies for the different requirements definition.

3 Overview of the Proposed Ontology Based Authentication Framework

The proposed framework is designed to allow different types of identification. It express the abilities of a patient with a formal specification. For each user, the system determinate a personalized method of authentication. The data is collected from different devices like: body sensors worn by the user, ambient sensors surrounding the user or smart devices, as phone, tablet, etc. Body sensors are used to capture the health profile of the patient, viz, vital signs, motion, location, etc. Ambient sensor reflect an image of the patient's environment, viz, ambient temperature, lightness, existence of a caregiver, etc. Smart devices are basically used to allow the communication between the user and the system and between users, viz sending an alert to user about a patient's situation, monitoring a patient, etc. We suppose that a caregiver or doctor is authorized to enter the mental situation the abilities of the patient and edit it in case of any changes. Thus, the basis of the designed system is to provide the appropriate identification method for each user deduced from its role (Patient, Doctor, Caregiver, FamilyCaregiver, etc), the collected data of its current situation, the already described data of its mental situation and abilities and security-related knowledge. As described by Fig. 1, the general architecture of this framework is containing:

Sensing Component: a set of sensors and smart devices related directly to the user. Their role is to collect all the context data: health data, ambient data, location,

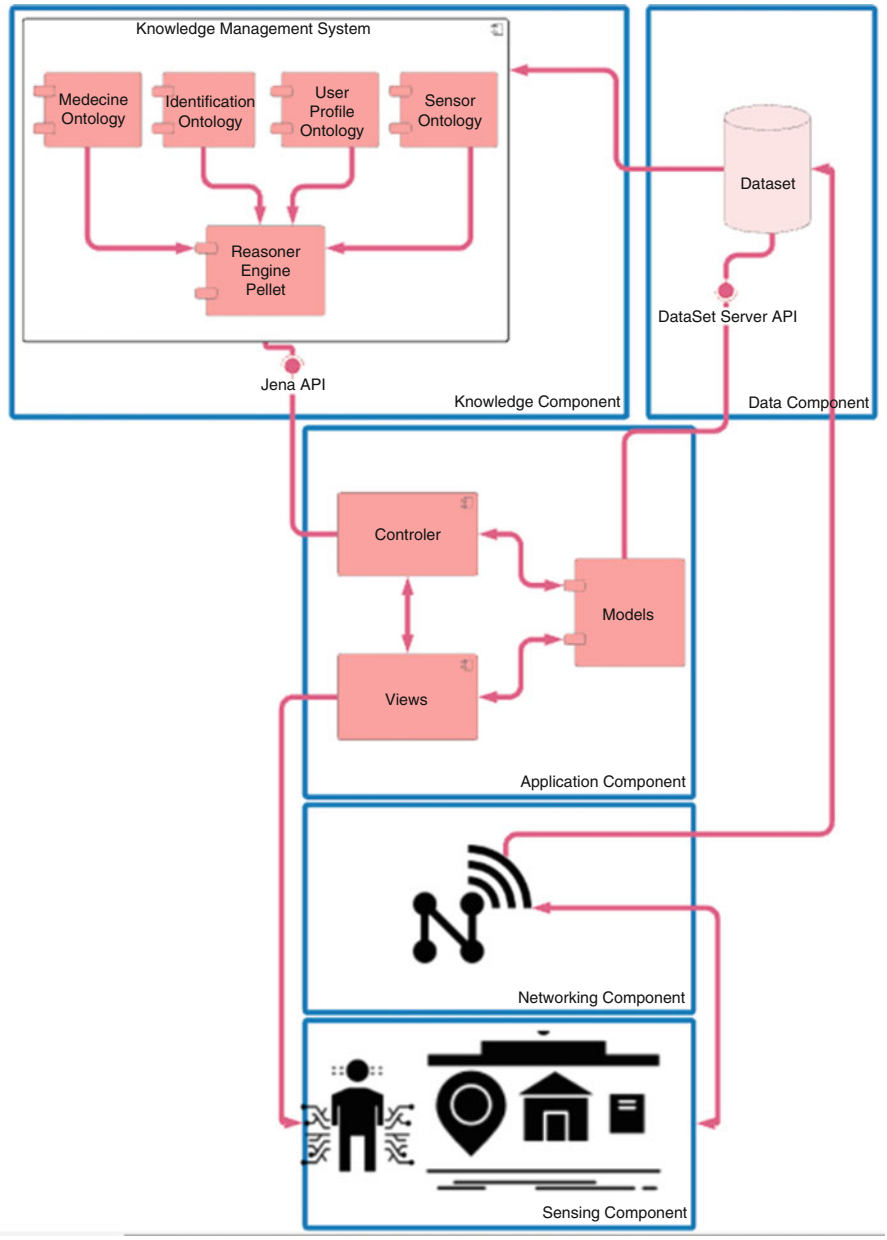

Fig. 1 General architecture of ontology based authentication framework

motion, personal information, etc. This set of sensors are related to one user and they are composing a smart platform.

Networking Component: a set of networking device allowing the communication between the different physical elements and the connection of those elements to the internet. Networking elements also allow the data exchange between the sensing layer and the knowledge component.

Data set Component: is a server hosting all the data: current data collected in real time and saved information about the user. It is providing instances enriching the ontologies from the knowledge component.

Application Component: is the implementation of all the features of the healthcare application providing all the services for ubiquitous and continuous medical monitoring. It is a MVC[1] application.

Knowledge Component: is playing a fundamental role in this architecture because it is the responsible for the knowledge base and the reasoning. It is composed of four ontologies and a reasoner engine (Pellet). This component is the responsible to provide the appropriate authentication method. The Fig. 2 explains the general process of authentication.

4 Ontology Based Knowledge Management System

The main part in the general architecture of the proposed framework, presented in Sect. 3, is the knowledge Management System. It decides the identification method associated to each user. It is composed basically from a set of ontologies: personal profile ontology, sensor ontology, medicine ontology, security ontology and a reasoner. Our ontologies are the extension of standard ontologies such as FOAF for personal profile, SSN and SOSA for sensors ontology and ICNP for medicine ontology. Those standard ontologies are merged with the security ontology containing basically a set of SWRL rules corresponding to the security rules. In the following, we present the different ontologies and the links between their entities.

Personal and health profile: we are using FOAF to present the personal profile of users. FOAF:person is representing all information related to the user, viz, account details, name, familyName, age, gender, etc. In the same time the ontology ICNP is providing an entity Individual presenting the health profile of a user as height, weight. We have specified FOAF:person equivalent to ICNP:Individual. ICNP is also describing an entity Role precising if the individual is Patient, Doctor, Caregiver, Nurse, etc. The property named hasLocation from ICNP associates a location to each patient.

Sensor ontology: The ontology SSN is providing an entity named Platform. It is a concept used to gather different entities as sensors, actuators, other platforms

[1] MVC: Model View Control

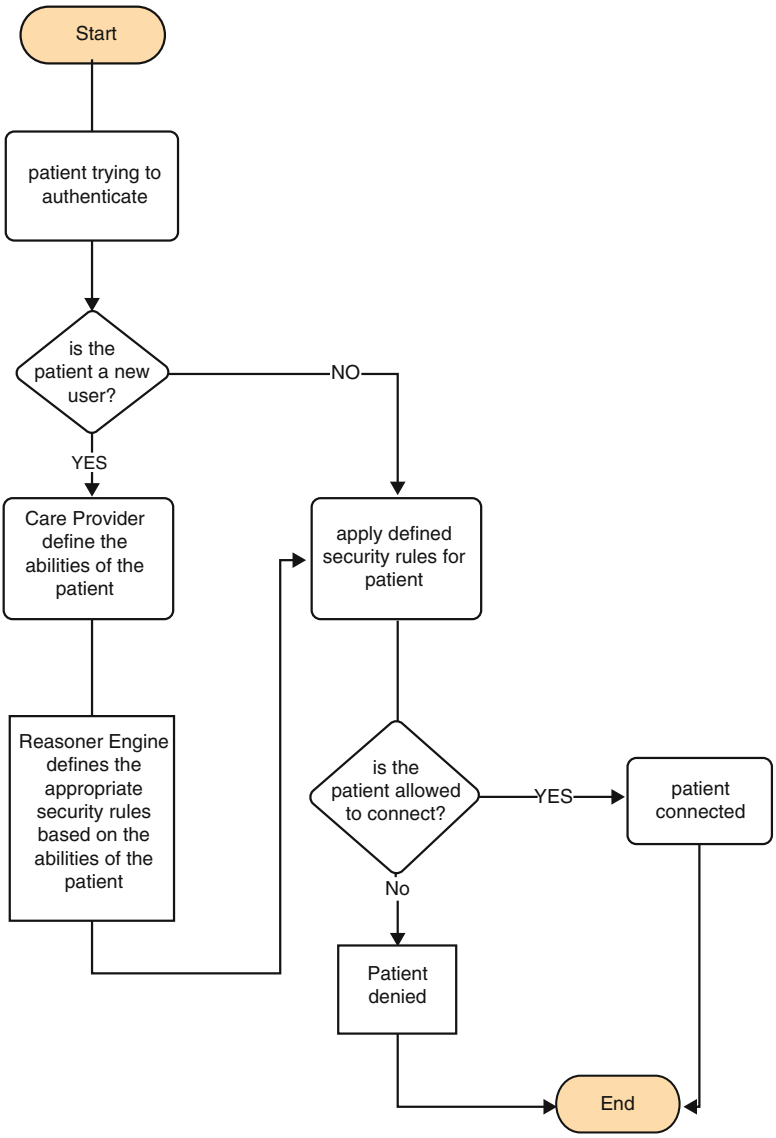

Fig. 2 Flow chart of authentication process

hosted in the same platform. SSN:Platform is associated to a user using the personalized property hasPlatform. The class SSN:Sensor is specified with two sub-classes BodySensors presenting sensors worn or attached to the body of the user and AmbientSensors presenting sensors existing in its environment. For each entity from the platform, we define its location using the same property hasLocation.

Medicine Ontology: ICNP provides an entity AbilityStatus with a set of sub-classes defining all the possible abilities of a person. Each ability contains two sub-classes an actual positive ability, in the case of safe ability, and actual negative ability, in the case of lost ability. For instance, ActualNegativeAbilityToSee is defining the disability of a patient to see. The property hasAbsoluteJudgeState is expressing the state of each ability for a user.

Security Ontology: the class IdentificationMethods contains a sub-classes for each identification methods. This list contains the different following entities: ByCareGiver, ByCornea, ByDoctor, ByEnteringPassword, ByFingerPrint, ByLocation, ByVoicePrint. The relation implementedBy related each method to its implementation. The property IdentifyBy is relating a user to his identification method.

SWRL Security Rules This ontology contains a set of SWRL rules used later by the reasoner to calculate the appropriate identification method and they are mainly authentication rules. For example, if all the abilities of a patient have ActualPositive for the hasAbsoluteJudgeState property, the authentication can be processed using classical authentication method using password, i.e. the property IdentifyBy for this patient is ByEnteringPassword. However, if a patient is blind, the property IdentifyBy for this patient is ByFingerPrint, ByCareGiver or ByDoctor.

5 Conclusions and Perspectives

This paper presents a new ontology based framework to personalize the authentication method to each user of a healthcare ubiquitous and continuous monitoring PPPM system. This new technique is very helpful for users with limited abilities or particular health situation. The identification method is defined depending on different parameters, viz, the user's personal information, his health situation, his mental situation, the possible identification methods, the available device to the user, etc. This work is based also on context and rules based authentication specified with SWRL. As a continuation of this work, we are aiming to develop the complete components constituting the system. We will also evaluate the performance of our system and compare it to other identification methods.

Acknowledgments The authors would like to express their gratitude to King Khalid University, Saudi Arabia for providing administrative and technical support.

References

1. Agadakos, I., Hallgren, P., Damopoulos, D., Sabelfeld, A., Portokalidis, G.: Location-enhanced authentication using the IoT: because you cannot be in two places at once. In: Proceedings of the 32nd Annual Conference on Computer Security Applications, pp. 251–264. ACSAC'16, ACM, New York (2016). https://doi.org/10.1145/2991079.2991090
2. Al-Fuqaha, A., Guizani, M., Mohammadi, M., Aledhari, M., Ayyash, M.: Internet of things: a survey on enabling technologies, protocols, and applications. IEEE Commun. Surv. Tutorials **17**(4), 2347–2376 (2015)
3. Alharam, A.K., El-madany, W.: Complexity of cyber security architecture for IoT healthcare industry: a comparative study. In: 2017 5th International Conference on Future Internet of Things and Cloud Workshops (FiCloudW), pp. 246–250. IEEE (2017)
4. Baker, S.B., Xiang, W., Atkinson, I.: Internet of things for smart healthcare: technologies, challenges, and opportunities. IEEE Access **5**, 26521–26544 (2017)
5. Bernal Bernabe, J., Hernandez-Ramos, J.L., Skarmeta Gomez, A.F.: Holistic privacy-preserving identity management system for the Internet of things. Mob. Inf. Syst. **2017**, 1–20 (2017)
6. Chen, D., Jin, D., Goh, T.T., Li, N., Wei, L.: Context-awareness based personalized recommendation of anti-hypertension drugs. J. Med. Syst. **40**(9), 202 (2016)
7. Ciuciu, I., Claerhout, B., Schilders, L., Meersman, R.: Ontology-based matching of security attributes for personal data access in e-health. In: OTM Confederated International Conferences on the Move to Meaningful Internet Systems, pp. 605–616. Springer (2011)
8. El-Sappagh, S., Ali, F.: Ddo: a diabetes mellitus diagnosis ontology. In: Applied Informatics, vol. 3, p. 5. SpringerOpen (2016)
9. ICD10: https://bioportal.bioontology.org/ontologies/ICD10
10. ICNP: https://bioportal.bioontology.org/ontologies/ICNP
11. Kumar, T., Braeken, A., Liyanage, M., Ylianttila, M.: Identity privacy preserving biometric based authentication scheme for naked healthcare environment. In: 2017 IEEE International Conference on Communications (ICC), pp. 1–7. IEEE (2017)
12. Poulymenopoulou, M., Malamateniou, F., Vassilacopoulos, G.: A virtual PHR authorization system. In: IEEE-EMBS International Conference on Biomedical and Health Informatics (BHI), pp. 73–76 (June 2014). https://doi.org/10.1109/BHI.2014.6864307
13. Shahzad, M., Singh, M.P.: Continuous authentication and authorization for the Internet of things. IEEE Internet Comput. **21**(2), 86–90 (2017)
14. Shone, N., Dobbins, C., Hurst, W., Shi, Q.: Digital memories based mobile user authentication for IoT. In: 2015 IEEE International Conference on Computer and Information Technology; Ubiquitous Computing and Communications; Dependable, Autonomic and Secure Computing; Pervasive Intelligence and Computing, pp. 1796–1802. IEEE (2015)
15. SNOMED CT: https://bioportal.bioontology.org/ontologies/SNOMEDCT
16. Souag, A., Salinesi, C., Comyn-Wattiau, I.: Ontologies for security requirements: a literature survey and classification. In: International Conference on Advanced Information Systems Engineering, pp. 61–69. Springer (2012)
17. Trnka, M., Cerny, T.: Authentication and authorization rules sharing for Internet of things. Softw. Netw. **2018**(1), 35–52 (2018)

DeepLCP: Towards a DeepLearning Approach to Prevent Lung Cancer

Mayssa Ben Kahla, Dalel Kanzari, and Ahmed Maalel

1 Introduction

Lung cancer is considered to be one of the leading causes of death, mainly because of the late detection of the disease's symptoms and the lack of prevention's means. According to the National Cancer Institute: lung cancer is the fourth most common cancer in France. Also, according to the International Agency for Research on Cancer: Lung cancer is the second most common cancer in Tunisia with a 14.2% incidence and 21.1% mortality. This disease has many (a) risk factors, for example personal history of disease, family history of cancer, diet, smokers, etc., and many (b) symptoms, for example chest pain, persistent cough, Spitting blood, etc. The aim of our approach is to accurately calculate the probability of having lung cancer disease based on (a) and (b) by combining two technologies; the natural language processing (NLP) [1, 2] and the convolutional neural network (CNN) [3]. This paper describes in Sect. 2 the related work in Sect. 3 our approach, named DeepLCP, and in Sect. 4 the experimental validation of DeepLCP.

M. Ben Kahla (✉)
Higher Institute of Applied Science and Technology, University of Sousse, Sousse, Tunisia

D. Kanzari · A. Maalel
Higher Institute of Applied Sciences and Technology, University of Sousse, Sousse, Tunisia

National School of Computer Sciences, RIADI Laboratory, University of Manouba, Manouba, Tunisia

L. Chaari (ed.), *Digital Health in Focus of Predictive, Preventive and Personalised Medicine*, Advances in Predictive, Preventive and Personalised Medicine 12,
https://doi.org/10.1007/978-3-030-49815-3_3

2 Related Works

Several works deal with the cancer disease using the Deeplearning [4] paradigm, we quote, for example, the work of Gruetzemacher et al. [5] which use the architecture DNN for a revolutionary image recognition method to distinguish large and small pulmonary nodules from potentially malignant lung nodules.Besides uncertainty and high cost of computation, this work achieves high false positive in the detection step. Esteva et al. [6] deal with the CNN technique to classify the skin lesion and to detect the cancer disease by giving the probability of malignancy or benignity. But, this work complains by the variance of accuracy. Park et al. [7] develops a Deep learning algorithm, called DeepNEAT-Dx, to predict the presence or absence of lung cancer in a chest X-ray. The problem of "DeepNEAT-Dx", spend 40 h to train. Also, the study by D. Yang et al. [8], presents advanced AI (artificial intelligence) technology for the early detection of lung cancer and a classification model based on the DCNN system. Bychkov et al. [9] chose to combine convolutional (CNN) and recurrent (RNN) architectures to form a deep network to predict colorectal cancer outcomes from images of tumor tissue samples. But, this work has obtained low accuracy. All these works use image as input data, furthermore, there exist other works that use text as input data, such as those of Baker et al. [10] that apply the convolutional neural network (CNN) to classify the biomedical input texts. The disadvantages of this work the Cost of calculation and complexity. Also, John et al. [11] deal with the convolutional neural network (CNN), to extract ICDO-3 topographic codes from a corpus of breast and lung cancer pathology reports. The limitation of this corpus study included pathology reports for which the truth on the ground came only from the final diagnostic section of the report We summarize the different works that deal with deep learning, associated with text or image input data, to detect the cancer disease in Table 1.

The works presented in Table 1 contain a lot of limits like precision problem, cost calculation and complexity. Moreover, we note that most of these works apply convolutional neural networks (CNN) to detect only the lung cancer. They use CNN in a delayed phase where the patient made the diagnosis by imaging. For example, [7] used CNN to detect lung cancer from CXRs images and [11] use the CNN with medical reports after diagnosis. The problem with imaging, in case of lung cancer, is that the disease can't be discover early and the remedy is hardly difficult.

3 Proposed Approach

Inspired from Zhang Y. & Wallace (2015) [12] works, our approach, aim to combine two advanced methods; the natural language processing **(NLP)** and the convolutional neuronal network **(CNN)**. As illustrated in Fig. 1, our architecture is composed of an NLP layer, CNN layers, and a disease classification output.

Table 1 Synthesis of related works

Reference	Algorithm	Architecture	Accuracy	Error rate	Input image	Input text
[5]	Maxpooling, softmax	DNN	81.08–82.10%	_	✓	
[6]	Partitioning algorithm (PA)/Inference algorithm/t-SNE (t-distributed stochastic neighbor embedding)	CNN (GoogleNet)	55.4–72.1%	_	✓	
[7]	Genetic algorithm/ DeepNEAT-Dx/ Backpropaga-tion/SchiffMan encoding	CNN	96.00%	7.97%	✓	
[8]	_	DCNN	90–97%	10–24%	✓	
[9]	SVM/Naïve Bayes classifier/logistic regression	CNN-RNN (LSTM)	69%	_	✓	
[10]	NLP-WORD2VEC word embeddings	CNN	97.1%	2.9%		✓
[11]	Adadelta adaptive gradient descent/NLP-WORD2VEC/N-grams	CNN	71%	30%		✓

3.1 Natural Language Processing (NLP)

In the **NLP** part we use the word2vec model [13] to convert the sentences extracted from our online form to raw matrix. each sentence is a feature. The weights will choose according to the user's response and semantic transformation rules.

Semantic Transformation Rules give each information weights. All the rules defined by two doctors from hospital Farhat Hached Sousse and Hospital Taher Sfar Mahdia. We use 31 semantic rules formed by the formal Z language[14], then we implement these rules in python the construction of our raw semantic matrix. Figure 2 shows an example of these rules.

This rule means if the person answered in our online form that his gender is a man then the first column weight of VC matrix is a value of the interval [0.6..0.9]. Else if the answer is a woman then the weight of the first VC matrix column is a value

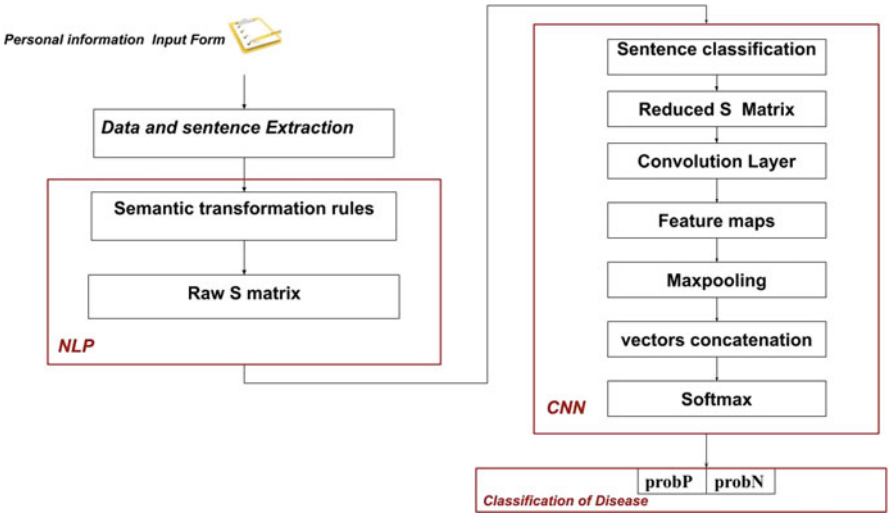

Fig. 1 DeepLCP architecture

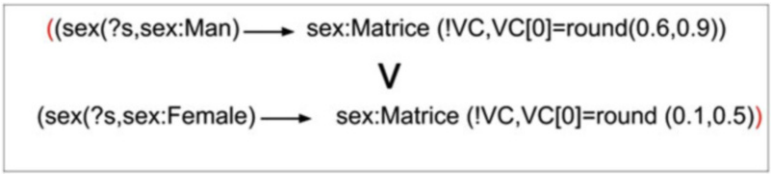

Fig. 2 Semantic transformation rules

of the interval [0.1..0.5]. These intervals are suggested by the doctor "Pr. Bouaouina Noureddine" chief radiotherapy department in the hospital Farhat hached Sousse and the doctor "Dr. Jalel Knani" Pneumologist in the Tahar Sfar Hospital because the Man have the risk of having the disease that the woman.

Raw S Matrix after the transformation we obtain the raw semantic matrix as illustrated in Fig. 3 with size [31*13].

- **31**: is the number of features.
- **13**: is the maximum number of words in the longest sentence.

3.2 Convolutional Neural Network (CNN)

In this part we apply two semantic classifications on the raw semantic matrix to obtain the reduced semantic matrix. Then we apply the CNN on this matrix to obtain the probability of detecting the disease.

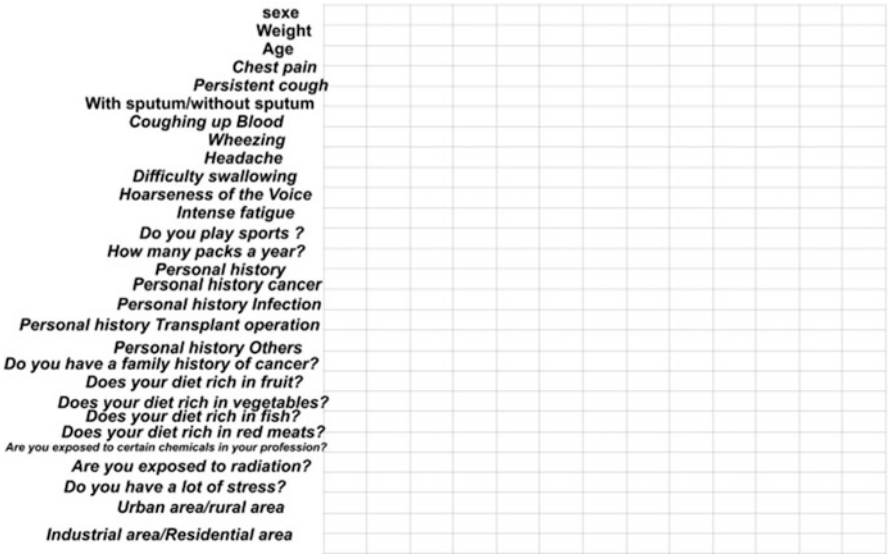

Fig. 3 Raw semantic matrix

- **Reduced S Matrix**
  To obtain the reduced semantic matrix we apply two type of classifications:
  - **Classification By Categories:** we classify data according to three categories: **Minor risk factors, Major risk factors, symptom**.
  - \+ **Classification By Themes:** we classify data into six themes:
    - **Thoracic signs:** this matrix represents the average of the matrices "chest pain", "wheezing" and "abnormal breathlessness".
    - **Cough:** this matrix contains the average of the matrices of "persistent cough", "with/without spitting" and "spitting of blood".
    - **Feeding:** this matrix contains the average of the matrices "diet rich in fruits", "diet rich in vegetables", "food rich in fish" and "diet rich in red meat".
    - **Consumer:** this matrix contains the average of the matrices "how many packets tobacco", "passive smoking", "alcohol".
    - **Personal antecedent:** this matrix contains the average of the matrices "Cancer", "infection", "Transplant operation of an organ".
    - **Residence:** this matrix indicates either the average of the matrices "urban area" and "industrial zone", either the average of the matrices "urban area" and "residential area", either the average of the matrices "rural area" and "residential area".

After classification we obtain the reduced semantic matrix with size [18*13] as illustrated in Fig. 4.

Fig. 4 Reduced matrix

We used the reduction to optimize the complexity. With the reduction will not lose any information.

- **Convolution Layer**
  In this layer we have 3 region size (5, 6, 7) and 2 filters for each region size. So, we have six filters in the total. All the filters will scan all the matrix input with stride 1 to give us one feature maps for each filter. For each feature map we will apply the maxpooling to get one value for each feature map accordingly concatenate all the maxpooling and apply the activation function "softmax".
- **Disease Classification** Our output is two probability "probP": probability of having the disease and "probN": probability of not having the disease.

4 Validation

In the validation part, we use validation set with 490 real cases divided into 315 of the patient who have the disease and 175 who haven't. Also, we use 111 real cases for test set divided into 40 patients affected by the disease and 71 who not affected. As it is shown in Figs. 5 and 6 the accuracy for our model is 94.59% with a 5.41% error rate and the test lost 15.90%.

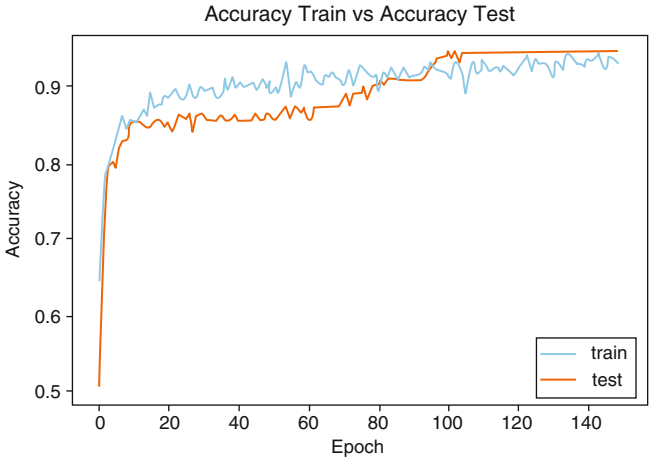

Fig. 5 Accuracy train vs accuracy test DeepLCP

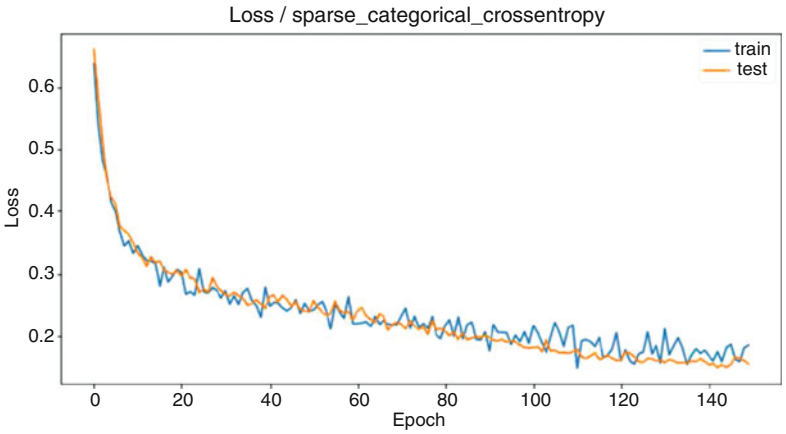

Fig. 6 Loss train vs loss test DeepLCP

5 Discussion

We tested our dataset with four machine learning algorithms:

- The **k-nearest neighbors (KNN)**: it provides a 86.48% precision rate and a 13.52% Error rate.
- The **Decision Tree algorithm**: it returns a 93.69% precision rate and a 6.31% error rate.
- The **Random Forest**: it results a 91.89% precision rate and a 8.11% error rate.
- The **Artificial Neural Network (ANN)**: it provides a 85.59% precision rate and a 14.41% error rate.

Based on these results we find that our "DeepLCP" model provides the best accuracy rate and the lowest error rate.

6 Conclusion

In this article we present a new model for the prevention of lung cancer. Our model named "DeepLCP" is a combination of NLP and CNN. In the NLP part we use semantic transformation rules. the accuracy of validation test is 94.5% which confirm that our model give an efficient result.

References

1. Otter, D.W., et al.: A survey of the usages of deep learning in natural language processing. CoRR, abs/1807.10854 (2018)
2. Towards Datascience: https://towardsdatascience.com/natural-language-processing-nlp-for-machine-learning-d44498845d5b. Last accessed 13 June 2019
3. Analytics Vidhya: https://www.analyticsvidhya.com/blog/2018/12/guide-convolutional-neural-network-cnn/. Last accessed 14 June 2019
4. Pattanayak, S.: Pro Deep Learning with TensorFlow: A Mathematical Approach to Advanced Artificial Intelligence in Python. Apress, Berkeley (2018)
5. Gruetzemacher, R., Gupta, A.: Using deep learning for pulmonary nodule detection & diagnosis. In: AMCIS, Association for Information Systems, San Diego (2016)
6. Esteva, A., et al.: Dermatologist-level classification of skin cancer with deep neural networks. Nature **542**, 115–118 (2017)
7. Michael Park, H., Monahan, C.: Genetic deep learning for lung cancer screening. Innovation Dx Inc. 23 Aug (2017)
8. Yang, D., Powell, C.A., et al.: Deep convolutional neutral networks based artificial intelligence system for pulmonary nodule detection and diagnosis in United States and Chinese dataset. In: ATS, San Diego (2018)
9. Bychkov, D., et al.: Deep learning based tissue analysis predicts outcome in colorectal cancer. In: Scientific Reports, Feb (2018)
10. Baker, S., et al.: Cancer hallmark text classification using convolutional neural networks. In: BioTxtM@COLING (2016)
11. John, X., et al.: Deep learning for automated extraction of primary sites from cancer pathology reports. IEEE J. Biomed. Health Inf. **22**, 244–251 (2018)
12. Zhang, Y., Wallace, A.: Sensitivity analysis of (and practitioners' guide to) convolutional neural networks for sentence classification. arXiv preprint arXiv:1510.03820 (2015)
13. Dataanalytics Post: https://dataanalyticspost.com/Lexique/word2vec/. Last accessed 14 June 2019
14. Bowen, J.P.: Formal Specification and Documentation Using Z: A Case Study Approach. International Thomson Publishing, London/Boston, June (2003)

A Sleep Monitoring Method with EEG Signals

Yessrine Abichou, Siwar Chaabene, and Lotfi Chaari

1 Introduction

One of the crucial issues in the development of cognitive and clinical neuroscience is undoubtedly the ability to track over time and to precisely locate human brain activity. Sleep detection is one of the most active research topics in biomedical signal processing. This involves the acquisition and recording of a set of physiological signals, followed by visual analysis to establish the diagnosis. Assessing sleep disorders is also an important step to prevent further physical and mental complications. This could be done for instance to predict and prevent sleep apnea.

Several methods for sleep exploration have been proposed during the last decades. The basic examination, called polysomnography, allows to group the recording of several variables by mentioning for example the electrical activity of the brain, the activity of the muscles of the face and the chin, sometimes muscles legs, the activity of eyeballs and also the electrical activity of the heart.

This study is mainly based on the electroencephalogram (EEG) signal which presents the result obtained by a recording of electrical signals transmitted by means of electrodes applied on the scalp. This recording is a potential difference between the electrodes excited by the neurons.

In 2009 with Li et al. [7], the EEG signals are analyzed with the Hilbert-Huang transformation, the energy frequency distribution of the EEG is used as a function

Y. Abichou · S. Chaabene
MIRACL laboratoty, University of Sfax, Sfax, Tunisia

Digital Research Centre of Sfax, Sfax, Tunisia

L. Chaari (✉)
University of Toulouse, IRIT-ENSEEIHT, Toulouse, France
e-mail: lotfi.chaari@enseeiht.fr; lotfi.chaari@toulouse-inp.fr

L. Chaari (ed.), *Digital Health in Focus of Predictive, Preventive and Personalised Medicine*, Advances in Predictive, Preventive and Personalised Medicine 12,
https://doi.org/10.1007/978-3-030-49815-3_4

parameter for each sleep stage. This method gave a classification rate of 81.7% using the k nearest neighbor method. In 2010, Tagluk et al. [9] used frequency analysis, specifically using the power spectral density. An artificial neural network technique is the used for classification. This system gave a recognition rate up to 76.8%.

In 2012, Fraiwan et al. [2] used Hilbert transformations and continuous wavelet transformations to extract the characteristics with an accuracy rate of 83%, relying on a random forest classification method.

In 2013, Lajnef et al. [6] used variance, Skewness, Kurtosis and energy permutations as features, and the SVM classification method was considered achieving an accuracy level of 92%. The performance of the method was evaluated using polysomnographic data of 15 subjects (electroencephalogram (EEG), electro oculography (EOG) and electromyogram (EMG) recordings.

In 2015 Kayikcioglu et al. [5] reached a 91% classification rate with LPC (Partial Least Squares Regression) using an auto-regressive method. The results were compared with those of other classifiers, such as k nearest neighbor (k-NN), linear discriminant (LDC) and Bayes classifiers.

More recently, Alickovic et al. [1] used the decomposition based on iterative filtering with SVM as classifier. This system achieved a classification rate of 91.1%.

In this work, a feature-based method for EEG data classification is proposed with additional features and a dimension reduction strategy.

The rest of this paper is organized as follows. Section 2 formulates the problem. The proposed method is then presented in Sect. 3, while experimental results are drawn in Sect. 4. Finally, conclusions and future work are given in Sect. 5.

2 Problem Formulation

The EEG signal is complex, its inspection gives inaccurate information; to improve its sensitivity, the plot is cut into short observation windows. Each window undergoes a mathematical analysis intended to extract quantitative parameters. In this paper,the parameters extracted from EEG signal in order to identify the recognition of the state through a study of classifications. Secondly, we go on to describe the method used in our work that specifies the performance of our research.

3 Proposed Method

The basic structure of the method proposed in this paper is given in Fig. 1. It can be seen that it has three main modules: the first is Data Preparation; the second is feature extraction; the third is dimension reduction; and finally classification. In this section, we provide detailed explanation of each module.

We performed a windowing with a frame in 2 s. Then we varied the size of the window (3 s). The best results were obtained for the size of 2 s. So we decided to

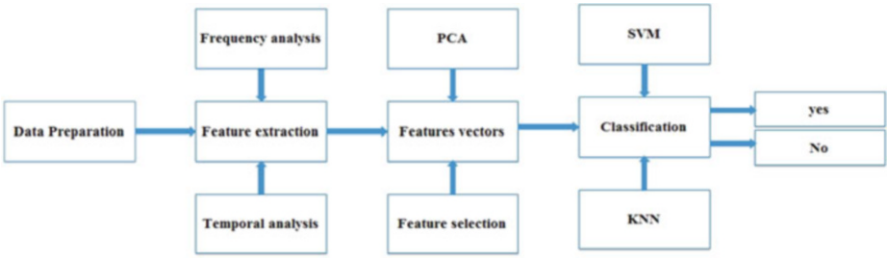

Fig. 1 Structural diagram of the proposed method for sleep monitoring

decrease the frame to have a better result we advocated to 1 and 0.5 s. Which leads to deduce that the window a second is the one that suits the most.

3.1 Feature Extraction

The main interest in signal processing is to extract as much information as possible on the temporal or frequency structure of these signals. It is therefore necessary to break down the signal on functions well localized in both time and frequency.

3.1.1 dwt

The discrete wavelet transform analysis the signal at different frequency bands with different resolutions by decomposing the signal with a rough approximation and detailed information. The basic principle of the discrete wavelet transform is to separate the signal into two components, one representing the shape of the signal, the other representing its details. The general appearance of a function is represented by its low frequencies, the details by its high frequencies.

3.1.2 Energy

The most traditional features among wavelet-based methods is the measurement of energy in each sub-band. Mathematically, it is presented as follows:

$$ED_i = \sum_{j=1}^{N} |D_{ij}|^2. \tag{1}$$

$$EA_i = \sum_{j=1}^{N} |A_{ij}|^2. \tag{2}$$

3.1.3 Shannon's Entropy

The entropy here is a reflection of the amount of information present at each sub-band, where X is a discrete scalar random variable with realizations x_1,..., x_n and the probability distribution p_1,..., p_n measure his disorder. For a source X having n symbols, a symbol i having a probability pi to appear, the entropy H of the source X is defined as:

$$H(x) = -\sum_{i=1}^{n} p_i log_2 p_i. \tag{3}$$

3.1.4 Variance

Variance is the measure of the dispersion of a set of data points around their mean value, it is defined as follows:

$$v(x) = \frac{\sum_{i=1}^{n}(x_i - \overline{x})^2}{n}. \tag{4}$$

avec $\overline{x} = \sum_{i=1}^{n} p_i x_i$ et n: total number of data points.

3.1.5 Mean

We can define the mean M of a data vector X as follows:

$$M = \frac{1}{n}\sum_{i=1}^{n} x_i. \tag{5}$$

3.1.6 Minimum

This is the minimum value of an X data vector.

3.1.7 Maximum

This is the maximum value of a data vector X.

3.1.8 Energy Ratio

Each of the brainwaves (delta, theta, alpha and beta) occupy a quantity of the energy of the EEG signal. We proceed to a quantitative study of the energetic ratios of each of the waves compared to the global energy of the signal. The energy ratio is calculated by the ratio between the wave energy (E_0) and the total energy of the signal (E_s).

$$RE = \frac{E_0}{E_s}. \tag{6}$$

3.1.9 Frequency Analysis

The frequency characteristics of a time series can be written by calculating its power spectral density (DSP).

$$DSP(v) = \lim_{N_k \to \infty} \frac{1}{2N_k+1} E(|FFT(v)|^2). \tag{7}$$

3.2 Dimension Reduction

3.2.1 PCA

Which consists of replacing the initial set of data with a new reduced set constructed from the initial set of characteristics.

3.2.2 Feature Selection

Which consists in selecting the most relevant characteristics from the dataset of the variables describing the phenomenon studied.

3.3 Classification

3.3.1 SVM

Is a binary classification method by supervised learning. This method relies on the existence of a linear classifier in an appropriate space. Since this is a two-class classification problem, this method uses a learning dataset to learn the model's parameters.

3.3.2 KNN

Is a method based on memory, which unlike other statistical methods, requires no learning. It works according to the intuitive principle that the closest objects are most likely to belong to the same category. Thus, with the k nearest neighbors method, forecasts are based on a set of prototype examples that are used to predict new data.

4 Experimental Results

4.1 Data Set

Our database is a record taken from the "Physio Bank" [3], in the form EDF "European Data Format"; EDF is a file that contains separate lines according to the samples. It can have several sampling frequencies as it can contain several signals; in our case he can present an EEG and an EOG together. This database is registered for eight Caucasian people (men and women) between the ages of 21 and 35, healthy (who do not have trouble sleeping) and without medication. The records are named sc4002e0.rec, sc4012e0.rec, sc4102e0.rec, sc4112e0.rec, st7022j0.rec, st7052j0.rec, st7121j0.rec, st7132j0.rec. These signals are recorded through the electrode FpzCz (E1), PzOz (E2) against C4-A1 and C3-A2 according to the alternative placement of the electrodes during the automatic detection of sleep. Four recordings are obtained by four volunteers during 23 h: 45 min during their normal lives, while using a modified tap tape cassette. The other four recordings lasted one night of sleep in a hospital, while using a 100 Hz sampling rate miniature telemeter with a frequency response equal to −3 dB per point, a 14-bit representation per sample, and a total noise equal to −2V p-p.

4.2 Experimental Setup

According to the exploitation of the Daubechies wavelet decomposition method (db5) we found the 5 brain waves: alpha, theta, gamma, beta, delta (please see Figs. 2 and 3).

The calculation of these parameters is done on each EEG rhythm, that is to say for each wave we will calculate the 7 features (energy, variance, maximum, minimum, average, entropy, energy ratio).

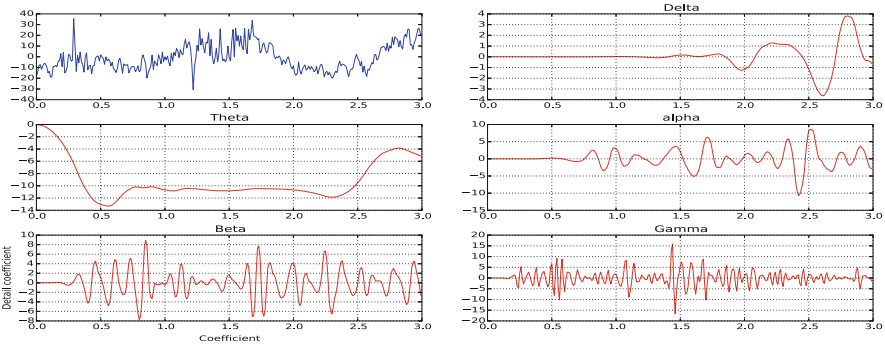

Fig. 2 Decomposition with a window of 3 s

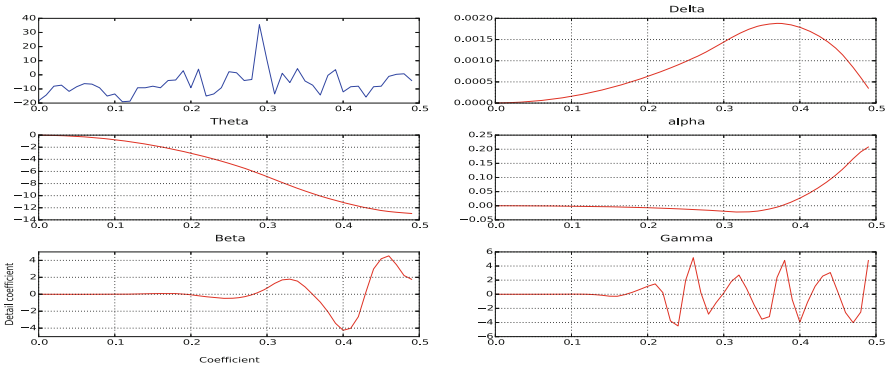

Fig. 3 Decomposition with a window of 0.5 s

Table 1 Best accuracy obtained

	OneClassSVM	KNN
Without reduction	84%	82.5%
PCA	91.5%	79.7%
SF	**93%**	88.2%

From the FFT, we calculated the DSP of our signal. We used this method to subdivide the signal into subband and we started with 2 then 3 then 4 and finally 5 bands. In order to grasp the exact choice we had to try with all the frequencies proposed in the classification.

The following table shows the results without and with reduction. This table shows that we have succeeded, on two levels of reduction, in improving the recognition rate and reducing by more the number of characteristics used. By reducing the characteristics, a small subset of examples containing only those that seem to influence the class separation capability can be selected from the training set. Our contribution comes within this framework. The proposed method makes it possible to significantly reduce the number of characteristics of the database then to make an offline learning. The results obtained show the performance of this solution using the OneClassSVM classification method with electrode 2 (Table 1).

4.3 Comparison with the Existing Methods

Our detection results are compared with those of the literature to better position our algorithm with other recent methods of sleep detection. The choice of articles to make the comparison was based on the methods used and their similarities to our algorithm (Table 2).

Table 2 Comparison of performance of previous studies

Methods	Accuracy
Li et al. [7]	81.5%
Hassan et al. [4]	87.5 %
sharma et al. [8]	90%
Kayikcioglu et al. [5]	91 %
Proposed method	93 %

5 Conclusion

This study proved that statistical features can be used with standard accuracy. This proposed methods provides convincing classification accuracy of 93% using statistical parameters of EEG signal. Future work will focus perform parallel analysis using electro oculography (EOG) and electrocardiography (ECG).

References

1. Alickovic, E., Subasi, A.: Ensemble SVM method for automatic sleep stage classification. IEEE Trans. Instrum. Meas. **67**(6), 1258–1265 (2018)
2. Fraiwan, L., Lweesy, K., Khasawneh, N., Wenz, H., Dickhaus, H.: Automated sleep stage identification system based on time–frequency analysis of a single EEG channel and random forest classifier. Comput. Methods Prog. Biomed. **108**(1), 10–19 (2012)
3. Goldberger, A.L., Amaral, L.A., Glass, L., Hausdorff, J.M., Ivanov, P.C., Mark, R.G., Mietus, J.E., Moody, G.B., Peng, C.K., Stanley, H.E.: Physiobank, physiotoolkit, and physionet: components of a new research resource for complex physiologic signals. Circulation **101**(23), e215–e220 (2000)
4. Hassan, A.R., Bashar, S.K., Bhuiyan, M.I.H.: On the classification of sleep states by means of statistical and spectral features from single channel electroencephalogram. In: 2015 International Conference on Advances in Computing, Communications and Informatics (ICACCI), pp. 2238–2243 (2015)
5. Kayikcioglu, T., Maleki, M., Eroglu, K.: Fast and accurate pls-based classification of EEG sleep using single channel data. Expert Syst. Appl. **42**(21), 7825–7830 (2015)
6. Lajnef, T., Chaibi, S., Ruby, P., Aguera, P.E., Eichenlaub, J.B., Samet, M., Kachouri, A., Jerbi, K.: Learning machines and sleeping brains: automatic sleep stage classification using decision-tree multi-class support vector machines. J. Neurosci. Methods **250**, 94–105 (2015)
7. Li, Y., Yingle, F., Gu, L., Qinye, T.: Sleep stage classification based on EEG Hilbert-Huang transform. In: 2009 4th IEEE Conference on Industrial Electronics and Applications, pp. 3676–3681 (2009)
8. Sharma, R., Pachori, R.B., Upadhyay, A.: Automatic sleep stages classification based on iterative filtering of electroencephalogram signals. Neural Comput. Appl. **28**(10), 2959–2978 (2017)
9. Tagluk, M.E., Sezgin, N., Akin, M.: Estimation of sleep stages by an artificial neural network employing EEG, EMG and EOG. J. Med. Syst. **34**(4), 717–725 (2010)

Numerical Simulation of Venous System Blood Flow for Hepatic Donor Patient and Portal Hypertension's Proposed Measurement

Safa Ben Cheikh Souguir, Raouf Fathallah, Asma Ben Abdallah, Badii Hmida, and Mohamed Hedi Bedoui

1 Introduction

Concerning hepatic blood flow, clinicians require reproducible and non-invasive methods. In clinical practice, we quote two useful non-invasive methods in hepatic flow measurement despite their known limitations such as Doppler ultrasound (US) and Phase-contrast magnetic resonance imaging (PC-MRI). However, results in the literature suggest that these methods may in some cases show diverse analysis. Furthermore, in velocity measured by US doppler, there is great errors' percentage that may reach 20% in reference to blood velocity estimation [1]. In this case, a comparative study was done in order to set the variability of parameters using these methods [2, 3].

Nowadays, Numeric simulation of blood circulation opens up predictions and perspectives for doctors in terms of performing a surgery. Virtual simulation provides useful biomechanical models for clinicians in different blood flow systems. However, like any technic or method, the virtual simulation will be used with well-defined conditions in order to be verified in terms of capability and performance.

Little work has been done to study blood flow in the portal vein. The work reported in the literature has mentioned the hemodynamic simulation of blood flow in different organs such as the cerebral arterial circle [4], the carotids [5]

S. B. C. Souguir (✉)
National Engineering School of Sousse, Sousse, Tunisia

Laboratory Technology and Medical Imaging, Monastir, Tunisia

A. B. Abdallah · M. H. Bedoui
Laboratory Technology and Medical Imaging, Monastir, Tunisia

B. Hmida
Medical Imaging Services, CHU Fattouma Bourguiba, Monastir, Tunisia

L. Chaari (ed.), *Digital Health in Focus of Predictive, Preventive and Personalised Medicine*, Advances in Predictive, Preventive and Personalised Medicine 12,
https://doi.org/10.1007/978-3-030-49815-3_5

and cardiovascular system [6] etc. The numerical simulation of venous system was rarely approached due to its complex geometry as well as its difference of elasticity with respect to the arterial system.

The purposes of this research will focus mainly on studying the normal venous blood circulation in the liver of a female donor through the determination of blood's pressure and velocity by the chosen hypothesis and condition, validating results, understanding the phenomenon of portal hypertension [7] that can be seen in several pathologies such as cirrhosis or thrombosis, as well as proposing portal pressure's measure related to a young receiver patient before and after chirurgical intervention.

2 Methods

We propose to simulate the 3D blood flow of the venous system based on 2D database. Our approach is as follows: We segmented series of anatomical images about the venous system, along with a 3D reconstruction extracting iso-surfaces. Subsequently, from the generated 3D triangular mesh, we modelled the volume of our structure by the "Reverse Engineering" method. Finally, we prepared a CFD study Fig. 1.

2.1 Segmentation and 3D Reconstruction

The anatomical structure was obtained from native cuts using a thoraco-abdominopelvic CT scan of liver donor patient before the chirurgical inter-

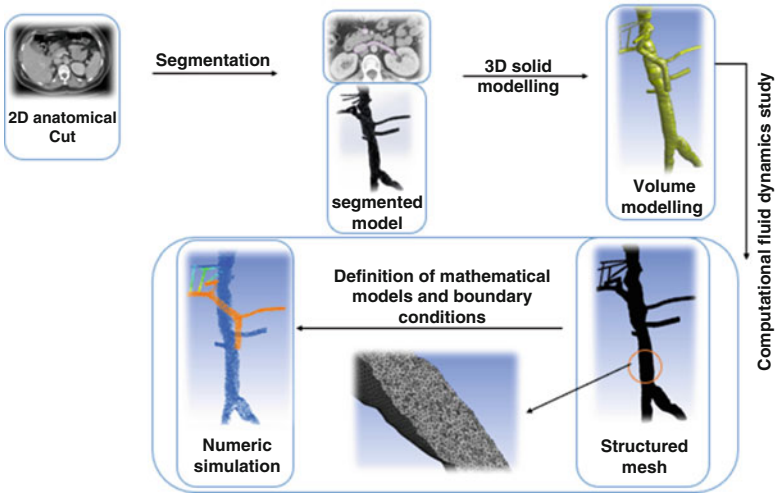

Fig. 1 Methods and approach

vention. We identified different veins and segmented the 2D anatomical cuts (0.7 × 0.7 × 1.25 mm) after injection of the contrast medium. Indeed, for each anatomical section we surround the concerned veins and control the appearance of the following line using AMIRA software. The segmentation has been validated by radiologist experts.

2.2 3D Volume Modelling

the next step is to prepare a volume model through the Reverse Engineering method which used to generate a three-dimensional digital model from 2D data [8]. This method consists of designing a series of parallel curves relating to the generated 3D triangular mesh and connecting them with surface sections in order to obtain a closed surface. It is noteworthy to mention; this surface model has been transformed into a volume model by filling the material.

2.3 CFD Study

In this section, we performed a CFD study consisting of the following steps:

2.3.1 Finite Elements Mesh

In CFD analysis, the flow domain is subdivided into smaller subdomains. For this geometry, a structured mesh has been conducted in which domain has been discretized into purely tetrahedral elements.

This figure depicts a mesh quality study about the size and number of geometric primitives which forms the tetrahedral mesh after choosing one of these five meshes composed of 2,138,653 elements from which the pressure is almost constant. This volume mesh allowed us to have a reliable result along with optimizing the calculation time Fig. 2.

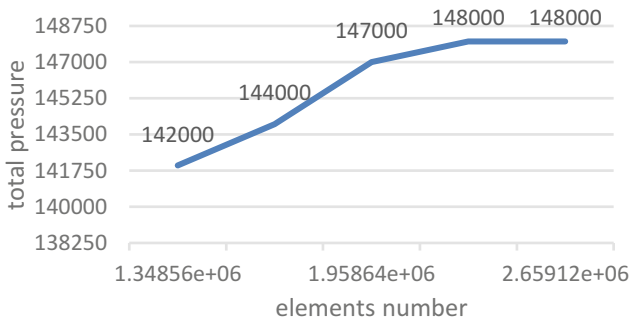

Fig. 2 Pressure variation according to the number of elements

2.3.2 Parameter Definition: Mathematical Model and Boundary Conditions

The flow is assumed to be isothermal so the energy equations have been neglected, while the Navier Stokes equations of continuity and momentum equations 1 and 2 have been solved numerically under stable conditions and for an incompressible fluid.

$$\frac{\partial \rho}{\partial t} + div \rho \vec{V} = 0 \tag{1}$$

$$\rho \frac{\partial \vec{V}}{\partial t} + \bar{=}grad \vec{V}.\rho \vec{V} = \rho \vec{F} - \vec{grad}\, p + \mu \left(\Delta \vec{V} + \vec{grad}\, div \vec{V} \right) \tag{2}$$

V: Vector fluid velocity, p: momentum, F: External forces exerted on the fluid, ρ: density of the fluid.

We use the hypothesis of a perfectly rigid wall. Blood is a non-Newtonian fluid its viscosity depends on mechanical shear stress. Several models can describe this behaviour between mechanical stress and deformation. Recently, comparative research has been conducted in order to identify the most useful model within blood circulation. Power Law model was recommended which defined by the following Eq. (3) and parameters [9].

$$\mu = \mu_0 (\dot{\gamma})^{n-1} \tag{3}$$

γ: Shear rate, n: power-law index, $\mu_0$initial Viscosity.

Blood density usually depends on the sex and age group of human beings. We took on average density equal to 1060 kg / m3. The flow is defined laminar since the Reynolds coefficient Re (4) does not exceed 1500.

$$R_e = \frac{\rho V D}{\mu} \tag{4}$$

ρ: density (kg.m-3), μ: Dynamic viscosity, V: Characteristic velocity (m / s), D: Largest vein diameter (m).

Due to the complexity and orientation of venous system's shapes, the flow must be considered as turbulent. That is why we examined both laminar and turbulent cases. Although there are numerous turbulence models, we used two turbulence models named K Epsilon and K Omega [10].

In addition, we know that the definition of boundary conditions plays an indispensable role in the numeric experience. We have affected the entry velocities of the veins that feed the liver and vena cava. In CFD study, the input velocity values are obtained from in vivo measurement and are specified in Table 1. For the output values, we used a flow ratio of 1 at the level of the right atrium.

Table 1 Boundary Conditions

Veins	Velocity	Diameter
Left iliac vein	14 (cm/s)	13 (mm)
Right iliac vein	14 (cm/s)	13 (mm)
Left renal vein	15 (cm/s)	8 (mm)
Right renal vein	15 (cm/s)	8 (mm)
Superior mesenteric vein Splenic vein	18 (cm/s) 16 (cm/s)	11 (mm) 7 (mm)

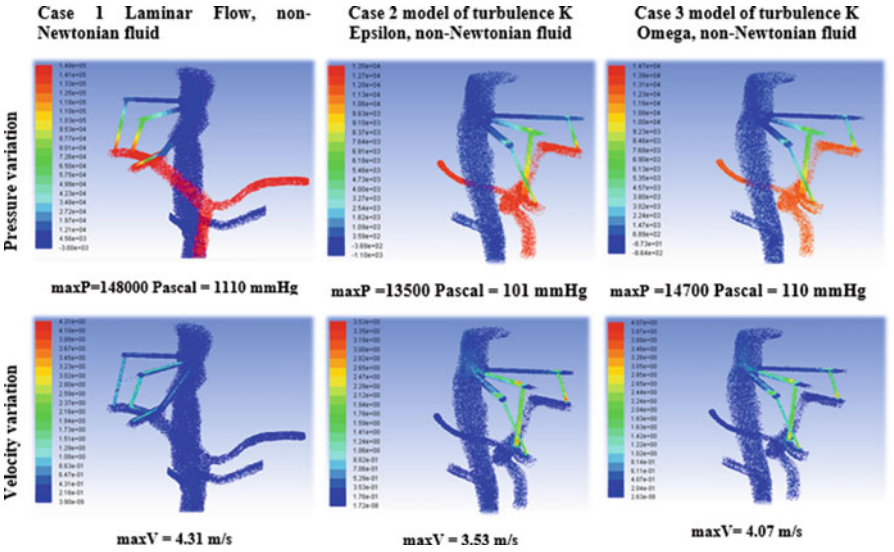

Fig. 3 Results of virtual simulation

3 Results and Conclusions

Regarding the figure below, it is concluded that the laminar model diverged from measured data. In contrast, turbulence models provide an accurate result. Indeed, virtual velocity in the portal vein is 20 cm/s, this result shows a significant correlation with the result measured by Us Doppler which is between 15 and 20 cm/s. Maximum pressure is concentrated at the liver while maximum velocity appears in capillaries situated between sus-hepatics veins and portal branches. Moreover, this research opens perspectives on studying the phenomena explaining portal hypertension through a mechanical model starting by data acquisition, segmentation, 3D reconstruction and numerical simulation. Indeed, there is a growing need for clinicians to detect portal hypertension by measuring hepatic pressure gradient using numeric simulation. Furthermore, we are going to simulate a hepatic pressure gradient for a receiver patient suffering from portal hypertension after and before chirurgical interventions, and to determinate wall shear stress in order to predict variceal bleeding risk (Fig. 3).

References

1. Carlisle, K.M., Halliwell, M., Read, A.E., Wells, P.N.: Estimation of total hepatic blood flow by duplex ultrasound. Gut. **33**, 92–97 (1992). https://doi.org/10.1136/gut.33.1.92
2. Hepatic vascular flow measurements by phase contrast MRI and doppler echography: A comparative and reproducibility study – Yzet – 2010 – J. Magnet. Reson. Imaging – Wiley Online Library. https://onlinelibrary.wiley.com/doi/full/10.1002/jmri.22079. Accessed 9 Jun 2019
3. Annet, L., Materne, R., Danse, E., et al.: Hepatic flow parameters measured with MR imaging and Doppler US: correlations with degree of cirrhosis and portal hypertension. Radiology. **229**, 409–414 (2003). https://doi.org/10.1148/radiol.2292021128
4. Reorowicz, P., Obidowski, D., Klosinski, P., et al.: Numerical simulations of the blood flow in the patient-specific arterial cerebral circle region. J. Biomech. **47**, 1642–1651 (2014). https://doi.org/10.1016/j.jbiomech.2014.02.039
5. Lancellotti, R.M., Vergara, C., Valdettaro, L., et al.: Large eddy simulations for blood dynamics in realistic stenotic carotids. Int. J. Numer. Methods Biomed. Eng. **33**, e2868 (2017). https://doi.org/10.1002/cnm.2868
6. Morris, P.D., Narracott, A., von Tengg-Kobligk, H., et al.: Computational fluid dynamics modelling in cardiovascular medicine. Heart. **102**, 18–28 (2016). https://doi.org/10.1136/heartjnl-2015-308044
7. Lebrec, D., Moreau, R.: Hypertension portale : avancées et perspectives. Gastroenterol. Clin. Biol. **33**, 799–810 (2009). https://doi.org/10.1016/j.gcb.2009.04.001
8. Yu C-C., & Cheng, H-Y.: Study of biomechanical behavior on temporomandibular joint during jaw movement using reverse engineering 3D technology (2018). https://www.ingentaconnect.com/content/asp/jbte/2018/00000008/00000012/art00012. Accessed 20 Oct 2019
9. Johnston, B.M., Johnston, P.R., Corney, S., Kilpatrick, D.: Non-Newtonian blood flow in human right coronary arteries: steady state simulations. J. Biomech. **37**, 709–720 (2004). https://doi.org/10.1016/j.jbiomech.2003.09.016
10. Zhang, J., Zhang, P., Fraser, K.H., et al.: Comparison and experimental validation of fluid dynamic numerical models for a clinical ventricular assist device. Artif. Organs. **37**, 380–389 (2013). https://doi.org/10.1111/j.1525-1594.2012.01576.x

Medical Decision-Making: Incompressible Blood Flow Simulation for the Coronary Artery and Bifurcation Stenosis with CFD Module

Houneida Sakly, Mourad Said, and Moncef Tagina

1 Background

Recently, cardiovascular disease is considered dramatically increased. The common type of death that is mainly due to heart disease or stroke, which is caused by the accumulation of plaques on the endothelial walls of the coronary arteries [1]. The coronary artery disease (CAD) induces to a reduction in the oxygen level at the myocardium and this has been related to the antecedents of cardiovascular disease such as myocardial infarction, stroke and unstable angina [2]. Despite the diversification of risk factors, in particular high cholesterol, diabetes and hypertension, being of a systemic nature, the plaques are located at specific sites of the coronary artery where an endothelial shear disorder occurs [3–5]. In recent years, the additional explanation that has been shown for plaque formation is blood pressure/shear stress [6, 7].

The appearance of atherosclerosis that is based on observation plays a role in the identification of blood behavior. According to the distribution of vascular inflammation and plaques near the lateral branches or arterial stenosis, the blood trajectory n It is not uniform and at the slightest curvature of curvatures where blood flow is relatively low [8, 9]. The inflow of blood flow on the vessel wall is caused by shear stress is reflected via the behavior of endothelial cells. The shear stress leads to shear deformation of the cells and subsequently the inflammatory component and the progression of the plaque [10].

H. Sakly (✉) · M. Tagina
COSMOS Laboratory -National Institute of Computer Sciences – Campus University of Mannouba, Mannouba, Tunisia
e-mail: houneida.sakly@esiee.fr

M. Said
Radiology and Medical Imaging Unit, International Center Carthage Medical, Monastir, Tunisia

L. Chaari (ed.), *Digital Health in Focus of Predictive, Preventive and Personalised Medicine*, Advances in Predictive, Preventive and Personalised Medicine 12,
https://doi.org/10.1007/978-3-030-49815-3_6

The main objective in our study is to analyze the impact of CFD modules on a 3D artery model for a blood flow of normal physical characteristic and detect if there are anomalies via velocity value study and pressure.

2 Related Works

The detection of coronary stenosis is crucial for decision making in coronary revascularization. With the advancement of digital fluid dynamics (CFD), flow accuracy is limited due to the adopted modeling approach. To overcome this problem, a new non-invasive method based on CFD is proposed [11]. The study in [12] focuses on examining the effects of hyperemic flow, such as velocity, shear wall in 3D coronary artery models with and without stenosis on the hydrodynamic parameters. 3D coronary artery models suffer from a > 50% shrinkage of the light surface to simulate the hyperemic flow condition. In contrast, the decrease in pressure was found downstream of the stenosis relative to the coronary artery without stenosis. The analysis provides a view of the distribution of shear stress and pressure drop across the walls to understand the effect of hyperemic flow under both conditions. The research developed in [13] shows the effectiveness of 3D modeling of the artery on the Coronary CT Angiography-derived Fractional Flow Reserve via the Machine Learning Algorithm versus Computational Fluid Dynamics technique. The severity of the stenosis is assessed relative to invasive angiography and angiographic stenosis and does not necessarily apply with hemodynamic accuracy when the fractional flow reserve is used as a reference. In this context, Machine Learning algorithms improve the performance of CTA by correctly reclassifying hemodynamically no significant stenosis and CFD-based CT [14]. The study of the correlation between left coronary bifurcation angle and coronary stenosis as assessed by coronary angiography coronary angiography (CCTA) analysis generated by digital fluid dynamics (CFD) [15]. MV *et al* [16] proposes a reconstruction of the right coronary artery from the angiogram of a patient. The flow analyzes were performed using the Digital Fluid Dynamics (CFD) method focusing on the geometry of the stenosis characterized by areas of stasis, multidirectional velocity, and high wall shear stress. A clinical review was proposed by JM *et al* [1] for the prognostic indications for quantifying the severity of coronary artery disease and invasive and non-invasive imaging technologies to quantify the anatomical parameters of coronary stenosis. The application of image-based CFD simulation techniques [17, 18] to elucidate the effects of hemodynamics in vascular physiopathology on the initialization and progression of coronary artery disease. At this stage Blood flow presents the key for localization and progression of coronary heart disease [19]. CFD simulation based on 3D luminal reconstructions is used to analyze local flow fields and flow profile due to changes in vascular geometry. It helps to identify the risk factors for the development of coronary heart disease [20].

2.1 Methods and Materials

A 3D model of the artery has been reconstructed with a geometry that contains 4 nodes, 6 edges, 4 faces. The Hex-dominant algorithm for only CFD module has been adopted with internal meshing mode and moderate finesses. The Blood-type fluid parameterization was set with a Newtonian model viscosity, (ν) Kinematic viscosity = 0.00004 m^2/s, (ρ) Density = 1056 kg/m^3. A second 3D for this bifurcation model is composed of two nodes, 6 edges, 6 faces, 1 volumes. The mesh was generated with Max global cells = 100,000,000, Resolve feature angle = 30, Solver iterations = 150, Relax iterations = eight. Therefore, the boundary conditions is defined as follows: Pressure inlet = 1184 (Pa), the turbulence kinetic energy = 0.00375 (m^2/s^2) and the specific dissipation rate = 3.375 (1/s) for the blood fluid.

3 CFD Studies on Coronary Artery Disease

In order to predict the flow field, particle transport and related phenomena in the region of interest, the numerical methods are used by computational fluid dynamics to solve the set of main equations (continuity and Navier-Stokes equations) for blood flow). The CFD procedure includes the pre-processing phase, which essentially contains the construction of the geometry (artery) to represent the domain of interest, discretization of the domain with meshes as well as the description of the physical model and the boundary conditions. The post-processing part is dedicated for the presentation of the results and the numerical resolution of the equations. The coronary arteries are very curved and are mobile and deformable; this is why the flow study is considered a hard task which leads to in-depth studies on CFD to analyze coronary artery disease in recent decades. To minimize the numerical diffusion and to reduce the number of elements, the generation of the coronary artery model consists of defining the fluid and structural domains that are meshed with hexahedral cells.

4 Results and Discussion

4.1 Dedicated for Coronary Artery Analysis

A model of coronary stenosis acquired with CT with a maximum diameter 3.27 mm, minimum diameter 1.08 mm, length 29.66 mm, and a main tortuosity 0.11 mm presented in Fig. 1a was selected. The reconstruction of the 3D model was generated in Fig. 1b.

In order to minimize the numerical diffusion and to reduce the number of elements we adopted the geometry of the artery in Fig. 2. For the generation of

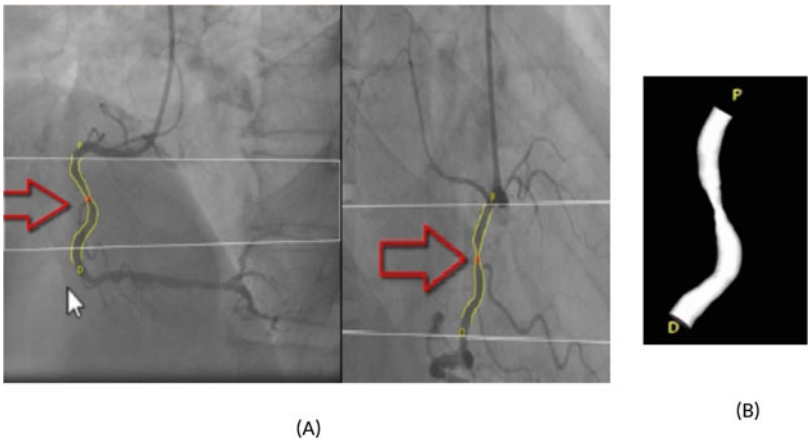

Fig. 1 Reconstruction of the 3D coronary artery model

Fig. 2 Model of the artery in 3D

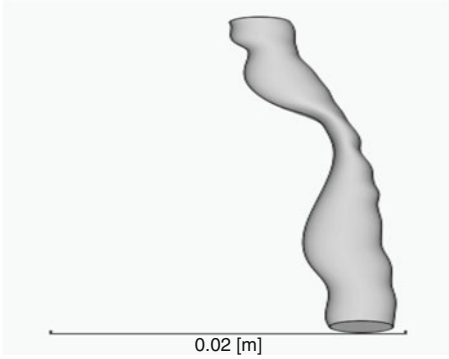

the model of coronary artery, the fluid and structural domains are in mesh with the hexahedral cells.

The next step is to define the meshing mode. We have used an internal meshing, which is typically used for pipe flow and valves. It will place the mesh inside the body and attempt to generate multiregional and will surround the materiel point and extend until the boundaries of the artery as shown in Fig. 3.

The mesh quality are depicted in Table. 1 as follows after finishing parallel processing:

Due to the variation of the blood flow with the cardiac cycle, the flow in the coronary artery is unstable. The inflow and outflow conditions allow the observation of the hemodynamic changes of the arterial system, including the coronary artery. Therefore, the boundary conditions is defined as follows: velocity inlet and outlet = 0.2 m/s and arterial pressure = 76 mmHg in the diastole phase [21]. The fluid solver completed the parallel computation for execution time = 318.52 s and ClockTime = 340 s and the residual simulation is presented as follows in Fig. 4.

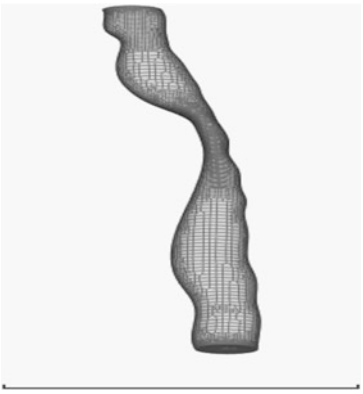

Fig. 3 Mech of the artery

Table 1 Mesh quality metrics

Mesh quality metrics	
Median	1.043005289846296
Min	1.0000000202514494
Max	59.82625634572443
Average	2.7749034006189257
Standard deviation	3.3558916335140054

0-th percentile: 1.0000000202514494
20-th percentile: 1.006279489227181
40-th percentile: 1.0199218383015278
60-th percentile: 1.1554712432086376
80-th percentile: 6.693254767354305
100-th percentile: 59.82625634572443

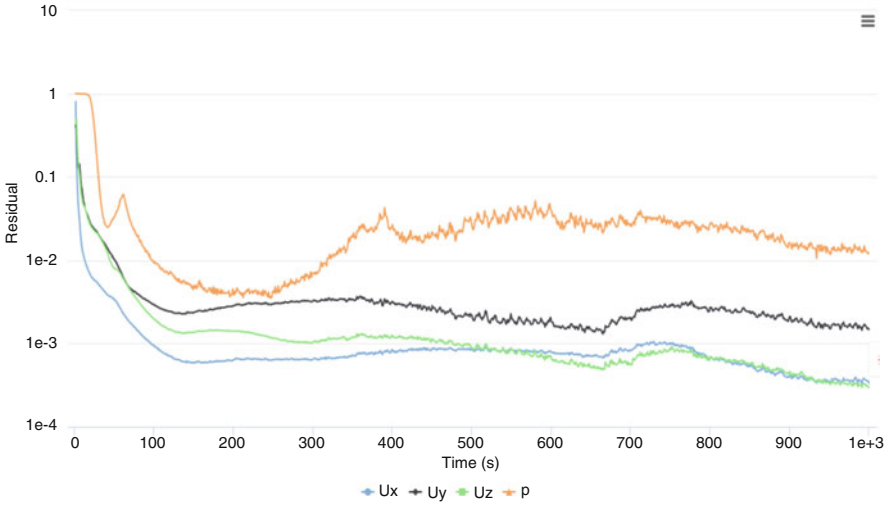

Fig. 4 The residual simulation

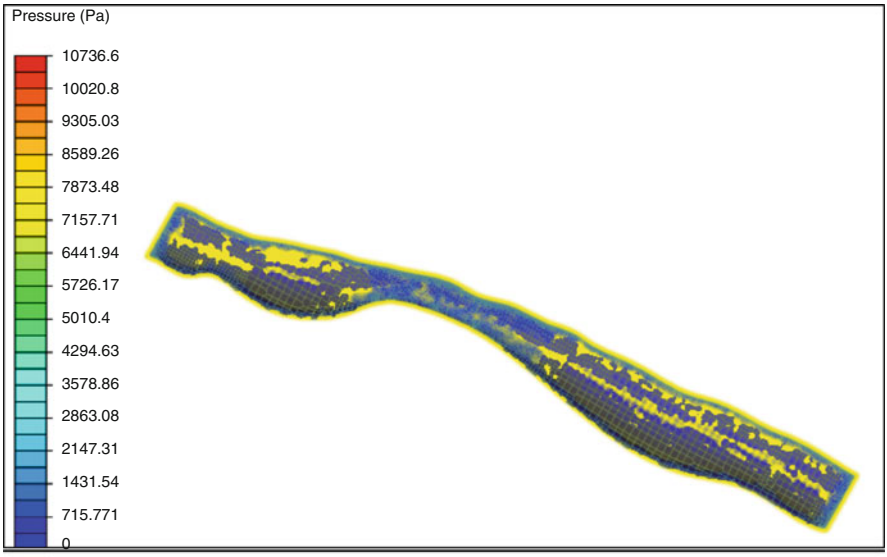

Fig. 5 Simulation of the pressure

The inlet and outlet boundary conditions are based on a physiological flow rate and pressure of the aorta. The average blood flow in the left coronary artery is estimated to be about 57 ml / min, reaching a maximum of 105 ml/min during the diastolic phase according to average human coronary blood flow data that are available in the literature [22–24]. A flow simulation is conducted over a time-span of several cardiac cycles, which are represented by time steps. The time steps can be divided into a number of coupling iterations, with each time step converged to a residual target of less than 1×10^{-4} by approximately 100 iterations. A total of 600 time steps are required to achieve satisfactory convergence for fluid simulation when all velocity component changes from iteration to iteration are less than 10^{-6} [25, 26]. The solution field simulation shows a decrease in pressure as well as the velocity value in the stenotic segment as shown in Figs. 5 and 6.

4.2 Dedicated Bifurcation Analysis

In a research setting, coronary arterial analysis (QCA) is used after coronary angiography or intervention to evaluate the effectiveness of treatments such as ballooning, stenting, or drug therapy. For coronary device studies, QCA is performed on images acquired before treatment, immediately after treatment and follow-up. The main dedicated laboratories usually perform the analysis for independent analysis. The most important search parameters, calculated using QCA, are: the acute luminal gain; MLD which gives insights on the acute efficacy of the device and is defined as

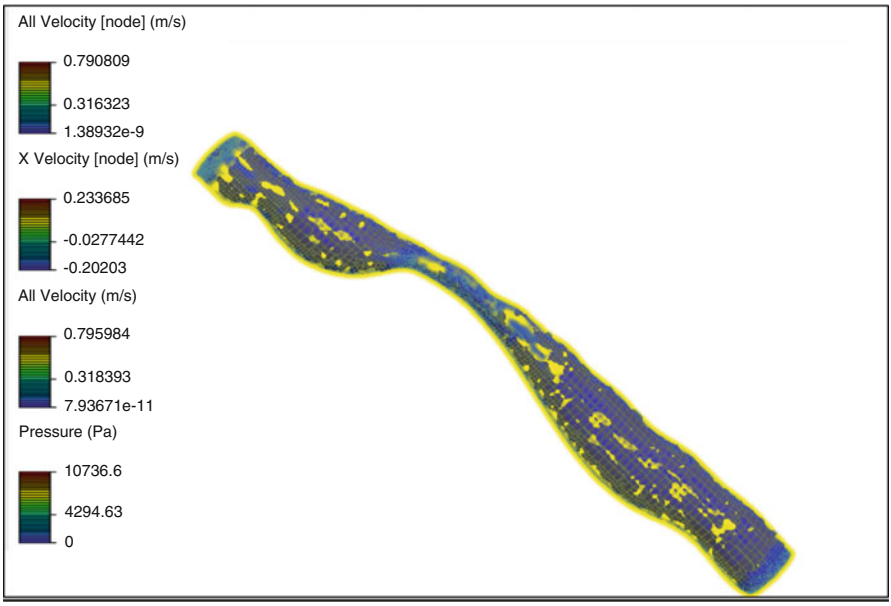

Fig. 6 Simulation of the velocity

post-procedural, the luminal loss which is the estimator for restenosis and defined as post-procedural MLD and the binary angiographic restenosis which is the incidence of percent diameter stenosis>50% [27].

By adopting the same methodology for the conception of coronary artery QCA offers a dedicated bifurcation analysis option to overcome the major challenges in quantifying bifurcation lesions as seen in Fig. 7:

The processed model is a pathological case with occlusion 60%. A second 3D for this bifurcation model is composed of two nodes, 6 edges, 6 faces, 1 volumes. The mesh was generated with Max global cells = 100,000,000, Resolve feature angle = 30, Solver iterations = 150, Relax iterations = eight. Therefore, the boundary conditions is defined as follows: Pressure inlet = 1184 (Pa), the turbulence kinetic energy = 0.00375 (m^2/s^2) and the specific dissipation rate = 3.375 (1/s) for the blood fluid. The final processing of the Solver finished with the initial residual = 8.49079723516e-07, Final Residuel = 8.49079723516e-07, average solving K: 7.12500637921e-05, Execution Time = 1923.11 s and Clock Time = 2075 s as showed in Fig. 8.

The results of analysis of the arterial bifurcation with the CFD modules represent a considerable advantage, because now, for these cases also, the previous and subsequent data can be compared and these patients can be included. Due to blood reflux in the stenotic segment, velocity as well as pressure take up significantly negative values, which may give indications for detecting the position of the stenosis as indicated in Fig. 9.

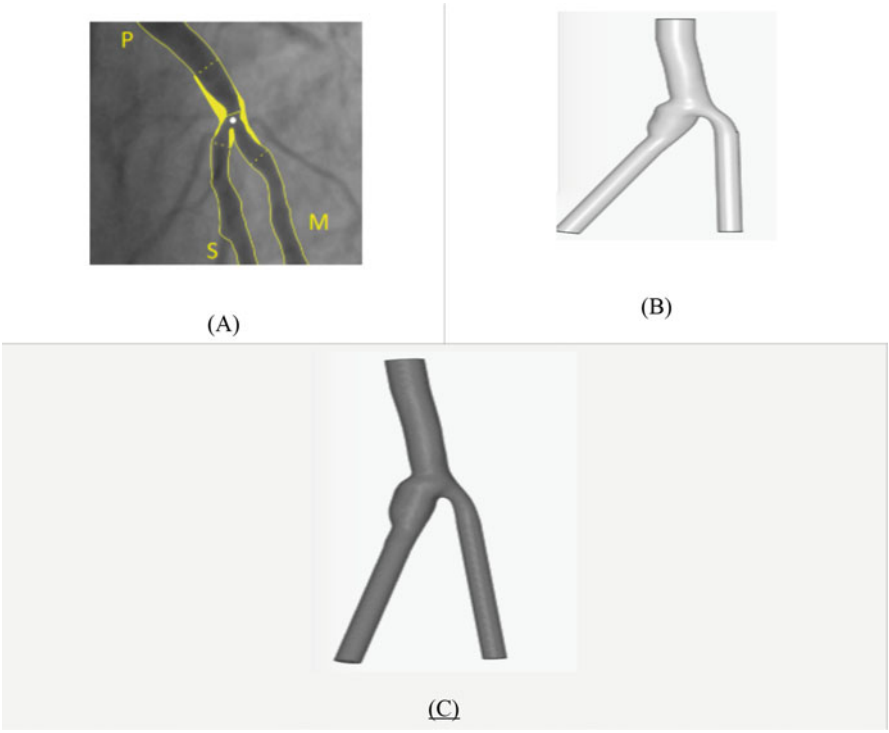

Fig. 7 (**a**) Reconstruction of the 3D bifurcation model;(**b**) Model of the bifurcation in 3D; (**c**) Mech of the bifurcation

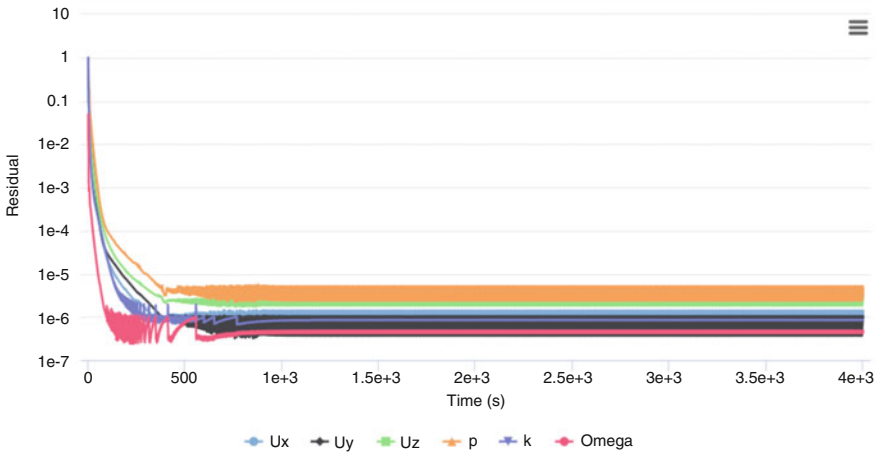

Fig. 8 Convergence plot of the solution

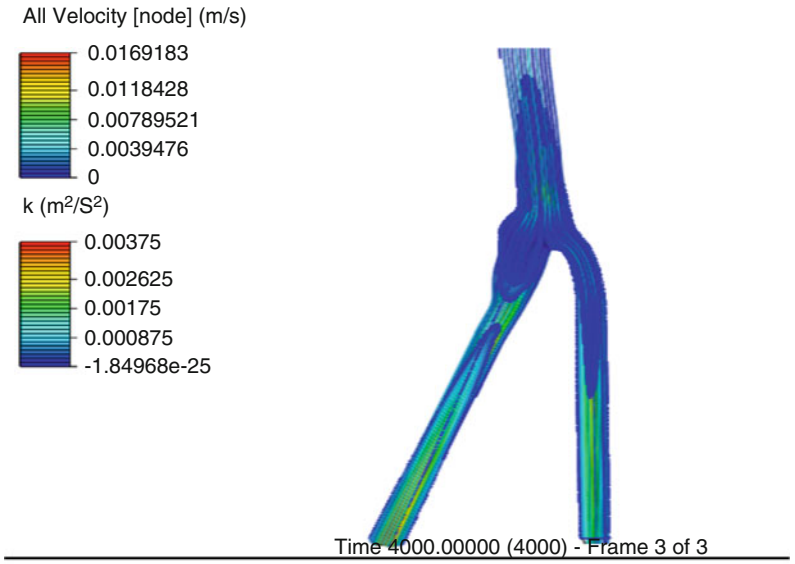

(a)

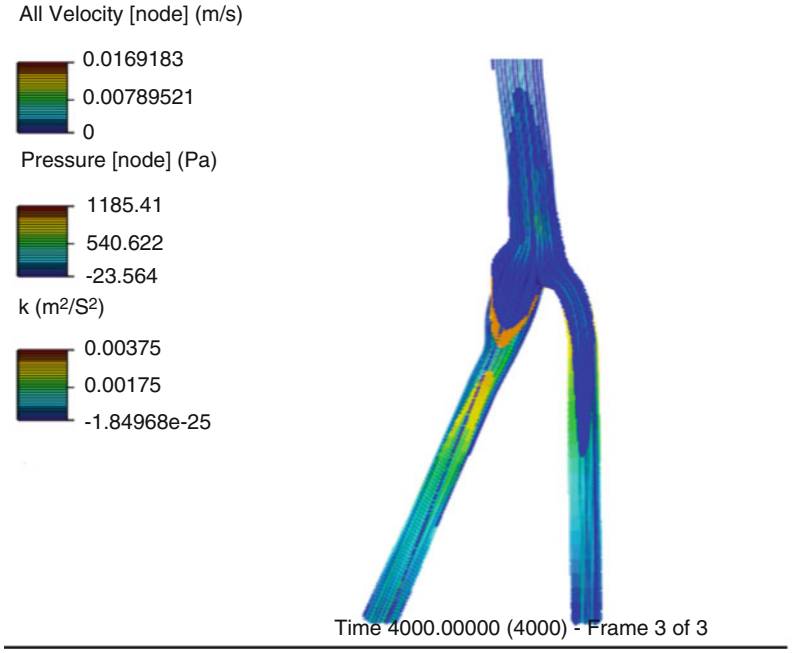

(b)

Fig. 9 (**a**) simulation of the velocity (**b**) simulation of the pressure

5 Conclusion

In summary, promising results have been depicted with the use of CFD for the diagnosis of coronary artery disease. With the advancement of CFD methods and image processing techniques, the detection of additional indications for coronary heart disease will be elucidated using specific CFD applications [28–31].

References

1. Zhang, J.-M., et al.: Perspective on CFD studies of coronary artery disease lesions and hemodynamics: a review. Int. J. Numer. Methods Biomed. Eng. **30**(6), 659–680 (2014)
2. Heitzer, T., Schlinzig, T., Krohn, K., Meinertz, T., Münzel, T.: Endothelial dysfunction, oxidative stress, and risk of cardiovascular events in patients with coronary artery disease. Circulation. **104**(22), 2673–2678 (2001)
3. Caro, C.G., Fitz-Gerald, J.M., Schroter, R.C.: Arterial wall shear and distribution of early atheroma in man. Nature. **223**(5211), 1159–1160 (1969)
4. Friedman, M.H., Hutchins, G.M., Bargeron, C.B., Deters, O.J., Mark, F.F.: Correlation between intimal thickness and fluid shear in human arteries. Atherosclerosis. **39**(3), 425–436 (1981)
5. Lutz, R.J., Cannon, J.N., Bischoff, K.B., Dedrick, R.L., Stiles, R.K., Fry, D.L.: Wall shear stress distribution in a model canine artery during steady flow. Circ. Res. **41**(3), 391–399 (1977)
6. Shaaban, A.M., Duerinckx, A.J.: Wall shear stress and early atherosclerosis: a review. AJR Am. J. Roentgenol. **174**(6), 1657–1665 (2000)
7. Wang, Y., et al.: High shear stress induces atherosclerotic vulnerable plaque formation through angiogenesis. Regen. Biomater. **3**(4), 257–267 (2016)
8. Davies, P.F., Polacek, D.C., Shi, C., Helmke, B.P.: The convergence of haemodynamics, genomics, and endothelial structure in studies of the focal origin of atherosclerosis. Biorheology. **39**(3–4), 299–306 (2002)
9. Chaichana, T., Sun, Z., Jewkes, J.: Computation of hemodynamics in the left coronary artery with variable angulations. J. Biomech. **44**(10), 1869–1878 (2011)
10. Helderman, F., et al.: Effect of shear stress on vascular inflammation and plaque development. Curr. Opin. Lipidol. **18**(5), 527–533 (2007)
11. Xie, X., Zheng, M., Wen, D., Li, Y., Xie, S.: A new CFD based non-invasive method for functional diagnosis of coronary stenosis. Biomed. Eng. Online. **17**(1), 36 (2018)
12. Kamangar, S., et al.: Influence of stenosis on hemodynamic parameters in the realistic left coronary artery under hyperemic conditions. Comput. Methods Biomech. Biomed. Engin. **20**(4), 365–372 (2017)
13. Tesche, C., et al.: Coronary CT angiography-derived fractional flow reserve: Machine learning algorithm versus computational fluid dynamics modeling. Radiology. **288**(1), 64–72 (2018)
14. Coenen, A., et al.: Diagnostic accuracy of a Machine-learning approach to coronary computed tomographic angiography-based fractional flow reserve: result from the MACHINE consortium. Circ. Cardiovasc. Imaging. **11**(6), e007217 (2018)
15. Sun, Z., Chaichana, T.: An investigation of correlation between left coronary bifurcation angle and hemodynamic changes in coronary stenosis by coronary computed tomography angiography-derived computational fluid dynamics. Quant. Imaging Med. Surg. **7**(5), 537–548 (2017)
16. Caruso, M.V., De Rosa, S., Indolfi, C., Fragomeni, G.: Computational analysis of stenosis geometry effects on right coronary hemodynamics. Conf. Proc. Annu. Int. Conf. IEEE Eng. Med. Biol. Soc. IEEE Eng. Med. Biol. Soc. Annu. Conf. **2015**, 981–984 (2015)

17. Zhang, J.-M., et al.: Numerical simulation and clinical implications of stenosis in coronary blood flow. Biomed. Res. Int. **2014**, 514729 (2014)
18. Papafaklis, M.I., et al.: Functional assessment of lesion severity without using the pressure wire: coronary imaging and blood flow simulation. Expert. Rev. Cardiovasc. Ther. **15**(11), 863–877 (2017)
19. Javadzadegan, A., Moshfegh, A., Qian, Y., Ng, M.K.C., Kritharides, L., Yong, A.S.C.: The relationship between coronary lesion characteristics and pathologic shear in human coronary arteries. Clin. Biomech. Bristol. Avon. **60**, 177–184 (2018)
20. Sun, Z.: Coronary CT angiography: beyond morphological stenosis analysis. World J. Cardiol. **5**(12), 444–452 (2013)
21. Vignaux, O.: Imagerie cardiaque: scanner et IRM, 2nd ed. Elsevier Masson (2011)
22. Vlachopoulos, C., O'Rourke, M., Nichols, W.W.: McDonald's blood flow in arteries: theoretical, experimental and clinical principles, 6th edn. CRC Press, London (2011)
23. Berne, R. M., Levy, M. N.: Cardiovascular physiology. The C.V. Mosby Company, (1967)
24. Boutsianis, E., et al.: Computational simulation of intracoronary flow based on real coronary geometry. Eur. J. Cardio-Thorac. Surg. Off. J. Eur. Assoc. Cardio-Thorac. Surg. **26**(2), 248–256 (Aug. 2004)
25. Siauw, W.L., Ng, E.Y., Mazumdar, J.: Unsteady stenosis flow prediction: a comparative study of non-Newtonian models with operator splitting scheme. Med. Eng. Phys. **22**(4), 265–277 (2000)
26. Elhadj, S., Akers, R.M., Forsten-Williams, K.: Chronic pulsatile shear stress alters insulin-like growth factor-I (IGF-I) binding protein release in vitro. Ann. Biomed. Eng. **31**(2), 163–170 (2003)
27. Ramcharitar, S., et al.: A novel dedicated quantitative coronary analysis methodology for bifurcation lesions. Euro Intervent. J. Eur. Collab. Work. Group Interv. Cardiol. Eur. Soc. Cardiol. **3**(5), 553–557 (2008)
28. Frauenfelder, T., et al.: Flow and wall shear stress in end-to-side and side-to-side anastomosis of venous coronary artery bypass grafts. Biomed. Eng. Online. **6**, 35 (2007)
29. Knight, J., et al.: Choosing the optimal wall shear parameter for the prediction of plaque location-a patient-specific computational study in human right coronary arteries. Atherosclerosis. **211**(2), 445–450 (2010)
30. Wellnhofer, E., Osman, J., Kertzscher, U., Affeld, K., Fleck, E., Goubergrits, L.: Flow simulation studies in coronary arteries–impact of side-branches. Atherosclerosis. **213**(2), 475–481 (2010)
31. Chaichana, T., Sun, Z., Jewkes, J.: Impact of plaques in the left coronary artery on wall shear stress and pressure gradient in coronary side branches. Comput. Methods Biomech. Biomed. Engin. **17**(2), 108–118 (2014)

Accurate Left Ventricular Segmentation Based on Morphological Watershed Transformation Towards 3D Visualization

Khouloud Boukhris, Ramzi Mahmoudi, Badii Hmida, and Mohamed Hédi Bedoui

1 Introduction

Cardiac magnetic resonance imaging (cMRI) represents the golden reference method for assessing the LV function and analyzing the myocardial diseases [1], using mainly short-axis cine images. With the aim of obtaining full exploitation of the information contained in these MRI images, the automated extraction and segmentation of the myocardium contours, which are often drawn manually by cardiologists, are proving to be crucial [2].In this paper, we propose to compare a set of existing methods dealing with ventricular segmentation in short axis cine MR images, in order to prove the accuracy of our proposed method. This comparison was also assessed against manual segmentations performed by cardiologist. The main issue with an accurate LV segmentation is to ensure its faithful 3-D reconstruction. This paper is organized as follows: Sect. 2 describes the previous work aiming to segment the heart cavities. Sects. 3 and 4 are dedicated to introduce then evaluate the proposed segmentation process to extract the LV myocardium. Section 5 depicts resulting 3D visualization. Finally, Sect. 6 presents the conclusion.

K. Boukhris (✉) · M. H. Bedoui
Faculty of Medicine of Monastir, Medical Imaging Technology Lab – LTIM-LR12ES06, University of Monastir, Monastir, Tunisia

R. Mahmoudi
Faculty of Medicine of Monastir, Medical Imaging Technology Lab – LTIM-LR12ES06, University of Monastir, Monastir, Tunisia

Gaspard-Monge computer-science laboratory, Paris-Est University, Mixed Unit CNRS-UMLV-ESIEE UMR8049, BP99, ESIEE Paris City Descartes, 93162 Noisy Le Grand, France

B. Hmida
Radiology Service- UR12SP40 CHU Fattouma Bourguiba, Monastir, Tunisia

L. Chaari (ed.), *Digital Health in Focus of Predictive, Preventive and Personalised Medicine*, Advances in Predictive, Preventive and Personalised Medicine 12,
https://doi.org/10.1007/978-3-030-49815-3_7

2 Review of Ventricular Segmentation Methods in cMRI

Cardiac Magnetic Resonance Imaging (cMRI) is used to help visualizing the internal structures of the human heart in order to highlight the medical management of patients. MRI cardiac planes include short axis, horizontal long axis (four-chamber view), and vertical long axis (two-chamber view) [3]. Various segmentation methods have been proposed by different researchers using generally the short-axis view [4]. These existing methods can be divided into two main categories: "segmentation based on no or weak prior" and "segmentation based on a strong prior". Approaches based on no or weak prior are very contingent upon the gray-level histograms and the thresholding techniques. These approaches include image-based methods [5–7], pixel classification and deformable models [8, 9]. However, approaches based on strong prior are characterized by the use of statistical models which are mainly divided into three categories: deformable models based segmentation with strong prior, Active shape ("ASM") [10, 11] and active appearance models ("AAM") [12] and atlas based ones [9, 13, 14].

3 Proposed Method Based on Watershed Transform

Since the early work of Serge Beucher [15], the watershed transform has been successfully applied in thousands of applications, including medical ones. Our approach is based mainly on the watershed transformation method [16] and considers prior properties. The set of prior knowledge that will allow an accurate segmentation are: topology (the left ventricular myocardium LVM is delimited by two surfaces: endocardium and epicardium), geometry (the endocardium cannot exceed the epicardium) and brightness (the endocardium is a very bright object). Our proposed method to automatically segment the LVM in 3D + t short-axes images is composed of two consecutive steps: endocardium segmentation, followed by the epicardium segmentation. Thereafter, the myocardium extraction (LVM) consists in applying the ensemblist difference between the epicardial and the endocardial civility. The segmentation of the endocardium is performed by geodesic dilations. Its recognition is ensured by extracting a connected set of pixels that belongs to the endocardium (thanks to its brightness). The delineation is then performed by dilating this marker in a mask made to be a candidate that belongs to the endocardium. The epicardium segmentation is consequent to the endocardium one preserving certain anatomical constraints. We propose to separate the myocardial cavity from the ventricular background. To achieve this goal, we propose to dilate the endocardium contour in order to obtain the first epicardial marker (EPm).To extract the EPm, the idea is to dilate the endocardium segmented cavity (ENC) as much as possible by ensuring that the resulting set is included in the real ENC, according to the prior:

$$Epicardium\_Boundary \cap Endocardium\_Boundary = \emptyset \quad (1)$$

The next step consists of finding a marker for the left ventricular background (LVBm) that does not belong to the myocardium: composed of several tissues including the liver, the stomach, the right ventricle and the lungs. In order to extract the LV background marker (LVBm), we propose a second dilatation, based on the prior that the myocardium thickness cannot exceed a certain threshold. Then, the delineation is performed by the topological watershed transformation approach cited in [16] using the above-selected markers as inputs. The delineation is followed by a smoothing post-processing using shape filters coming from mathematical morphology. Thus, in order to obtain the final segmentation, we use the alternating sequential filter (ASF) [17] to regularize the epicardial boundary (Ep) and to restore a correct shape of the intensity information. The ASF is a sequence of intermixed morphological openings and closings by balls of an increasing size.

4 Validation of the Proposed Segmentation

In our experiment, we used 4D cine MR images of 20 patients to segment. For the evaluation, the same dataset was manually segmented by two different experts, called below Exp1 and Exp 2.

4.1 Point to Surface Measurement

Given two surfaces S and S′ represented by two polygons, the point-to-surface measurement (P2S) defined in [18] estimates the mean distance between the vertices of these surfaces (S and S′).

From our proposed segmentation, the endocardial and the epicardial surfaces (EndoS and EpiS) were used to compute the P2S in order to compare them with those obtained by other groups on their own datasets [6, 9, 11, 12, 14, 19–22]. In Table 1, different distance measures similar to P2S where used: APD (Average Perpendicular distance), Hausdroff distance and image volumes. The comparison demonstrates that the distance (P2S) evaluation results averaged favorably across our proposed method and those obtained by previous works. The P2S was computed from the segmentations resulting from our proposed method and the two experts. In order to assess the inter-observer variability, the P2S of both experts is also provided as shown in Table 2.

The obtained results are convergent (PM vs.exp. and exp. vs. exp) with a distance that does not exceed 2 mm, thus evidencing the reliability of the proposed segmentation.

Table 1 Literature values of left ventricle delineation errors

	Distance (mm)	
	EndoS	EpiS
Mitchell and al [11]	2.75	2.63
Kaus and al [19]	2.28	2.62
Lötjönen and al [14]	2.01	2.77
Van Assen and al [12].	1.97	2.23
Lorenzo-Valdes and al [9]	1.88	2.75
Jolly and al [6]	2.48	2.91
Ying-Li Lu and al [20]	2.07	1.92
Huaifei Hu and al [21]	2.3	2.2
Irshad and al [22]	2.1	3.1
Proposed method	1.52	1.75

Table 2 Results of the P2S(mm) measurements from our proposed method (PM)

		PM VS. EXP1	PM VS.EXP2	EXP1 VS.EXP2
End-diastolic time	EndoS	1.62	1.52	1.46
	EpiS	1.81	1.60	1.62
End-systolic time	EndoS	1.45	1.30	1.44
	EPIS	**1.82**	**1.42**	**1.63**

4.2 False Negative and False Positive Volume Fraction

These two measures are recommended by [18] to characterize the delineation accuracy. Considering Struth the set of image pixels containing 'true' delineations of the LV and Spm the segmentation to be compared to the ground truth to be evaluated, we set False Negative Ejection Fraction FNEF and False Positive Ejection Fraction FPEF:

$$FPVF\,(Spm, Struth) = \frac{|\ Spm \backslash Struth\ |}{Struth} \tag{2}$$

$$FNVF\,(Spm, Struth) = \frac{|\ Struth \backslash Spm\ |}{Struth} \tag{3}$$

Figure 1 illustrates the meaning of these measures: A false positive volume fraction (FPVF)indicates the amount of pixels falsely extracted to be considered as a fraction of the true delineation (considered as the reference segmentation) and the false negative volume fraction (FNVF) depicts the fraction of pixels that was missed. These metrics were computed for the three segmented areas: the epicardium, the endocardium and the myocardium. Table 3 depicts their mean values between the proposed method PM and the two experts at end-systolic and end-diastolic time. In order to achieve an accurate assessment, these measures were also provided between

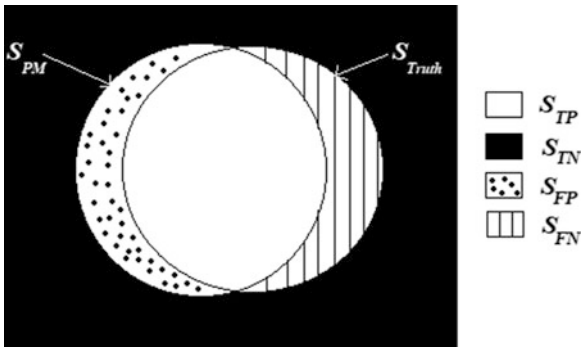

Fig. 1 Illustration of the accuracy factors from a binary case segmentation

Table 3 FPVF and FNVF values for the segmentation of the endocardium, the epicardium and the myocardium at end-systolic and end-diastolic time

		PM vs. exp1	PM vs.exp2	Exp1 vs. exp2	Exp2 vs. exp1
End-systolic-time					
Endocardium	FPVF	0.04	0.05	0.15	0.02
	FNVF	0.12	0.07	0.03	0.14
Epicardium	FPVF	0.08	0.14	0.06	0.09
	FNVF	0.21	0.06	0.10	0.12
Myocardium	FPVF	0.02	0.10	0.25	0.09
	FNVF	0.04	0.22	0.14	0.08
End-diastolic-time					
Endocardium	FPVF	0.06	0.12	0.09	0.12
	FNVF	0.12	0.23	0.21	0.10
Epicardium	FPVF	0.09	0.11	0.09	0.06
	FNVF	0.14	0.02	0.13	0.07
Myocardium	FPVF	0.04	0.08	0.18	0.21
	FNVF	0.03	0.13	0.09	0.04

the two experts. The inter-expert segmentations results (exp1 vs.exp2 and exp2 vs. exp1) compare well to those obtained between the proposed method and expert segmentations (PM vs. exp1 and PM vs. exp2). The Dice metric can be expressed in terms of true positives (TP), false positives (FP) and false negatives (FN) as:

$$Dice\,(A, B) = (2 * TP) / (2 * TP + FP + FN) \tag{4}$$

Comparing our method to both experts, the best segmentation result had a Dice Metric of 0.96 and the worst a DC of 0.73.

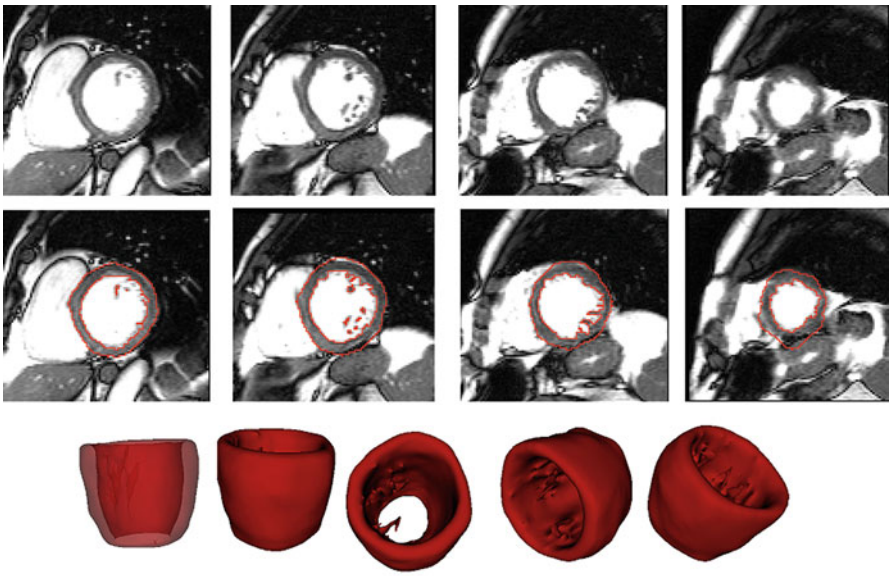

Fig. 2 Illustration of the myocardium segmentation results: The first row shows the pseudo slices from apical to basal direction without any contours. The second row depicts the extraction of myocardial contours. The third row shows the extracted mesh from different corners

5 The 3D Visualization

Searching for a means to display the segmentation results proved to be important. To achieve it, we start by generating meshes from the binary images resulting from the proposed segmentation. The ability to visualize the LV meshes would be a significant advantage. To generate these meshes we applied the method defined in [23] using the marching cube algorithm [24].The ensuing step consists on applying Laplacian smoothing steps [25] on these resulting meshes and save them in the vtk format [27]. Figure 2 depicts an example of myocardium segmentation ranging from apical to basal plane and the extracted mesh from different corners.

6 Conclusion

The purpose of this work was to provide an automatic and accurate LV myocardial segmentation method for 3D cine-MRI images. Extraction of the LV endo- and epicardium has provided accurate and consistent results. Our Proposed method has achieved a mean Dice metric of 0.87 for the endocardium and 0.82 for the epicardium. Therefore, we focused on the volumetric object reconstruction (3D visualization) by exporting the endocardial and the epicardial extracted contours

as 3D surface meshes [24]. This reconstruction is ensured throughout a complete cardiac cycle (from systole to diastole) to allow dynamic visualization of the LV.

References

1. Olimulder, M.A.G.M., Van Es, J., Galjee, M.A.: The importance of cardiac MRI as a diagnostic tool in viral myocarditis-induced cardiomyopathy. Netherlands Heart J. **17**(12), 481–486 (2009)
2. Buser, P.T., et al.: Noninvasive evaluation of global left ventricular function with use of cine nuclear magnetic resonance. J. Am. Coll. Cardiol. **13**(6), 1294–1300 (1989)
3. Ginat, D.T., et al.: Cardiac imaging: Part 1, MR pulse sequences, imaging planes, and basic anatomy. Am. J. Roentgenol. **197**(4), 808–815 (2011)
4. Petitjean, C., Dacher, J.-N.: A review of segmentation methods in short axis cardiac MR images. Med. Image Anal. **15**(2), 169–184 (2011)
5. Katouzian, A., Prakash, A., Konofagou, E.: A new automated technique for left-and right-ventricular segmentation in magnetic resonance imaging. 2006 International Conference of the IEEE Engineering in Medicine and Biology Society. IEEE (2006)
6. Jolly, M.: Fully automatic left ventricle segmentation in cardiac cine MR images using registration and minimum surfaces. MIDAS J. Cardiac MR Left Ventricle Segment. Challenge. **4**, 59 (2009)
7. Lin, X., Cowan, B.R., Young, A.A.: Automated detection of left ventricle in 4D MR images: experience from a large study. In: International conference on medical image computing and computer-assisted intervention. Springer, Berlin/Heidelberg (2006)
8. Pednekar, A., et al.: Automated left ventricular segmentation in cardiac MRI. IEEE Trans. Biomed. Eng. **53**(7), 1425–1428 (2006)
9. Lorenzo-Valdés, M., et al.: Segmentation of 4D cardiac MR images using a probabilistic atlas and the EM algorithm. Med. Image Anal. **8**(3), 255–265 (2004)
10. Pennell, D.J., et al.: Clinical indications for cardiovascular magnetic resonance (CMR): consensus panel report. J. Cardiovasc. Magnet. Reson. **6**(4), 727–765 (2004)
11. Mitchell, S.C., et al.: 3-D active appearance models: segmentation of cardiac MR and ultrasound images. IEEE Trans. Med. Imaging. **21**(9), 1167–1178 (2002)
12. Van Assen, H.C., et al.: SPASM: a 3D-ASM for segmentation of sparse and arbitrarily oriented cardiac MRI data. Med. Image Anal. **10**(2), 286–303 (2006)
13. Zhuang, X., et al.: Robust registration between cardiac MRI images and atlas for segmentation propagation. Medical Imaging 2008: Image Processing. Vol. 6914. International Society for Optics and Photonics, (2008)
14. Lötjönen, J., et al.: Statistical shape model of atria, ventricles and epicardium from short-and long-axis MR images. Med. Image Anal. **8**(3), 371–386 (2004)
15. Beucher, S.: Use of watersheds in contour detection. In: Proceedings of the International Workshop on Image Processing. CCETT (1979)
16. Mahmoudi, R., Akil, M., HédiBedoui, M.: Concurrent computation of topological watershed on shared memory parallel machines. Parallel Comput. **69**, 78–97 (2017)
17. Couprie, M., Bertrand, G.: Topology preserving alternating sequential filter for smoothing two-dimensional and three-dimensional objects. J. Electr. Imaging. **13**(4), 720–731 (2004)
18. Udupa, J.K., et al.: A framework for evaluating image segmentation algorithms. Comput. Med. Imaging Graph. **30**(2), 75–87 (2006)
19. Kaus, M.R., et al.: Automated segmentation of the left ventricle in cardiac MRI. Med. Image Anal. **8**(3), 245–254 (2004)
20. Lu, Y.-L., et al.: Automatic functional analysis of left ventricle in cardiac cine MRI. Quant. Imaging Med. Surg. **3**(4), 200 (2013)

21. Hu, H., et al.: Automatic segmentation of the left ventricle in cardiac MRI using local binary fitting model and dynamic programming techniques. PLoS One. **9**(12), e114760 (2014)
22. Irshad, M., et al.: Automatic segmentation of the left ventricle in a cardiac MR short axis image using blind morphological operation. Eur. Phys. J. Plus. **133**(4), 148 (2018)
23. Lachaud, J.-O., Montanvert, A.: Deformable meshes with automated topology changes for coarse-to-fine three-dimensional surface extraction. Med. Image Anal. **3**(2), 187–207 (1999)
24. Lorensen, W.E., Cline, H. E.: Marching cubes: a high resolution 3D surface construction algorithm. ACM siggraph computer graphics, nol. 21. No. 4. ACM (1987)
25. Vollmer, Jörg, Robert Mencl, and Heinrich Mueller. "Improved laplacian smoothing of noisy surface meshes." Computer Graphics Forum. 18 3. Oxford/Boston: Blackwell Publishers Ltd, 1999
26. Wesarg, S.: AHA conform analysis of myocardial function using and extending the toolkits ITK and VTK. International Congress Series, vol. 1281. Elsevier (2005)

A Smart Search Functionality for a Memory Prosthesis: A Semantic Similarity-Based Approach

Fatma Ghorbel, Wafa Wali, Elisabeth Métais, Fayçal Hamdi, and Bilel Gargouri

1 Introduction

In the context of the VIVA[1] project («*Vivre Paris avec Alzheimer en 2030 graçe aux nouvelles technologies*»), we are proposing a memory prosthesis, called Captain Memo [1], to help Alzheimer's patients to palliate mnesic problems. Data are structured semantically using an ontology, called PersonLink[2] [2]. It is a multilingual ontology for storing, modeling and reasoning about interpersonal relationships and describing people. This prosthesis supplies a set of services. Among these services, one is devoted to "remember things about people", i.e., retrieving information about a person (e.g., preferences, gifts exchanged and shared events). However, these particular users, living in a form of uncertainty, can substitute words having the same meaning and have an increased difficulty in naming things. For instance, they may enter "the brothers having the same birthday" instead of "the twins".

[1] http://viva.cnam.fr/

[2] http://cedric.cnam.fr/isid/ontologies/files/PersonLink.html

F. Ghorbel (✉)
CEDRIC Laboratory, Conservatoire National des Arts et Métiers (CNAM), Paris, France

MIRACL Laboratory, University of Sfax, Sfax, Tunisia

W. Wali · E. Métais · F. Hamdi
CEDRIC Laboratory, Conservatoire National des Arts et Métiers (CNAM), Paris, France
e-mail: wafa.wali@fsegs.rnu.tn; wafa.wali@fsegs.rnu.tn; faycal.hamdi@cnam.fr

B. Gargouri
MIRACL Laboratory, University of Sfax, Sfax, Tunisia

L. Chaari (ed.), *Digital Health in Focus of Predictive, Preventive and Personalised Medicine*, Advances in Predictive, Preventive and Personalised Medicine 12,
https://doi.org/10.1007/978-3-030-49815-3_8

Captain Memo aims to offer a smart search functionality. It is able to deal with all kinds of input e.g., full sentence, sentence fragments or keyword, natural language text. It takes into account that the user may substitute the words/sentences that express the same meaning. To address this issue, we estimate the semantic similarity score between the user's search filed entry and the saved personal data of the user.

Several approaches for sentences similarity estimation have been proposed. However, they are applied only to the English language. Moreover, many knowledge elements, e.g., the semantic class, the thematic role and the relationship between them, are not taken into account when measuring the sentences similarity.

In this paper, we propose a multilingual semantic similarity-based approach to estimate the similarity between the user's search filed entry and the patient's saved personal data. Compared to related work, it is mainly based on semantic information notably the synonymy relationships between words and syntactico-semantic information especially semantic class and thematic role. It supported three languages: English, French and Arabic. It is mainly proposed to be integrated in Captain Memo. However, it can be used on others applications.

The remainder of the paper is structured as follows. Section 2 details some related work. The approach is presented in Sect. 3. Section 4 discusses some experimental results. Finally, in Sect. 5, we conclude and we give perspectives.

2 Related Work

Several approaches have been proposed to measure the semantic similarity between sentences. We classify them into *(i)* syntactic-based, *(ii)* semantic-based and *(iii)* hybrid approaches. An example of a syntactic-based approach is [3]. An example of a semantic-based approach is [4]. An example of a hybrid approach is [5].

However, these approaches are applied to the English language and they do not support the specific particularities of the French and Arabic languages. Moreover, they estimate the semantic similarity based only on the syntactic structure of sentence notably word order or the syntactic dependency and the synonymy relationship between terms. They do not take into consideration the semantic arguments notably the semantic class and thematic role in computing the semantic similarity.

3 Proposed Approach

The proposed approach allows estimating a semantic similarity score between the user's search input sentence (USIS) and the others saved in data tier (DTS). It supports three languages: English, French and Arabic. It includes an extension of previous strategies by taking into account the most important linguistics and the syntactico-semantics information. Compared to related work, it also takes into account the semantic arguments notably the semantic class and thematic role.

It is composed of two modules: *(i)* "Preprocessing" and *(ii)* "Similarity Score Attribution".

3.1 Preprocessing

Before estimating the similarity score between USIS and DTS, three sub-steps are proposed:

- Tokenization: USIS and DTS are decomposed into authentication tokens (words). This step filters the answers and tags the words into their part of speech and labels them accordingly. WordNet [6] handles only relationships between noun-noun and verb-verb. The other parts of speeches are not taken onto account. Therefore, to reduce the time and space complexity of the approach, we only consider nouns and verbs to calculate the similarity.
- Removal of the punctuation signs: For the two sentences, all punctuation signs are removed.
- Lemmatization: morphological variables are reduced to their base form using the Stanford Morphological analyzer [7].

3.2 Similarity Score Attribution

To estimate the similarity score between USIS and DTS, three similarity level are measured: lexical, semantic and syntactico-semantic.

The lexical similarity score (SL(USIS, DTS)) is computed using the lexical units that compose the two sentences to extract the words that are lexically the same. It is computed based on the Jaccard coefficient [8].

$$SL\,(USIS, DTS) = MC/\,(MA_{USIS} + MA_{DTS} - MC) \tag{1}$$

MC is the number of common words between USIS and DTS; MA_{USIS} is the number of words contained in USIS; and MA_{DTS} is the number of words contained in DTS.

The measurement of the semantic similarity is reinforced by means of the WordNet database in order to extract the synonyms of each sentence's words. Also, we use the NOOJ platform [9] to determine the named entities. We also use the OpenCyc ontology to extract common sense facts (for instance, twins have the same birthday).

The computing process of the semantic resemblance between USIS and DTS involves primarily the creation of a set of joint words from the two sentences $W = \{W_1 \ldots W_m\} = SW_{USIS} \cap SW_{DTS}$. For each sentence, only the words returned by the "Preprocessing" component are taken into consideration. Then, we calculate the semantic vector $V = \{V_{USIS}, V_{DTS}, W\}$. For each $W_i \in W$, if $W_i \in SW_{USIS}$,

V_{USIS} is set as one (case1). In the other case ($W_I \notin \in SW_{USIS}$), a set of semantic similarity scores between W_i and all the words contained in SW_{USIS} are estimated ($SIM(W_I,SW_J)$). The closest word to W_J in the answer is the one that has the highest semantic similarity score. T_{USIS} is set to this score. To estimate the semantic similarity scores, we rely on synonymy link of the WordNet database.

$$SIM\,(W_I, SW_J) = MC/\,(MW_I + MSW_J - MC) \tag{2}$$

where, MC is the number of common words between the two synonym sets; MW_I is the number of words contained in the W_I synonym set and MSW_J is the number of words contained in the SW_J synonym set.

On the basis of the semantic vector previously calculated, the semantic similarity score (SM(USIS, DTS),) is computed by applying the Cosine similarity.

$$SM\,(USIS, DTS) = (V_{USIS}.V_{DTS})\,/\,(||V_{USIS}||\,.\,||V_{DTS}||) \tag{3}$$

The estimation of the syntactico-semantic similarity score consists of extracting the characteristics of the semantic arguments of USIS and DTS from the VerbNet database for the French and English languages [10] and LMF Arabic dictionary for the Arabic language [11]. As a consequence, a syntactic parser is used to identify, on the one hand, the syntactic behavior of the sentences and, on the other hand, the semantic predicates from the databases which is very rich in semantic predicates. Moreover, the meanings of the lexical entry (such as the verb of the sentence) and the predicative representation that connects the syntactic behavior and the semantic predicate pre-defined in the first stage are looked up in the databases. Then, when the predicative representation is caught, the semantic arguments will be extracted. Once the pairs of semantic argument have the same thematic role and semantic class, they are considered similar. After that, the degree of the syntactico-semantic similarity between two elements of each pair of the sentence is computed based on the common semantic arguments of the elements of the pair of sentences, which are called SSM(USIS,DTS) by using the Jaccard coefficient.

$$SSM\,(USIS, DTS) = ASC/\,(\,AS_{USIS} + AS_{DTS} - ASC) \tag{4}$$

Where, ASC is the number of common semantic arguments between USIS and DTS; AS_{USIS} is the number of semantic arguments contained in USIS; and AS_{DTS} is the number of semantic arguments contained in DTS.

The similarity score between USIS and DTS (SS(USIS,DTS)) is a USIS and DTS is a weighted sum of the three mentioned scores.

$$\begin{aligned} SS\,(USIS, DTS) =& SL\,(USIS, DTS)\,.\alpha + SM\,(USIS, DTS)\,.\beta \\ &+ SSM\,(USIS, DTS)\,.\gamma \end{aligned} \tag{5}$$

We propose to use the automatic learning in order to define the appropriate coefficients α, β and γ.

4 Experimentations

A Java-based prototype is implemented based on the proposed approach.

4.1 Integration in Captain Memo

The prototype is integrated in Captain Memo. A set of similarity scores are estimated between the user's search input sentence and all saved data. To consider that the data having the higher similarity score is right, it ought to be greater than 0,9. Figure 1 shows an example of the system's response for the following user's search entry: "the brothers having the same birthday".

4.2 Evaluation

We evaluated the efficiency of the proposed approach in determining the correctness of the responses given by the user. This evaluation was done in the context of Captain Memo. A total of 20 Alzheimer's patients $\{P_1 \ldots P_{20}\}$ and their associated caregivers $\{C_1 \ldots C_{20}\}$ were recruited to participate in this study. All caregivers are first-degree relatives. Most Alzheimer's patients were living in a nursing home

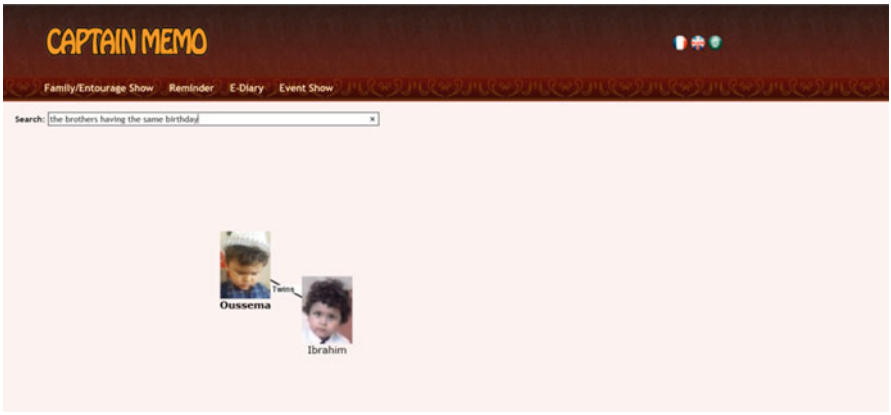

Fig. 1 An example of the system search's response

in Sfax/Tunisia. We asked each patient's legal sponsor for the consent letter. We excluded participants with overt behavioral disturbances, sever aphasia and sever auditory and/or visual loss.

The evaluation consisted of one test session for each patient. Its duration depends on the cognitive performance of the Alzheimer's patient. At mean, it was about 1 h. At the beginning of each session, we gave a brief introduction and a live demo of Captain Memo. Each patient uses the search functionality about 20 times. We classify these attempts according to the length of user's search filed entry. For each patient P_i, two scenarios had been tested:

- The first scenario, called "One or a part of sentence scenario", represents only user's search filed entries formed only by one or a part of sentence. $T_{S1/i}$ represents the total of the search's results related to the patient P_i and recorded as true responses. $GS_{S1/i}$ represents the "gold standard" responses. There are given by the caregiver C_i.
- The second scenario, called "Two or more sentences scenario", represents only user's search filed entries responses formed by two or more sentences. $T_{S2/i}$ represents the total of the search's results related to the patient P_i and recorded as true responses. $GS_{S2/i}$ given by the caregiver C_i represents the "gold standard" responses. There are given by the caregiver C_i.

For each scenario, we compare the generated response against the golden standard ones. The exact Precision measures Pi@S1 ($(|T_{S1/i} \cap GS_{S1/i}| / |T_{S1/i}|)$) and Pi@S2 represent respectively, the precision values related to the first and second scenarios of the patient P_i. The results obtained are encouraging. The means of the Precision measures related to the first scenario is estimated to 82,98 and the one related to the second scenario is estimated to 74,58. We noticed that the analysis of short sentences presents the highest measures of precision. As the sentence gets longer, there will be a more complex calculation, which reduces the system's performance. We believe that these results can be improved. In fact, we think that we can improve the learning stage by adding other features besides the lexical, semantic and syntactico-semantic features.

5 Conclusion

This paper proposed a multilingual approach to estimate the semantic similarity between the user's search filed entry and the saved personal data of the user. Compared to related work, it takes into account the synonymy relations between words and the semantic argument properties notably semantic class and thematic role. It supports three languages: English, French and Arabic. A prototype based on the approach is implemented. It is integrated in Captain Memo to allow a smart search functionality for Alzheimer's patients.

We plan to extend the proposed approach to be able to deal with spelling mistakes ungrammatical text entries.

References

1. Métais, E., Ghorbel, F., Herradi, N., Hamdi, F., Lammari, N., Nakache, D., Ellouze, N., Gargouri, F., Soukane, A.: Memory prosthesis. Non-pharmacol. Therapies Dementia. **3**(2), 177–180 (2015)
2. Herradi, N., Hamdi, F., Metais, E., Ghorbel, F., Soukane, A.: PersonLink: an ontology representing family relationships for the CAPTAIN MEMO memory prosthesis. In: ER 2015 (Workshop AHA). Lect. Notes Comput. Sci. **9382**, 3–13 (2015)
3. Li, Y., Mclean, D., Bandar, Z.A., O'Shea, J.D., Crockett, K.: Sentence similarity based on semantic nets and corpus statistics. Knowl. Data Eng. IEEE Trans. **18**(8), 1138–1150 (2006)
4. Kozlowski, M.: Opi: Semeval-2014 task 3 system description. SemEval. **2014**, (2014)
5. Md Arafat Sultan, Steven Bethard, Tamara Sumner. Dls@ cu: Sentence similarity from word alignment. In Proceedings of the 8th International Workshop on Semantic Evaluation (SemEval 2014), pp. 241–246 (2014)
6. Miller, G.A.: Wordnet: a lexical database for english. Commun. ACM. **38**(11), 39–41 (1995)
7. Manning, C.D., Surdeanu, M., Bauer, J., Finkel, J., Bethard, S.J., McClosky, D.: The Stanford CoreNLP natural language processing toolkit. In: Association for Computational Linguistics (ACL) System Demonstrations. pp. 55–60 (2014),
8. Jaccard, P.: Etude comparative de la distribution orale dans une portion des Alpes et du Jura. Impr. Corbaz (1901)
9. Silberztein, M., V_aradi, T., Tadi_c, M.: Open source multi-platform NooJ for NLP. In: Proceedings of COLING 2012: Demonstration Papers. pp. 401–408. The COL-ING 2012 Organizing Committee, Mumbai, India (2012)
10. Schuler, K.K.: VerbNet: A Broad-Coverage, Comprehensive Verb Lexicon. PhD thesis, University of Pennsylvania (2006)
11. Khemakhem, A., Gargouri, B., Ben Hamadou, A., Francopoulo, G.: Iso standard modeling of a large arabic dictionary. Nat. Lang. Eng. 1–31 (2015)

An Efficient Image Retrieval Using Medical-Dependent Features

Hajer Ayadi and Mouna Torjmen-Khemamkhem

1 Introduction

Facing the explosion in the amount of medical images, the image indexing and retrieval systems have seen an evolution to provide access to biomedical literature and satisfy the user information needs. In traditional text-based image retrieval (TBIR) approaches, the image meta-data (document) is represented as a bag of words and frequencies, that are used to compute its relevance score according to a given query. While this traditional approach served as a building block to several well-known retrieval models (e.g. vector model and language model), it is no longer satisfied due to the limits dealing with noun phrases, synonyms, abbreviations and variants of terms mismatch problems. Moreover, the semantic relatedness between query terms and document terms need to be considered. To overcome these linguistic problems, several research and indexing studies known as "concept-based" have appeared [5]. The conceptualization is known as a step leading to a higher level of abstraction of text content, as well as a method to bridge the gap between surface linguistic form and meaning. However, this kind of approach is extremely time consuming, rendering it less effective. This issue was the subject of several indexing and retrieval studies such as "MDF-Feature-based" approach [1]. Recently, exploiting features within the retrieval process has received high attention in the information retrieval (IR) domain. The key benefits of using medical-dependent features(MDF) in TBIR are the following: First, they are specific for TBIR. In fact, they display the textual specificity for image retrieval as they denote a set of imaging modality (e.g. x-ray, MRI), image dimensionality (e.g. micro, macro), and so on. Second, they are specific to the medical domain as they contain a

H. Ayadi (✉) · M. Torjmen-Khemamkhem
ReDCAD Laboratory, National School of Engineering of Sfax, Sfax University, Sfax, Tunisia
e-mail: hajer.ayadi@redcad.org; mouna.torjmen@redcad.org

L. Chaari (ed.), *Digital Health in Focus of Predictive, Preventive and Personalised Medicine*, Advances in Predictive, Preventive and Personalised Medicine 12,
https://doi.org/10.1007/978-3-030-49815-3_9

set of medical terminology (e.g. Ultrasound, Dermatology). This paper investigates the performance of MDF based medical image indexing and retrieval according to both criteria: efficiency and effectiveness. Our main findings are: (1) the MDF based approach gives accuracy results comparable to those found by concept based approach, meaning that MDF based approach may be applied to any medical image collection; and (2) the MDF approach has several strengths compared to literature indexing approaches, especially as regards space-time occupancy. The remainder of this paper is organized as follows. In Sect. 2, we describe the related work. We present the MDF based image retrieval approach in Sect. 3. In Sect. 4, we set up our experimental environment. In Sect. 5, the experimental results are presented and discussed. Finally, we conclude our work briefly and discuss directions for future research in Sect. 6.

2 Related Work

In the literature, several text-based image retrieval (TBIR) approaches have been proposed. Their success highlight the area of image retrieval thanks to the relatively mature techniques of traditional information retrieval(such as query expansion, simple bag of words (BoW)). The largest number of medical retrieval systems which deal with annotated images exploits only the keywords of these images to search for relevant images in large collections. The standard approach is to represent the text as a "bag-of-words" and to associate a weight for each word using the Term Frequency-Inverse Document Frequency (TF-IDF) method [2]. Authors in [3] propose to extend the probabilistic Latent Semantic Analysis model to integrate the textual information from medical images. However, in [13] authors propose to extract textual information from patients records, such as the patient age, sex and medical history. Then, they use these textual attributes into retrieval process to search the possibly incomplete medical cases consisting of several images together with semantic information.

In many cases, the use of external resources, such as ontologies and thesaurus, significantly enhances the performance of TBIR systems. In [5], authors proposed a conceptual model to resolve the word sense ambiguity problem using the semantic relations between extracted concepts, through MetaMap[1] tool and UMLS Metathesaurus. In [7], the authors investigate the use of a query expansion strategy process using an advanced PubMed search. They conclude that the query expansion using external resources in PubMed improves the recovery efficacy. The query expansion was carried out, in [4], using the Mesh and UMLS ontologies and showed that using these ontologies improves the retrieval performance. Authors in [8], used conceptual language modeling with the additional use of the UMLS (Unified Medical Language System) metathesaurus to compute the similarity between a

[1] https://metamap.nlm.nih.gov/

given query and a document by simply computing the log-probability of the concept set of the document.

3 MDF Based Retrieval

In this section, we incorporate the MDFs into the retrieval process. First, we detail the set of MDFs; second, we present the used method to extract MDFs from documents/queries; finally, we applied the retrieval process based on MDF.

3.1 Medical-Dependentent Features

As our work falls into medical image retrieval field, we use MDFs [1, 15], which help in improving the retrieval performance. These features are detailed as follows:

- Radiology = {"Ultrasound Imaging", "Magnetic Resonance Imaging", "Computerized Tomography", "X-Ray", "2D Radiography", "Angiography", "PET", "Combined modalities in one image"}
- Microscopy = {"Light Microscopy", "Electron Microscopy", "Transmission Microscopy", "Fluorescence Microscopy"}
- Visible light photography = {"Dermatology", "Skin", "Endoscopy", "Other organs"}
- Printed signals and waves = {"Electroencephalography", "Electrocardiography", "Electromyography"}
- Generic Biomedical Illustrations = {"modality tables and forms", "program listing", "statistical figures", "graphs", "charts", "screen shots", "flowcharts", "system overviews", "gene sequence", "chromatography", "gel", "chemical structure", "mathematics formula", "non-clinical photos", "hand-drawn sketches"}
- Dimensionality = {"macro", "micro", "small", "gross", "combined dimensionality"}
- V-Spec = {"brown", "black", "white", "red", "gray", "yellow", "blue", "colored"}
- T-spec = {"finding","pathology", "differential diagnosis"}
- C-spec = {'Histology"}

3.2 MDFs Extraction Procedure

Although many approaches in the literature, such as conceptual approaches, have shown excellent retrieval results, most of them are very time and storage space consuming. In this work, we use the MDF based retrieval approach which saves both

indexing time and space occupancy. Usually, the indexes encode the whole internal representation of documents. However, this work addresses an indexing approach that is restricted on the occurrence of features values in the collection. Extracting features from both documents and queries requires several different operations. First, all features, represented with terms, pass through a snowball stemmer. The resulting stems are then recorded in the stemmed feature list. Each term in the image metadata ($docID$) passes through the same stemmer and is checked against the stemmed feature list. If this list already contains the stem of interest, this term is considered an MDF/value. Then, it is recorded in the image-feature list with the same identifier ($docID$). The representation of the text "Radiographic findings of osteomyelitis" using medical-dependent-features is "{2D Radiography, finding}". After this processing, the dataset considered in the retrieval process is a set of MDFs.

3.3 Retrieval Process

In this section, we present an approach for image retrieval based on MDFs. It is presented in three steps: first, we compute the relevance score that measures the similarity between a document and a query. This is the baseline score which represents the correspondence degree between document and query based on terms; second, we measure the relevance score of query and document representations through MDFs by using the same baseline model; finally, we combine the MDF score with the baseline score to form the new retrieval score ($MDF - BM$). In particular, we propose modeling the MDF-BM score by a simple and classic linear combination (Eq. 1). Before combining the two scores, we need to normalize the initial and feature based scores as follows:

$$MDF - BM = \alpha * \frac{BMScore}{max(BMScore)} + (1 - \alpha) * \frac{MDFScore}{max(MDFScore)} \quad (1)$$

Where α is a balancing parameter [0..1], $BMScore$ represents the initial ranking score for the image, and $MDF - BM$ is the MDF score of the same image, by using the same baseline. The normalized score is obtained by dividing the relevance score for a given document d by the highest relevance score in the whole collection.

4 Experimental Setting

4.1 Datasets and Evaluation Metrics

To evaluate the MDF based image retrieval, we use two ImageCLEF collections in medical Image Task: 2009 [10] and 2010 [11] presented in Table 1. In ImageCLEFmed datasets, each image has a textual annotation that may contain a caption,

Table 1 MedicalClef dataset

	MedicalCLEF dataset	
	2009	2010
# Total queries	25	16
# Total images	74,902	77,495

a link to the HTML of the full text article [16] and also the article title [10]. In this paper, we use both image caption and article title to evaluate the retrieval models. For measuring the IR effectiveness, we used three evaluation measures that are commonly used in Medical ImageCLEF: the Mean Average Precision (MAP), the precision at the top ranking results (P@5, P@10, P@15, etc.), and the Binary Preference (Bpref).

4.2 Review of Baseline Models

In order to show the effectiveness of the MDF based retrieval, we conduct comparative study with different models such as classic text-based model (BM25) which is used as baseline, and concept based model. Our experiments are conducted using the classic information retrieval system Terrier (Terrier 3.5) and its implementations.

4.2.1 Text-Based Image Retrieval

As a text-based model, we use the probabilistic model BM25 [14] as shown in Eq. (2).

$$RSV(q,d) = \sum_{t \in (q \bigcap d)} \frac{t_f}{t_f + nb * k_1} * \log\left(\frac{N - df_t + 0.5}{df_t + 0.5}\right) * q_{tf} \tag{2}$$

Where q is a query, d is a document, t_f is the term frequency in the document, df_t is the document frequency of the term t, N is total number of documents in the collection, q_{tf} is frequency of term t in the query, $k_1 = 1.2$ is a defaults parameter and nb is the normalization factor which may be calculated as: $nb = (1 - b) + b * \frac{t_l}{Avgt_l}$. With t_l is the number of terms in the document, $Avgt_l$ is the average number of terms in the document and b are default parameters. Also we have compared the specific feature based image retrieval model with the Dirichlet language model "DLM" [9] and Bo1 Pseudo-relevance feedback "Bo1-prf" [6]. In order to build a strong baseline, we conduct a set of experiments to tune the parameter b and we set it equals 0.75.

4.2.2 Concept Based Image Retrieval

As a concept based model, we use a simple but effective concept based image retrieval model. First, we extract the candidate concepts using METAMAP and UMLS; second, a concept based retrieval process is applied. Several works show the efficiency of the MetaMap tool with UMLS [12]. For this reason, we propose to map textual representation of images into concepts by applying the MetaMap tool. Extracted concepts are identified by a CUI (Concept Unique Identifier). Typically each term will relate to several possible concepts, whence, for each term, several concepts could be extracted. These concepts are called candidate concepts. Taking the phrase "Ocular complications" as an example, 6 UMLS concept candidates are identified by MetaMap and used for the conceptual representation of the text "Ocular complications". They are "{C0009566, C1171258, C0231242, C1522701, C0015392, C1555959}". After this processing, the dataset considered in the retrieval process is a set of medical concepts.

The retrieval process is presented in three main steps: first, we compute the relevance score that measures the similarity between a document and a query. This is the baseline score which represents the correspondence degree between document and query based on terms; second, we measure the relevance score of query and document representations through medical concepts by using the same baseline model; finally, in order to take advantages of both datasets (concept, text) we combine the medical concept (MC) score with the baseline (BM) score to form the new retrieval score (MC-BM), and thus by using a linear combination after a normalization step. In order to obtain the best linear combination, we conduct a set of experiments to tune the parameter α and we set it equals 0.4.

5 Experimental Results

5.1 Results of the Proposed Models

In these experiments, we evaluate the impact of MDF-BM, MC-BM, BM25 model using terms, according to the MAP. Figure 1 presents a comparison according to MAP values between the MDF-BM model results, the MC-BM model results and BM25 using the terms results for all datasets. Based on those barplots, we observe that the MAP values depend on the used model (BM25, MDF, MDF-BM). For both datatsets, we can clearly see that the MAP values of MDFBM and MC-BM are comparable. For example, the MAP value of 2009 dataset when using MDF model equals to 0.148 and achieved 0.39 by MDF-BM model. In addition, it equals to 0.216 when using only concepts (MC) for research and achieved to 0.393 when using combination (concept + term) MC-BM for retrieval. We have the same observation for 2010 collections. These results confirm that MDFs and concepts are good additional sources of evidence to enhance medical image retrieval. Using only

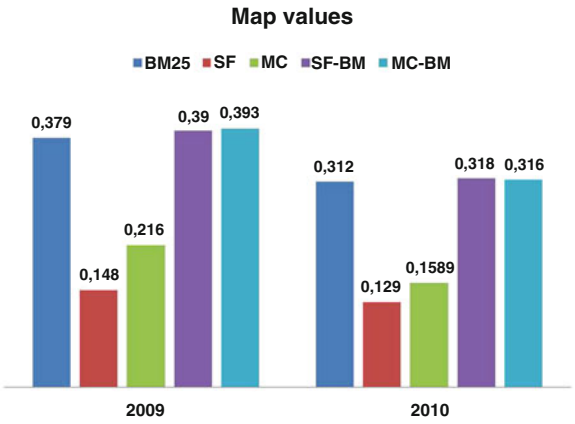

Fig. 1 Comparison based on the MAP values

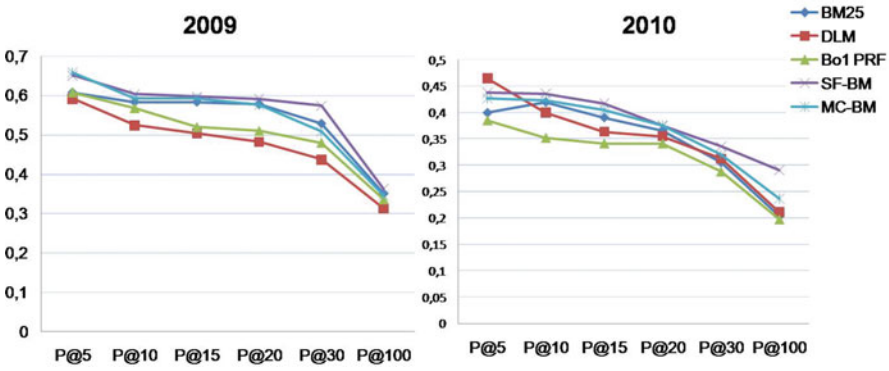

Fig. 2 Comparison of the precision at top ranks

features is not sufficient, and it is not surprising given the following explanation: A query cannot contain a large number of features, so it will be hard to find relevant images by using only features. Moreover, the decreasing MC results compared to BM25 may be explained by the fact that some UMLS concepts extracted based on image text are not correct. Consequently, it can negatively affect the obtained results. However, we can clearly see the improvement of results when combing feature/concept scores with BM25 scores.

5.2 Further Analysis and Discussion

In this experiment, we compare the precision at top ranks obtained by MDF-BM and MC-BM models to the state-of-the art models namely BM25, Dirichlet Language and Bo1 pseudo relevance feedback models. We use the same parameters for all datasets. Figure 2 presents the precision values for the different models.

Table 2 Comparison with the official imageCLEFmed approaches results

	Team	Rank	MAP	P@10	Bpref
2009	Liris	**1**	**0.43**	**0.66**	**0.46**
	MDF-BM	–	0.39	0.651	0.415
	MC-BM	–	0.393	0.623	0.41
	SINAI	2	0.38	0.62	0.39
	York	3	0.37	0.60	0.38
2010	Xrce	**1**	**0.338**	**0.506**	**0.382**
	AUEB	2	0.323	0.468	0.31
	MDF-BM	–	0.318	0.438	0.338
	MC-BM	–	0.316	0.427	0.34
	OHSU	3	0.302	0.431	0.34

According to the results, the MDF-BM model gives the best precision compared to other models. However, it is important to note that MC-BM results model has a comparable result with MDF-BM model. Our interpretations in regards to results of Fig. 2 are presented below. For 2009 and 2010 datasets, MDF-BM approach outperforms all other approaches according to all measures. More precisely, it outperforms BM25 which has the higher precision compared to other approaches.

5.3 A Comparative Study

In order to show how well our proposed approach performs compared to the state-of-the-art [10, 11] approaches, further comparative studies are conducted with the top three teams that achieved the best MAP using textual runs on the medical image retrieval task. Table 2 presents a comparison based on the MAP, P@10, and Bpref between the MDF-BM, the MC-BM model results, and the official imageCLEFmed approaches results. The results of the models (MDF-BM and MC-BM) are comparable to the results of the state of the art approaches, as shown in Table 2. For 2009 and 2010 datasets, our models do not outperform the highest values (MAP, p@10 and Bpref) founded by existing approaches. This can be explained by the fact that these models are highly dependent on the baseline results. However, for both datatsets, our models outperform the third highest values founded by existing approaches. This validates our assumption that our model has a positive impact on the retrieval performance.

5.4 Time and Space Complexity

In this paper, we used three datasets types (concept based, MDF based and text based) for retrieval approach. In this section, we present the indexing time and the

Table 3 Comparison of time/space occupancy

	2009			2010		
Index	Term	Concept	MDF	Term	Concept	MDF
Size(MB)	38.6	34.3	15.2	40.2	21.3	15.7
Time(s)	155.2	Few days	102.3	103.3	Few days	89.1

memory consumption using the three models: text-based, concept-based, and MDF-based. The experiment was conducted on a Pentium Dual Core 2.2 GHz machine with 2 GB DDR3 of RAM running ubuntu 12.04. As shown in Table 3, the size occupancy of MDFs, for the 2009 dataset, equals to 15.2 MB, while, for concept based indexing it is 34.3 MB and the term-based indexing, the size is 38.6 MB. The indexing time taken by MDFs approach is faster than the indexing time taken by term based and concept based indexing time. Based on result shown in Table 3, the indexing time is reduced from few days and 155.2–102.3 s by using MDFs. This reduction in indexing time as well as the size occupancy is due to the restriction of indexing on MDFs and thoughtlessness of all keywords of documents. This proves that these features are critical terms in the search process.

6 Conclusions and Future Work

In this paper, we studied the performance of medical-dependent-feature-based medical image indexing and retrieval according to both criteria: efficiency and effectiveness. MDFs are used to represent medical imageCLEF datasets as feature based representation. In addition, a classic retrieval method for computing the feature based score is used. We combined the feature based score with the baseline (BM25) score to form the new retrieval score. Using two medical imageCLEF collections (2009 and 2010), we compare the performance of MDF retrieval with approaches from the literature and analyze where it is effective. Results show that using that the MDF based approach gives accuracy results comparable to those found by concept based approach. In addition, the MDF approach has several strengths compared to literature indexing approaches, especially as regards space-time occupancy. In future work, we plan to include more MDFs that could cover more characteristics of any user information need in the context of image retrieval. Moreover, we plan to evaluate the performance of our model on other standard dataset collections.

References

1. Ayadi, H., Khemakhem, M.T., Daoud, M., Huang, J.X., Jemaa, M.B.: Mf-re-rank: a modality feature-based re-ranking model for medical image retrieval. JASIST **69**(9), 1095–1108 (2018)

2. Bouslimi, R., Messaoudi, A., Akaichi, J.: Using a bag of words for automatic medical image annotation with a latent semantic. CoRR abs/1306.0178 (2013)
3. Cao, Y., Steffey, S., He, J., Xiao, D., Tao, C., Chen, P., Müller, H.: Medical image retrieval: a multimodal approach. Cancer Informat. **2014**, 125–136 (2015)
4. Díaz-Galiano, M.C., García-Cumbreras, M.A., Martín-Valdivia, M.T., Ureña-López, L.A., Montejo-Ráez, A.: Query Expansion on Medical Image Retrieval: MeSH vs. UMLS, pp. 732–735. Springer, Berlin/Heidelberg (2009)
5. Gasmi, K., Khemakhem, M.T., Jemaa, M.B.: A conceptual model for word sense disambiguation in medical image retrieval. In: Information Retrieval Technology – 9th Asia Information Retrieval Societies Conference, AIRS 2013, Singapore, 9–11 Dec 2013. Proceedings, pp. 296–307 (2013)
6. He, B., Ounis, I.: Inferring query performance using pre-retrieval predictors. In: Proceedings of SPIRE, pp. 43–54 (2004)
7. Lu, Z., Kim, W., Wilbur, W.: Evaluation of query expansion using MeSH in PubMed. Inf. Retr. **12**(1), 69–80 (2009). https://doi.org/10.1007/s10791-008-9074-8
8. Maisonnasse, L., Gaussier, E., Chevallet, J.P.: Model Fusion in Conceptual Language Modeling, pp. 240–251 (2009)
9. Miller, D.R.H., Leek, T., Schwartz, R.M.: A hidden Markov model information retrieval system. In: Proceedings of the 22nd ACM SIGIR, pp. 214–221 (1999)
10. Muller, H., Kalpathy-Cramer, J., Eggel, I., Bedrick, S., Radhouani, S., Bakke, B., Khan, C.E., Jr., Hersh, W.R.: Overview of the CLEF 2009 medical image retrieval track. In: Proceedings of CLEF, pp. 72–84 (2009)
11. Müller, H., Kalpathy-Cramer, J., Eggel, I., Bedrick, S., Reisetter, J., Khan, C.E., Jr., Hersh, W.R.: Overview of the CLEF 2010 medical image retrieval track. In: CLEF (Notebook Papers/LABs/Workshops) (2010)
12. Pratt, W., Yetisgen-Yildiz, M.: A study of biomedical concept identification: Metamap vs. people. AMIA ... Annual Symposium Proceedings. AMIA Symposium, pp. 529–33 (2003)
13. Quellec, G., Lamard, M., Bekri, L., Cazuguel, G., Roux, C., Cochener, B.: Medical case retrieval from a committee of decision trees. Trans. Info. Tech. Biomed. **14**(5), 1227–1235 (2010)
14. Robertson, S.E., Walker, S.: Some simple effective approximations to the 2-poisson model for probabilistic weighted retrieval. In: Proceedings of SIGIR, pp. 232–241 (1994)
15. Souissi, N., Ayadi, H., Khemakhem, M.T.: Text-based medical image retrieval using convolutional neural network and specific medical features. In: Proceedings of the 12th International Joint Conference on Biomedical Engineering Systems and Technologies (BIOSTEC 2019) – Volume 5: HEALTHINF, Prague, 22–24 Feb 2019, pp. 78–87 (2019)
16. Wu, H., Sun, K., Deng, X., Zhang, Y., Che, B.: UESTC at imageCLEF 2012 medical tasks. In: Proceedings of CLEF, pp. 1–1 (2012)

Brain Image Processing Using Deep Learning: An Overview

Rahma Kadri, Mohamed Tmar, and Bassem Bouaziz

1 Introduction

Lately with the availability of smart technologies such as wearable technologies and the brain imaging tools, there have been great leaps forward the brain imaging processing and neuroscience. This discipline allows to better understand the mechanisms of the brain and the way we process and record information. One of the most challenging questions regarding this context is the automatic brain diseases and disorders diagnosis. Toward this end neuroscientists around the world collect data about brain function, structure and behavior using various neuroimaging tools at an ever-increasing rate. This data is the lifeblood of the brain behavior analysis. However the neuroimaging data are collected in various formats (text, image, video, sound..). The overarching challenge is how we can extract insights from it. Extracting knowledge is a tedious task that necessitates integration of well validated data described in a common standard and format. One interesting way to enable such process is to deal with a common international platform to collect, store, validate, analyze and publish neuroimaging data. The breakthrough in neuroimaging or brain imagining is the availability of powerful and advanced imaging modalities to understand the brain function. Brain imaging analysis encompasses many tasks such as the brain activity analysis, brain image segmentation, brain disease analysis and prediction. For this end, there are processing brain image modalities used to uncover and image the brain structure, behavior and activity.

R. Kadri (✉) · M. Tmar · B. Bouaziz
Higher Institute of Computer Science and Multimedia, University of Sfax, Sfax, Tunisia

L. Chaari (ed.), *Digital Health in Focus of Predictive, Preventive and Personalised Medicine*, Advances in Predictive, Preventive and Personalised Medicine 12,
https://doi.org/10.1007/978-3-030-49815-3_10

1.1 Brain Image Modalities

Typically brain imagining falls into two classes: the structural and the functional imaging.

Structural imaging which enables to illustrate the brain structure. Under this category there are the Computed Tomography (CT) and Magnetic Resonance Imaging (MRI) techniques.

- **C**T is a computerized x-ray imaging technique which provides axial images called slices.
- **M**RI is an advanced technique that produce detailed brain image structure. It allows to examine the brain anatomy in all three planes: axial, sagittal and coronal. the most commonly used MRI images are T1-weighted and T2-weighted.

Functional imaging is devoted to study the brain function. This technique uncovers the brain's information processing. It is based on well known scan techniques such as the Electroencephalography (EEG), functional Magnetic Resonance Imaging (fMRI), Positron Emission Tomography (PET) and the Magnetoencephalography (MEG).

- **fMRI**: is extremely used to detect the brain's functional anatomy by measuring the brain activity. It also examines the main changes in the brain.
- **(EEG)**: visualizes the electrical activity in the brain neurons. It also uncover the state of the brain.
- **(PET)**: uses a radioactive substance also known as tracer to illustrate the brain activity. This technique detects such injury on the brain.
- **(MEG)**: measures the magnetic fields relating to such electrical activity in the brain.

The automatic diagnosis and knowledge extraction from these tools became a hard question to meet. The tremendous success of deep learning meet the need of an efficient neuroimaging data analysis approaches. We investigate the recent application of deep learning regarding the neuroimaging data collection and analysis. Hence we define a set of research questions:

- RQ1: What are the most used datasets for each image brain analysis methods using deep learning. This question highlights the most used dataset sources for image brain analysis. The main motivation underlying this question is the need of data collection for the brain image analysis.
- RQ2: What are the most relevant contributions of deep learning regarding the brain image analysis. The underlying purpose of this question is to overview the current brain image processing methods and explore the recent publications and approaches within this context.

– RQ3: What are the preprocessing steps for an effective brain image analysis. The main motivation of this question is to figure out the main key preprocessing steps for the brain image analysis.
– RQ4: What are the main current challenges today regarding the brain image analysis.

We conducted a Systematic Literature Review (SLR) to investigate the recent existing publications in order to meet these research questions.

2 Brain Image Processing Using Deep Learning

Deep learning was widely used for different brain image analysis tasks:

Brain image reconstruction: is an active area that aims to create two or three-dimensional image from scattered or incomplete data. Brain image reconstruction is the key step for many tasks such as disease, classification and recognition. Further, this task is extremely applied for the reconstruction of the image from the brain activity.

Brain image super-resolution: medical image with high resolution is very expensive. For this end, the brain image super-resolution incorporates a set of techniques that aim to reconstruct a high-resolution MRI images from low-resolution image. This task is vital to ensure the relevant quantitative analysis.

Brain Image Segmentation: this task is critical for image brain analysis and understanding. It simplifies the representation of the image in order to make it easier to analyse.

Automated Brain Disorders Diagnosis: a lot of attention today is accorded to the brain disease classification. Examples include Alzheimer's disease, brain cancer, migraine disease and dementia.

Brain image generation and synthesis: data collection within the neuroimaging is challenging and difficult task. Brain image analysis using deep learning is relying on a huge amount of training data. Significant effort has been invested on this task such as the data augmentation and the synthetic image generation.

2.1 Data Preparation and Collection

Data preparation is a key pre-processing process consisting of data gathering, cleaning, structuring, organizing, augmentation, fusion and transforming into suitable data from for analysis task. Researchers adopt many methods to collect and prepare their data. The key challenge today within the brain image analysis is the lack of annotated brain images. There is an effective effort to ensure centralized access and data availability by creating tools for neuroimaging data exchange examples

includes (OpenfMR,[1] ADNI,[2] OASIS[3]). The data preparation and collection here depends on the target task such as brain image segmentation, reconstruction, super-resolution and brain disease detection. Within the context of the brain disease detection and analysis many researchers collect different brain image modalities. Jain et al. [1] collect T1-weighted MRI data of 150 subject 50 Alzheimer's Disease (AD) 50 Normal Control (CN), 50 Mild Cognitive Impairment (MCI) from the Alzheimer's Disease Neuroimaging Initiative (ADNI) for alzheimer's disease classification. The feature selection involves demographic characteristics of the selected subjects such as age, gender and Mind Mental State Examination (MMSE). They select the most informative RMI slices using an entropy function. They used a FreeSurfer software for the pre-processing. They adopt different preprocessing methods such as motion correction, non-uniform intensity normalization and skull stripping. Another intelligent selection of the most informative MRI slices from the ADNI dataset also was proposed by [2] for the prediction of Alzheimer's disease. An intelligent data augmentation process with balancing method is proposed by [3] using the same dataset also for the Alzheimer's disease. Here data selection involves 214 patients: 48 AD patients, 108 MCI and 58 NC. The input used images are T1-weighted Structural magnetic resonance imaging (sMRI) image and a Diffusion Tensor Imaging (DTI) image. They also adopt the age, gender and (MMSE) score as the demographic characteristics. For the preprocessing steps they applied a correction of eddy currents and head motion, skull stripping using the Brain Extraction Tool (BET) on the DTI brain images. For the same task [4] collect 18F-FDG PET images about 1002 patients with various scans. Here the dataset is from different sources such as (ADNI)-1, ADNI2 and ADNI-GO studies. To prepare data for analysis, they adopt a grid method based on the input images resampling to 2-mm isotropic voxels. Here the feature selection consists of extracting the caudal-most sections that represent more than $100 \times 100\,\text{mm}^2$ of brain parenchyma. For the brain voxels selection they utilize an Otsu threshold function. They also use a connected component analysis to extract the relevant imaging volume. For this end they find a use for Python Software Foundation.

Feng et al. [5] adopt 2 different brain image modalities MRI and PET also from the ADNI dataset for the diagnosis of Alzheimer disease. They applied different methods for the MRI preprocessing such as the image resampling, Anterior Commissure (AC), posterior commissure reorientation, skull striping and segmentation using Field Service Lightning(FSL) package. Here they applied different algorithms for elastic image registration using the hierarchical attribute matching method. Whereas [6] use a 3D FDG-PET images from the ADNI dataset about 339 patients: 93 AD patients, 146 MCI and 100 NC acquired by 30–60 min post-injection for the Alzheimer's disease classification. They use the same demographic characteristics of the previous contributions (age, gender, education..). Data preprocessing here

[1] openfmri.org

[2] adni.loni.usc.edu

[3] www.oasis-brains.org

includes the intensity normalization, the conversion to a uniform isotropic resolution of 8 mm FWHM, the image decomposition into 2D slices and the image size reduction. Yang et al. [7] use a small custom dataset for migraine classification including 21 migraine patients without aura, 15 migraineurs with aura, and 28 healthy controls. For the data acquisition they utilize a 3.0 Tesla MRI system and Echo-Planar Imaging (EPI). During this acquisition, patients were rest with their eyes closed and not to fall asleep. The key feature here is the feature mapping method in order to illustrate the brain activity and state. They calculated three functional maps for each subject the amplitude of low frequency fluctuations, the regional homogeneity and the brain functional connectivity state. Within the context of brain image segmentation [8] collect 2 medical datasets: the BraTS2016 and the LiTS2017 benchmark for brain tumor segmentation including MRI and CT images. They applied different preprocessing steps on the MRI images for example the intensity non-uniformity and the histogram matching. Further they perform a slice-wise fashion on the CT images. To remove the irrelevant object on the CT images, they calculated the Hounsfield Unit (HU) values. Finally they adopt the histogram equalization to improve the contrast. They introduce a patient-wise mini-batch normalization as preprocessing step to enhance the segmentation task. Ang et al. [9] collect an fMRI data about specific brain tissue such as gray matter, white matter, blood vessel, non-brain and cerebrospinal fluid also for brain tissue and tumor classification. For the preprocessing they adopt a motion correction, slice scan time correction and intensity normalization. Whereas for this task [10] use the Brats2017 training dataset. Here a few preprocessing steps are performed such as intensity normalization. Chen et al. [11] also collect data within the context of brain image segmentation from the MRBrainS challenge. They adopt different brain image modalities including the T1, T1-IR, and T2-FLAIR of patients with diabetes.

2.2 Training Process and Classification

The training and the learning process involves the main architectures used to meet such tasks on the brain image processing. The methods are based on different learning process algorithms. Examples include supervised learning methods based on the transfer learning, unsupervised learning and fusion methods.

2.2.1 Transfer Learning

The transfer learning is a machine learning method based on the reuse of a model which is created for solving specific task as a starting point for another task. Within the context of brain disease detection the transfer learning is widely used. Within the context of brain disease diagnosis and detection such as the Alzheimer's disease [1] adopt the transfer learning using a pretrained VGG16 for Alzheimer's disease classification. Whereas [2] use the VGG19 for Alzheimer's disease prediction. The

transfer learning meet the need of the huge amount of data for training. However the VGG network used in this works is slow to train due to the huge number of the network parameters. Another transfer learning based on the inception model was proposed by [4] with the same training dataset to predict a diagnosis of Alzheimer disease using 18F-FDG PET of the brain data. The network consists of 11 inception modules. Each module incorporates a convolution layers, pooling layers and convolutional filters with rectified linear units. The main advantage of this work over the previous methods is the multi-level feature extraction. Khvostikov et al. [3] present a 3D Convolution Neural Network (CNN) architecture which consists of a set of convolutions blocks using a sMRI and DTI images as inputs for alzheimer disease classification. Each block is composed by a 3D convolution, batch normalization, rectifier linear unit and 3D pooling. The discriminate feature of this work is the fusion method of 2 different image modalities(sMRI and MD-DT) using a hippocampal Region of interest pooling (ROI). Here the inception model allows the extraction of the local and global features at the same time. However this work just handles 2D images. A recent work [12] of the same researchers consists of using a 3D inception model. Compared with their previous work the inception model decreases the number of network parameters and enhances the feature extraction process. Yang et al. [7] address the problem of the migraine classification and compare the inception model with the Alexnet to classify healthy brains, brains affected by Migraines with aura (MWA) and brains affected by Migraines without aura (MWoA). Within the context of brain image segmentation, [8] propose a multitask convolutional neural network for tumor brain instance segmentation. The learning process involves 2 stages. The first stage is a tumor detection using a region proposal network correlated with the though transform technique. The second stage is the tumor segmentation using the VGG19 network. Chen et al. [11] present a new deep residual learning namely deep voxelwise residual networks for brain segmentation also from 3D MR images. They propose a stacked of residual module(25 volumetric convolutional/deconvolutional). The main advantage here is the multi-modality and auto-context information fusion to enhance the segmentation task. Their method holds different image sizes.

2.2.2 Fusion Methods

In order to enable an effective feature extraction from brain images. Researches adopt fusion methods that extract special and temporal features using the Recurrent Neural Network (RNN) such as the Long short-term memory (LSTM) and the Bidirectional gated recurrent unit (BGRU) combined with the convolution neural network. The application of CNNs for 3D volumetric classification is difficult to optimize. To improve the CNN performance regarding the Alzheimer's diagnosis, [5] combine a 3D-CNN and fully stacked bidirectional (FSBi-LSTM) using a RMI and PET images. They compare different fusion methods such as FSBi-RNN,

FSBi-GRU. They point out that FSBi-LSTM is the best fusion method. The key contribution of this method is the multi-modal fusion which yields good results of diagnosis than a single modality methods. Another fusion method on the same the context demonstrated by [6] consists of a convolutional and bidirectional gated recurrent neural network using FDG-PET images. The 2D CNN is trained to capture the intra-slice features and the BGRU for the inter-slice feature extraction. Different from the previous work, they adopt 2 activation functions Tanh for the BGRU and the Rectified Linear Activation Function (ReLU) for the CNN. To improve the segmentation task, [9] combine the CNN with the LSTM for automatic brain tissue tumor segmentation for fmri voxel classification into 5 classes gray matter, white matter, blood vessel, non-brain (NB) and cerebrospinal fluid. The training encompasses spatial and temporal feature extraction.

2.2.3 Unsupervised Learning

The unsupervised leaning overcome the lack of labeled data within the context of the neuroimaging. Regarding the context of brain disease detection, [13] introduce a method to model the progression of Alzheimer's disease in the MRI brain images. They modify the Wasserstein training process by a AdaBoost learning in order to extract the more extreme cases of AD on the ADNI training dataset. Mallick et al. [14] also propose an unsupervised learning using a combination of the deep wavelet autoencoder and the deep neural network for brain cancer detection. The main contribution here over the existing methods is the feature reduction and the image decomposition using an autoencoder and the wavelet transformation. Authors compare their proposed network with other methods such as Autoencoder-DNN and Deep Neural Network (DNN). Within the context of brain image segmentation [10] notice that it is vital to improve the spatial contiguity of the network output by using unsupervised learning. Toward this end, they adopt an adversarial network using tow different CNN networks. This adversarial learning consists of a generator that generates synthetic labels and the discriminator tries to distinguish between the truth and the synthetic labels produced by the generator. Data augmentation and brain image generation is another challenging task. The generative adversarial network is extremely used to meed this task. Han et al. [15] propose to generate synthetic brain MR images using a deep generative adversarial network. They adopt unsupervised learning basing on a generator and discriminator network. The generator used up-convolutions layers with a non-linearity and batch-normalization in order to create synthetic images. The discriminator is another network that distinguish between the real and the generated images. Han et al. [16] use a progressive Generative Adversarial Network (pGAN) for brain MRI augmentation. Han et al. [17] improve the data augmentation by a cascade method that combines different GAN architectures to generate brain MR images without and with tumors separately. For this end they combine the noise-to-image GANs and image-to-image GANs. They also adopt a pGAN to generate brain images. Dar et al. [18] propose a method for a multi-contrast MRI synthesis using the conditional

generative adversarial network. For the registered images they use a pGAN to learn the function map between the source and the target image. They use a cGAN for the unregistered images. Yang et al. [19] adopt a cycleGAN with structure-constrained for synthesizing CT images from brain MR images.

For the classification both methods are based on the softmax classifier.

2.3 Results

The transfer learning based on the convolution neural network was widely used for the context of brain disease detection such as the Alzheimer's disease. Jain et al. [1] achieve accuracy of 95.73% using the VGG 16 to classify brain sMRI 2D slices into 3 different classes: AD, NC and MCI. Over the CNN architecture the inception model yields the best accurate results. This is illustrated by many researchers such as [3]. Here authors reach 0.933% for AD/NC binary, 0.867% for AD/MCI, 0.733% for MCI/NC and 0.68% ternary for AD/MCI/NC classification problem. Ding et al. [4] reaches a good results using an inception model for Alzheimer's early prediction about 75.8 months before the final diagnosis. Fusion method based on the combination of the CNN and RNN architectures also shows an accurate results on this context such as [5]. Regarding the unsupervised learning the GAN and the autoencoder are widely used by researchers for the brain disease diagnosis. Bowles et al. [13] return relevant results regarding the illustration of the Alzheimer's disease progression using the GAN. Mallick et al. [14] with the combination of the deep network and the autoencoder obtain an accuracy of 93% to detect brain cancer. The convolution neural network is also used extremely for the brain image segmentation and tumor classification. A cascade method proposed by [9] reach a classification accuracy of 84.04% to classify brain tumor and segmentation. Chen et al. [11] achieve the first place in a challenge including 37 contributions on brain image segmentation. Rezaei et al. [8] present a prominent result regarding the brain tumor instance segmentation using a multitask convolution neural network basing on VGG19. Whereas [10] with the GAN architecture obtain more reliable results on the brain tumor segmentation. Regarding the context of the brain image synthesis and generation, the GAN architectures are the first choice of many researchers. Kazuhiro et al. [20] shows a good results using a deep GAN on the MRI image generation. Whereas the fusion method [17, 21] that based on the combination of the different architectures of the GAN such as pGAN, cGAN provide more accurate results.

3 Conclusion and Current Challenges

Neuroimaging is an interdisciplinary filed devoted to the study of the brain structure, function, behavior and activity. This domain brings different fields such

as medicine, statistics, biology and computer science. The advancement of the brain imaging technique enhances the brain analysis. However it is critical to extract the meaningful information within these techniques. Deep learning fill this need. In the present paper, we highlight the main techniques used on the deep learning networks for brain image processing such as the data preparation, augmentation and the training process. For the data preparation and collection, there is a hardest question to meet which is the lack of annotated datasets for the supervised learning.

The preprocessing and feature extraction are another key steps for an effective brain image analysis. Significant efforts have been made to handle different preprocessing for various brain image modalities. It is crucial today to ensure an analysis methods that handle different image brain modalities in order to exploit the information within these images.

The generative adversarial networks were extremely used for the data augmentation on the brain images analysis to enhance the training process. This network was also widely used for the brain image super-resolution and synthesis. The Convolution neural network was applied for the brain images classification and brain diseases classification. The inception model is the most used among the CNN architectures. To improve the CNN performance on the image brain analysis researches combine it with the RNN networks such as the LSTM and the BGRU. To enhance the training process and optimize the network, researchers utilize different regulations methods such as dropout layer, batch normalization and data augmentation. The brain image processing includes different tasks such as brain image segmentation, generation, brain disease prediction and brain image enhancement.

However there is a need today for the image to text within the context of neuroscience to enhance the brain image understanding which is not found on the recent deep learning application regarding this context. There are many challenges regarding the brain image analysis today such as the early prediction of the brain disease before years. However this needs a huge amount of medical data. Another challenge is ensuring a unified infrastructure to share neuroimaging data. The data augmentation and synthetic data generation is trending today due to the lack of the annotated datasets. The brain activity analysis is another key challenge.

References

1. Jain, R., Jain, N., Aggarwal, A., Jude Hemanth, D.: Convolutional neural network based Alzheimer's disease classification from magnetic resonance brain images. Cogn. Syst. Res. **57**, 147–159 (2019)
2. Khan, N.M., Abraham, N., Hon, M.: Transfer learning with intelligent training data selection for prediction of Alzheimer's disease. IEEE Access **7**, 72726–72735 (2019)
3. Khvostikov, A., Aderghal, K., Benois-Pineau, J., Krylov, A., Catheline, G.: 3D CNN-based classification using SMRI and MD-DTI images for Alzheimer disease studies, Jan (2018)
4. Ding, Y., Sohn, J.H., Kawczynski, M.G., Trivedi, H., Harnish, R., Jenkins, N.W., Lituiev, D., Timothy, P.: A deep learning model to predict a diagnosis of Alzheimer disease by using 18f-FDG PET of the brain. Radiology **290**(2), 456–464 (2019)

5. Feng, C., Elazab, A., Yang, P., Wang, T., Zhou, F., Hu, H., Xiao, X., Lei, B.: Deep learning framework for Alzheimer's disease diagnosis via 3D-CNN and FSBi-LSTM. IEEE Access **7**, 63605–63618 (2019)
6. Liu, M., Cheng, D., Yan, W.: Classification of Alzheimer's disease by combination of convolutional and recurrent neural networks using FDG-PET images. Front. Neuroinform. **12**, 35 (2018)
7. Yang, H., Zhang, J., Liu, Q., Wang, Y.: Multimodal MRI-based classification of migraine: using deep learning convolutional neural network. BioMed. Eng. Online **17**(1):138 (2018)
8. Rezaei, M., Yang, H., Meinel, C.: Instance tumor segmentation using multitask convolutional neural network. In: 2018 International Joint Conference on Neural Networks (IJCNN). IEEE, July 2018
9. Ang, S.P., Phung, S.L., Schira, M.M., Bouzerdoum, A., Duong, S.T.M.: Human brain tissue segmentation in fMRI using deep long-term recurrent convolutional network. In: 2018 Digital Image Computing: Techniques and Applications (DICTA). IEEE, Dec (2018)
10. Li, Z., Wang, Y., Yu, J.: Brain tumor segmentation using an adversarial network. In: Brainlesion: Glioma, Multiple Sclerosis, Stroke and Traumatic Brain Injuries, pp. 123–132. Springer International Publishing (2018)
11. Chen, H., Dou, Q., Yu, L., Qin, J., Heng, P.-A.: VoxResNet: Deep voxelwise residual networks for brain segmentation from 3D MR images. NeuroImage **170**, 446–455 (2018)
12. Khvostikov, A., Aderghal, K., Krylov, A., Catheline, G., Benois-Pineau, J.: 3D inception-based CNN with SMRI and MD-DTI data fusion for Alzheimer's disease diagnostics. arXiv preprint arXiv:1809.03972 (2018)
13. Bowles, C., Gunn, R., Hammers, A., Rueckert, D.: Modelling the progression of Alzheimer's disease in MRI using generative adversarial networks. In: Angelini, E.D., Landman, B.A. (eds.) Medical Imaging 2018: Image Processing. SPIE, Bellingham, Mar (2018)
14. Mallick, P.K., Ryu, S.H., Satapathy, S.K., Mishra, S., Nguyen, G.N., Tiwari, P.: Brain MRI image classification for cancer detection using deep wavelet autoencoder-based deep neural network. IEEE Access **7**, 46278–46287 (2019)
15. Han, C., Hayashi, H., Rundo, L., Araki, R., Shimoda, W., Muramatsu, S., Furukawa, Y., Mauri, G., Nakayama, H.: Gan-based synthetic brain MR image generation. In: 2018 IEEE 15th International Symposium on Biomedical Imaging (ISBI 2018), pp. 734–738. IEEE (2018)
16. Han, C., Rundo, L., Araki, R., Furukawa, Y., Mauri, G., Nakayama, H., Hayashi, H.: Infinite brain MR images: PGGAN-based data augmentation for tumor detection. arXiv preprint arXiv:1903.12564 (2019)
17. Han, C., Rundo, L., Araki, R., Nagano, Y., Furukawa, Y., Mauri, G., Nakayama, H., Hayashi, H.: Combining noise-to-image and image-to-image gans: brain MR image augmentation for tumor detection. arXiv preprint arXiv:1905.13456 (2019)
18. Dar, S.U.H., Yurt, M., Karacan, L., Erdem, A., Erdem, E., Çukur, T.: Image synthesis in multi-contrast MRI with conditional generative adversarial networks. IEEE Trans. Med. Imaging **38**, 2375–2388 (2019)
19. Yang, H., Sun, J., Carass, A., Zhao, C., Lee, J., Xu, Z., Prince, J.: Unpaired brain MR-to-CT synthesis using a structure-constrained cyclegan. In: Deep Learning in Medical Image Analysis and Multimodal Learning for Clinical Decision Support, pp. 174–182. Springer (2018)
20. Kazuhiro, K., Werner, R.A., Toriumi, F., Javadi, M.S., Pomper, M.G., Solnes, L.B., Verde, F., Higuchi, T., Rowe, S.P.: Generative adversarial networks for the creation of realistic artificial brain magnetic resonance images. Tomography **4**(4), 159–163 (2018)
21. Gu, J., Li, Z., Wang, Y., Yang, H., Qiao, Z., Yu, J.: Deep generative adversarial networks for thinsection infant MR image reconstruction. IEEE Access **7**, 68290–68304 (2019)

Discrete Optimization Model of Free-Fall-Flow-Rack Based Automated Drug Dispensing System

Dhiyaeddine Metahri and Khalid Hachemi

1 Introduction

Medicine is changing paradigm; it is switching from diagnosis and treatment to prediction and prevention. This is encompassed in the new concept of Predictive, Preventive and Personalized Medicine (PPPM). "True personalised medicine" is based on the "individual patient profile" directing to a tailored therapy that maximises the efficacy for that one patient in particular [12].

Going from a reactive medicine to a proactive medicine has multiple consequences for the management of the medication-use process within a healthcare structure, including an increase in the number of drug references underlying the individualization of treatments. In this context, automated dispensing systems are a key choice to meet the demands of speed and accuracy of patient service.

Materials handling technologies have enabled companies to control and manage their inventory. This can be achieved through an automated storage and retrieval system (AS / RS). AS / RSs are used in multiple industries and advanced manufacturing systems [30]. The main advantages of these systems are the saving of labor and floor space costs, the ease and speed of handling items and enhance throughput [21].

The main components of an AS/RS are storage racks, aisles, storage and retrieval (S/R) machines, Input/output stations (I/O) stations and the control system. Racks consist of several bins that can store items. The racks are separated by aisles, which allow the movement of storage and retrieval machines to pick up and drop off loads.

D. Metahri · K. Hachemi (✉)
Institute of Maintenance and Industrial Safety, Oran 2 Mohamed Ben Ahmed University, Oran, Algeria
e-mail: hachemi.khalid@univ-oran2.dz

L. Chaari (ed.), *Digital Health in Focus of Predictive, Preventive and Personalised Medicine*, Advances in Predictive, Preventive and Personalised Medicine 12,
https://doi.org/10.1007/978-3-030-49815-3_11

The Input/output stations (I/O) receive incoming and outgoing products. The control system is used for managing storage and retrieval operations.

There are different types of ASRS, namely, unit-load AS/RS, mini-load AS/RS, man-on-board AS/RS, carousel AS/RS, multi aisles AS/RS, Mobil-racks AS/RS, and flow-rack AS/RS (deep-lane AS/RS).

A new kind of flow-rack AS/RS has been introduced by MEKAPHARM [23], this system is served by a human operator or a single machine for storage operations, and combines the free-fall movement and a transport conveyor for retrieval operations. It can operate without any storage/retrieval machines, compared to the classic flow-rack AS/RS, where the system uses a (S/R) machine.

Since AS/RS require a very high investment, the design of AS/RS represents a crucial step during the feasibility conception study. In fact, once the AS/RS is implemented, it is very difficult to modify the rack layout and storage capacity. For this, the purpose of this paper is to find the optimal dimensions (length, height and depth) of the rack, which minimize the retrieval-travel-time. We formulate the optimization problem as a non-linear discrete model instead of a continuous model, which does not reflect the discrete nature of the rack. The aim of this study is to give a practical support to the AS/RS designer.

The structure of the paper is as follows. Section 2 gives an overview of the previous research. The FF-flow-rack AS/RS operation and structure are presented in Sect. 3. The optimization model and the obtained results are provided and discussed in Sect. 4. Section 5 draw conclusion and further research.

2 Literature Review

Different approaches have been proposed to increase the AS/RS performance by the means of request sequencing, storage assignment policy, and system configuration. The expected travel time was the main indicator used to assess the AS/RS performance.

Several studies exist on the modelling of the expected travel time. The most interesting approach to this issue has been proposed by Bozer and White [5]. They developed the expected single and dual travel time models of a rectangular rack under a random storage and for different positions of input/output point. Additionally, various dwell-point strategies for the storage/retrieval machine were examined. This model was used by Sari et al. [28], where they presented two mathematical models for the expected travel-time for a flow-rack AS/RS, which use two (S/R) machines. The first model is developed by using a continuous approach and compared with a second discrete model for accuracy via simulation. The authors conclude that the expressions based on continuous approach are extremely practical due to the difference in computation time.

For other flow-rack AS/RS variations, Sari and Bessnouci [27] have proposed a new kind of flow-rack AS/RS that using a single machine for both storage and retrieval operations instead of two machines. They developed analytical-travel-time

models of the storage and retrieval machine, under randomized storage assignment. Two dwell point positions were considered. Otherwise, De Koster et al. [10] used a lifting mechanism in the opposite face of the S/R machine for a flow-rack AS/RS. They presented a closed-form expression of expected retrieval travel-time for single-command cycles, and derived an approximate travel-time expression for dual command cycles of the system. Also, Chen et al. [7] designed a bi-directional flow-rack (BFR) in which bins in adjacent columns slope to opposite directions. They develop a travel-time model for BFR systems.

Various methods have been proposed to deal with reducing the travel time for the flow-rack AS/RS. Sari et al. [29] Studied the impact of P/D stations and restoring conveyor locations on expected retrieval-time and classified their optimal positions. Meghelli-Gaouar and Sari [22] used a two class-based storage policy for the flow-rack AS/RS, where each item is assigned to the same bin as closely as possible to the P/D point. This work was extended by Bessenouci et al. [4] by developing two metaheuristic algorithms (tabu search and simulated annealing) applied to the control of the S/R machine. Hachemi and Alla [13] presented an optimization method of retrieval sequencing where the AS/RS was represented by a colored Petri net model. In a recent paper, Hachemi and Besombes [14], extended the problem of retrieval sequencing for flow-rack AS/RS by integrating the product expiry date. They introduced an optimization method as a decision process which performs a real-time optimization into two phases and formulated as an integer program. Kota et al. [16] Developed analytical expressions for retrieval times and heuristic algorithms to determine optimal or near-optimal movement of objects in a high-density, puzzle-based storage system.

Various researchers study the sequencing problem for different type of AS/RS. Chung and Lee [8] **i**ntroduced heuristic methods to solve a generalized sequencing problem for unit-load AS/RS. These methods determine both specific bin locations for the retrieval requests and sequencing with the chosen bin locations. From a series of realistic case problems Kuo et al. [18] proposed a cycle-time model for class-based storage policies for automated unit load AS/RS that use autonomous vehicle technology. The model was designed specifically for the practice of AVS/RS design conceptualization by utilizing a network queuing approach. In order to minimize the distance travelled by the Storage and Retrieval (S/R) machine. Asokan et al. [3] implemented non-traditional optimization techniques (Adaptive Genetic Algorithm (AGA) and Particle Swarm Optimization (PSO)). In order to optimize the performance of man on board AS/RS, Dallari et al. [9] compares different storage policies with two tour construction heuristic. Authors conclude that the introduction of BI heuristic and class based storage policy provide substantial travel time reduction. According to (Fohn et al. [11]; Robert terry et al. [26]), AS/RS designs are difficult because these systems evolve in highly dynamic environments. For this, an optimal design procedure should be combined with control policies.

AS/RS design has received some attention in the literature. Ashayeri et al. [2] proposed a microcomputer-based optimization model to calculate the optimum number of racks and the optimum width and length of automated warehouses**.** Malmborg [20] studied the design and modelling of double-shuttle AS/RS.

Kuo et al. [17] proposed effective design calculation models for unit load AS/RS using autonomous vehicle technology. Yang et al. [32] deals with the optimization of 3D multi-deep AS/RS with a full turnover-based storage policy by considering the operating characteristics of the S/R machine, to close to the real operation of the compact warehouse.

De Koster et al. [10] derived the expressions of the expected travel time for single and dual command cycle of flow-rack AS/RS that used a lifting mechanism. They used these expressions to optimize the systems dimensions. The authors found that the cubic-in-time system (i.e. all dimensions are equal in time) is not the optimal configuration. This work was extended by Yang et al. [31], who considered the real operating characteristics of the S/R machine to obtain the optimal rack dimensions. Concerning the AS/RS introduced by Sari and Bessnouci [27]. Hamzaoui and Sari [15] determined the optimal dimensions of this AS/RS by using an enumeration technique. These dimensions minimize the expected travel times of the S/R machine.

An interesting study that was presented by Meneghetti et al. [24]. The authors proposed the adoption of a two-stage design approach of unit-load AS/RS by taking into account the economical and environmental perspectives (energy consumption, costs and carbon dioxide emissions). Based on discrete events simulation Caputo and Pelagagge [6] check and identify correct design choices for capacity upgrade of large-intensive material handling and storage systems. Asef-Vaziri et al. [1] designed and analyzed an automated container handling and storage system, which integrates AS/RS and Automated Guided Vehicle Systems (AGVS) for use at seaport terminals. They performed a computer simulation study to show the impact of such automation on the system performance (throughput, space utilization, and equipment utilization). Lättilä et al. [19] developed a decision-making tool based on the combination between static spreadsheet modelling and Monte Carlo simulation. This tool was used to compare warehouse design, calculate investment payback time of two suggested AS/RS investments, and to identify the main factors affecting their economic feasibility.

3 FF-Flow-Rack AS/RS

3.1 System Description and Structure

Mekapharm company® has launched a new type of flow-rack AS / RS, known under the trade name “APOTEKA” [23]. It is mainly used in all areas handling products resistant to free fall impact, and in particular for the automation of drug distribution in pharmacies. We are referring to the new type of AS / RS: the Free-Fall-flow rack AS/RS, or FF-Flow-rack AS/RS. The most important divergence between the FF-flow-rack AS/RS and the other types of flow-rack AS/RS presented by (Sari et al. [28]; De Koster et al. [10]; Sari and Bessnouci [27]) is that the picking operations

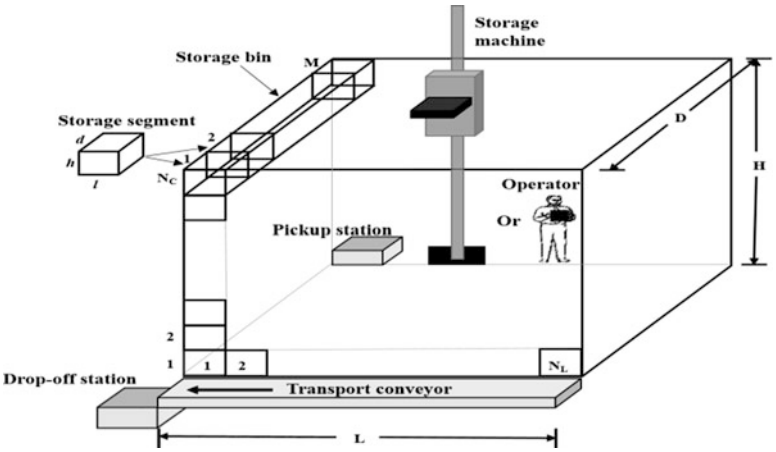

Fig. 1 Typical configuration of FF-flow-rack AS/RS

are realized by combining the free-fall movement and transport conveyor to replace the retrieval machine.

The use of FF-flow-rack AS/RS has several advantages like: saving the floor space, better inventory management, throughput increasing, and removal of the S/R machines. Especially, in the pharmaceutical distribution, this system offers the possibility of simultaneous retrieval of several drugs, reduces customer wait time, reduces queue sizes leading more time for advising customers, and reduces the dispensing error.

As shown in Fig. 1, the FF-flow-rack AS/RS structure is built of: a deep rack with a multitude of sloping bins, equipped with rolling wheels to allow the sliding of products by gravity from the storage to the picking side. Each bin is made of a set of segments (locations) that contains multiple identical products (the same SKU: Stock Keeping Unit) placed according to a FIFO file. A pickup station is located on the storage side, and a drop-off station is located on the retrieval side. A transport conveyor used to make the connection between the rack and the drop-off station. An operator or a storage crane performs the storage of items. The Fig. 2 shows a real view of the Apoteka© system.

As illustrated in Fig. 1, the rack dimensions are: length (L), height (H) and depth (D). The rack has (N_L) bins in each tier and (N_c) bins in each column. Each bin has (M) storage segments. Since the use of a person for the storage operation, the maximum height of the rack should be less than 3 m, in regard to practical and ergonomic considerations.

Fig. 2 Real view of the Apoteka system

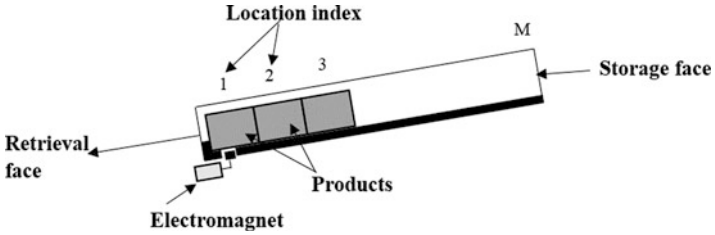

Fig. 3 Product layout inside a storage bin

3.2 System Operation

The FF-flow-rack AS/RS operating is as follows:

(a) The storage operation is fulfilled by a storage machine or an operator, where the products are moved from the pickup station to store them in the corresponding bins.
(b) The retrieval operation is done in two steps: The first one is the ejection of the item, where it is accomplished by the excitement of the electromagnet of the bin containing the desired product. This induces the free fall of the product on the transport conveyor. The second step is the product transport by the conveyor until the drop-off station.

The ejection of a product causes the progressive sliding by the gravity of all other products in the bin, as shown in Fig. 3 that highlight the layout of products inside a bin.

3.3 Retrieval Travel Time Model

Eq (1) gives expected retrieval-travel-time models that have been developed by Metahri and Hachemi [25].

$$E\left(T_g'\right) = \frac{1}{2\,V_c}L + \frac{2}{3}\sqrt{2H/g} \tag{1}$$

Where:

L, H the length and height of the rack
V_c the speed of the transport conveyor
g the acceleration due to gravity
$E\left(T_g'\right)$ the expected retrieval travel-time

4 Rack Dimensions Optimization

4.1 Problem Statement

The rack dimensions are a key of AS/RS performance improvement.

However, space constraints require that rack dimensions must not exceed the admissible values (L_A, H_A, D_A), the storage capacity is fixed into N storage segments, and the segment dimensions (l, h, d) are predefined. Consequently, there are several possible configurations to design this system (See Fig. 4), so what are the optimal rack-dimensions that lead to the minimum retrieval travel time? In order to solve this problem, we built an optimization model where the objective function to be minimized is the non-linear function of the retrieval travel time $E\left(T_g'\right)$.

To purchase this aim, we have developed a discrete optimization model which matches more accurately the real nature of the rack. Indeed, the enumeration technique is not practical because it leads to a combinatorial explosion, while a continuous model does not reflect the nature of the rack. In the continuous approach, approximating a solution to the nearest integer does not necessarily correspond to the optimal solution.

4.2 Optimization Model Formulation

Let us first introduce the following notations.

Parameters:

L_A, H_A, D_A the admissible length, height and depth of the rack
l, h, d the length, height and depth of a storage segment.

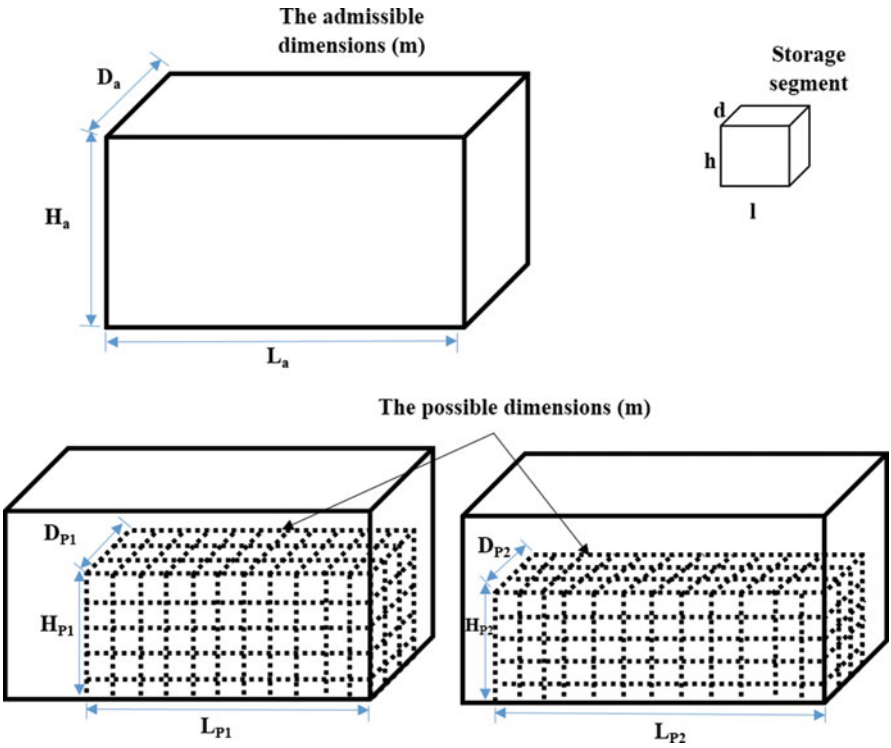

Fig. 4 Depiction of the admissible and possible rack dimensions

N_{LA}, N_{CA}, M_A the admissible number of bins per line, column and segments in each bin. Where: $N_{LA} = L_A/l$, $N_{CA} = H_A/h$, $M_A = D_A/d$.

V_c the speed of the transport conveyor

N the storage capacity (total number of bins)

N_A the admissible storage capacity

Variables:

m the number of bins per line

n the number of bins per column

q the number of segments in each bin

Recall that $E\left(T'_g\right) = \frac{1}{2\,V_c}L + \frac{2}{3}C\sqrt{H}$

$m = L/l$, $n = H/h$, $q = D/d$

So, the optimization problem can be formulated as follows:

$$\min \frac{1}{2\,V_c}m + \frac{2}{3}C\sqrt{n} \tag{2}$$

Subject to the following constraints:

$$m \leq N_{LA} \tag{3}$$

$$n \leq N_{CA} \tag{4}$$

$$q \leq M_A \tag{5}$$

$$m * n * q \geq N \tag{6}$$

$$m, n \text{ and } q \text{ are integer} \tag{7}$$

Where:

- The objective (2) minimizes the retrieval time,
- The constraints (3, 4 and 5) ensure that the dimensions of the rack are limited to the admissible values.
- The constraint (6) allows the rack storage capacity to be greater or equal to the admissible storage capacity.
- The constraint (7) ensures that decision variables are integers.

We propose a flow chart that effectively shows the different part of the discrete optimization model. As outlined in Fig. 5, the model evolves the following phases:

- Initialization of system parameters such as the storage capacity N, the admissible dimensions of the rack (L_A, H_A, D_A), the storage segment dimensions (l, h, d), and the transport conveyor velocity V_c.
- Determination of the resulted optimal dimensions of m, n, and q which are noted N_{Lo}, N_{Co}, M_o, respectively. Where: $N_{Lo} = L_o/l$, $N_{Co} = H_o/h$, $M_o = D_o/d$.

4.3 Optimization Results and Discussion

In order to show the effectiveness of the optimization method, we consider different configurations of industrial-sized problems with a storage capacity ranging from 400 to 27,000 segments. For each storage capacity, we assumed that the dimensions of storage segment are $(l, h, d) = (0.15; 0.10; 0.10)(m)$, and the transport conveyor velocity is: $V_C = 3m/s$.

Moreover, the optimization problem is solved using Generalized Reduced Gradient (GRG) solver, and executed on a PC with 2.17 GHz CPU and 2 GB RAM. In our study, we used the GRG solver because the optimized model is a discrete nonlinear problem.

To illustrate the optimization procedure, Table 1 presents the optimization results of 20 storage capacities. Columns 2, 3 and 4 of this table represent the studied storage capacity (N), the admissible dimensions (L_A, H_A, D_A) and the optimal

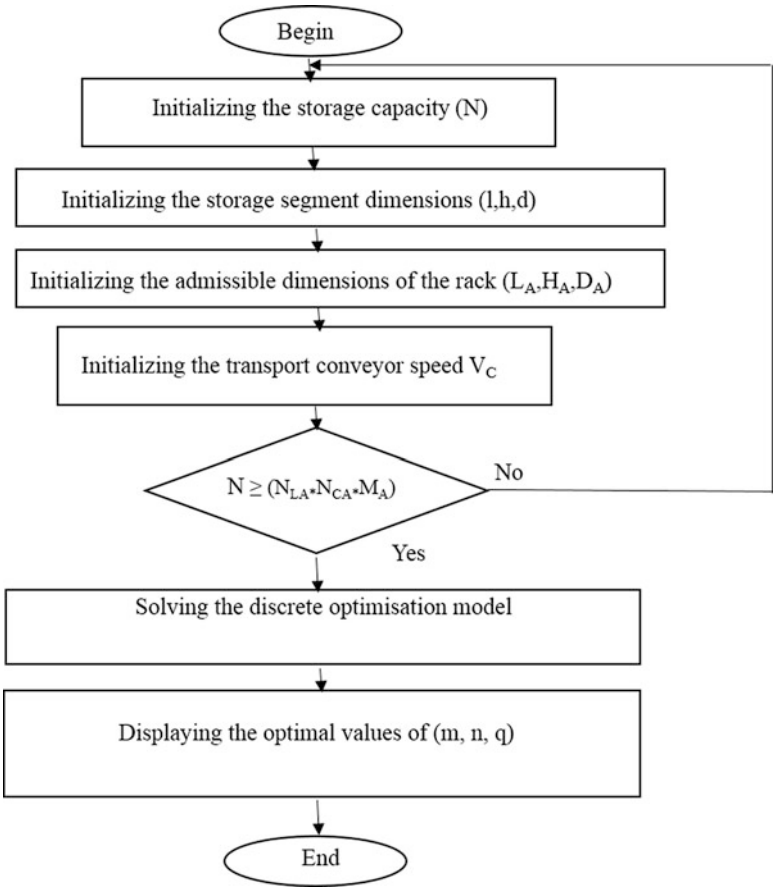

Fig. 5 Flow chart of the discrete optimization model

configuration (N_{Lo}, N_{Co}, M_o), respectively. While, Columns 5 and Column 6 represent the optimal dimensions (L_o, H_o, D_o) and their corresponding retrieval travel time $E\left(T_g'\right)$, respectively.

The analysis of the results allowed us to make the following insights:

- The optimal rack is not cubic-in-time (i.e. travel time along length, high, and depth are not equal).
- The optimization model tends generally to choose the maximum possible depth, and prevails rather the height to the length.
- The computing time is very short (few seconds).

Table 1 Optimal rack configuration for a different storage rack capacity

	N	The admissible dimensions (m)			The optimal configuration			The optimal dimensions (m)			$E\left(T_g'\right)$
		L_A	H_A	D_A	N_{Lo}	N_{Co}	M_o	L_O	H_O	D_O	
1	400	2	1	0.6	8	10	5	1.2	1	0.5	0.501016
2	500				10	10	5	1.5	1	0.5	0.551016
3	600				10	10	6	1.5	1	0.6	0.551016
4	900	4	1.5	0.8	10	15	6	1.5	1.5	0.6	0.618668
5	1000				20	10	5	3	1	0.5	0.801016
6	1200				10	15	8	1.5	1.5	0.8	0.618668
7	1400				20	10	7	3	1	0.7	0.801016
8	1800	6	2	1	9	20	10	1.35	2	1	0.650701
9	2000				10	20	10	1.5	2	1	0.675701
10	2500				25	10	10	3.75	1	1	0.926016
11	3000				15	20	10	2.25	2	1	0.800701
12	4000				20	20	10	3	2	1	0.925701
13	5000	8	2.5	1.2	20	25	10	3	2.5	1	0.975948
14	6000				20	25	12	3	2.5	1.2	0.975948
15	7000				28	25	10	4.2	2.5	1	1.175948
16	8000				32	25	10	4.8	2.5	1	1.275948
17	10,000	15	3	1.5	40	25	10	6	2.5	1	1.475948
18	21,000				50	28	15	7.5	2.8	1.5	1.753696
19	24,000				64	25	15	9.6	2.5	1.5	2.075948
20	27,000				60	30	15	9	3	1.5	2.021375

5 Conclusion

According to the fact that automated drug dispensing systems better meet the requirements of the PPP medicine, we are interested, in this paper, in the determination of the optimal configuration of an automated dispensing system based on a free-fall-flow-rack AS/RS. A useful way to do this is to determine the expression of the expected retrieval travel time and minimize it through an optimization model. We first presented an overview of the FF flow-rack AS/RS structure and then we presented its analytical retrieval time. Subsequently, we formulate this problem as a discrete nonlinear optimization model, which is solved by using Generalized Reduced Gradient (GRG) solver.

To show the power of the optimization method we applied the proposed model on different rack configurations under the constraints on the admissible dimensions and storage capacity. The results show that rack configuration has a significant effect on the expected retrieval time, and the optimal rack is not cubic-in-time (i.e. travel time along length, high, and depth are not equal). In addition, we find that the optimization model generally favors longer depth over the other two dimensions in retrieval time optimization. Note that the solving time for industrial sized rack configurations is very short (few seconds). This optimization method could be very useful for the AS/RS designer. Subsequently, according to numerical study the optimization model tends generally to choose the maximum possible depth then it prevails rather the height to the length. This optimization method could be used to give a decision support to the AS/RS designer.

In our future research, we will perform a comparison study in order to evaluate the gap between this approach and the continuous optimization approach, and investigate the optimal location of the drop-off station that minimize the retrieval travel time of the FF-flow-rack AS/RS.

References

1. Asef-Vaziri, A., Khoshnevis, B., Rahimi, M.: Design and analysis of an automated container handling system in seaports. Int. J. Agile Syst. Manag. **3**(1–2), 112–126 (2008)
2. Ashayeri, J., Gelders, L., Wassenhove, L.V.: A microcomputer-based optimization model for the design of automated warehouses. Int. J. Prod. Res. **23**(4), 825–839 (1985)
3. Asokan, P., Jerald, J., Arunachalam, S., Page, T.: Application of adaptive genetic algorithm and particle swarm optimisation in scheduling of jobs and AS/RS in FMS. Int. J. Manuf. Res. **3**(4), 393–405 (2008)
4. Bessenouci, H.N., Sari, Z., Ghomri, L.: Metaheuristic based control of a flow rack automated storage retrieval system. J. Intell. Manuf. **23**(4), 1157–1166 (2012)
5. Bozer, Y.A., White, J.A.: Travel-time models for automated storage/retrieval systems. IIE Trans. **16**(4), 329–338 (1984)
6. Caputo, A.C., Pelagagge, P.M.: Capacity upgrade criteria of large-intensive material handling and storage systems: a case study. J. Manuf. Technol. Manag. **19**(8), 953–978 (2008)
7. Chen, Z., Li, X., Gupta, J.N.: A bi-directional flow-rack automated storage and retrieval system for unit-load warehouses. Int. J. Prod. Res. **53**(14), 4176–4188 (2015)

8. Chung, E., Lee, H.F.: A generalised sequencing problem for unit-load automated storage and retrieval systems. Int. J. Ind. Syst. Eng. **2**(4), 393–412 (2007)
9. Dallari, F., Marchet, G., Ruggeri, R.: Optimisation of man-on-board automated storage/retrieval systems. Integr. Manuf. Syst. **11**(2), 87–93 (2000)
10. De Koster, R.M.B., Le-Duc, T., Yugang, Y.: Optimal storage rack design for a 3-dimensional compact AS/RS. Int. J. Prod. Res. **46**(6), 1495–1514 (2008)
11. Fohn, S.M., Greef, A.R., Young, R.E., O'Grady, P.J.: A constraint-system shell to support concurrent engineering approaches to design. Artif. Intell. Eng. **9**(1), 1–17 (1994)
12. Golubnitschaja, O., Baban, B., Boniolo, G., Wang, W., Bubnov, R., Kapalla, M., et al.: Medicine in the early twenty-first century: paradigm and anticipation-EPMA position paper 2016. EPMA J. **7**(1), 23 (2016)
13. Hachemi, K., & Alla, H. (2008). Pilotage dynamique d'un système automatisé de stockage/déstockage à convoyeur gravitationnel. J. Eur. Syst. Automatisés (JESA), 42(5/2008), 487–508
14. Hachemi, K., Besombes, B.: Integration of products expiry dates in optimal scheduling of storage/retrieval operations for a flow-rack AS/RS. Int. J. Ind. Syst. Eng. **15**(2), 216–233 (2013)
15. Hamzaoui, M.A., Sari, Z.: Optimal dimensions minimizing expected travel time of a single machine flow rack AS/RS. Mechatronics. **31**, 158–168 (2015)
16. Kota, V.R., Taylor, D., Gue, K.R.: Retrieval time performance in puzzle-based storage systems. J. Manuf. Technol. Manag. **26**(4), 582–602 (2015)
17. Kuo, P.H., Krishnamurthy, A., Malmborg, C.J.: Design models for unit load storage and retrieval systems using autonomous vehicle technology and resource conserving storage and dwell point policies. Appl. Math. Model. **31**(10), 2332–2346 (2007)
18. Kuo, P.H., Krishnamurthy, A., Malmborg, C.J.: Performance modelling of autonomous vehicle storage and retrieval systems using class-based storage policies. Int. J. Comput. Appl. Technol. **31**(3–4), 238–248 (2008)
19. Lättilä, L., Saranen, J., Hilmola, O.P.: Decision support system for AS/RS investments: real benefits out of Monte Carlo simulation. Int. J. Technol. Intell. Plan. **9**(2), 108–125 (2013)
20. Malmborg, C.J.: Interleaving models for the analysis of twin shuttle automated storage and retrieval systems. Int. J. Prod. Res. **38**(18), 4599–4610 (2000)
21. Mathisen, K.: From traditional stacks to an automated storage and retrieval system. Libr. Manag. **26**(1/2), 97–101 (2005)
22. Meghelli-Gaouar, N., Sari, Z.: Assessment of performance of a class-based storage in a flow-rack AS/RS. J. Stud. Manuf. **1**(2–3), 100–107 (2010)
23. MEKAPHARM: C. Fiche caractristiques de l'automate APOTEKA (2016). http://mekapharm.com/apoteka/.1999. Accessed 22 Oct 2016
24. Meneghetti, A., Borgo, E.D., Monti, L.: Decision support optimisation models for design of sustainable automated warehouses. Int. J. Shipp. Transport. Logist. **7**(3), 266–294 (2015)
25. Metahri, D., Hachemi, K.: Retrieval–travel-time model for free-fall-flow-rack automated storage and retrieval system. J. Ind. Eng. Int. **14**(4), 807–820 (2018)
26. Robert Terry, W., RAO, H.G., SON, J.Y.: Application of a computer-based approach to designing real-time control software for an integrated robotic assembly and automated storage/retrieval system. Int. J. Prod. Res. **26**(10), 1593–1604 (1988)
27. Sari, Z., Bessnouci, N. H.: Design & modeling of a single machine flow rack AS. RS, proceeding of IMHRC2012, Gardanne, France (2012)
28. Sari, Z., Saygin, C., Ghouali, N.: Travel-time models for flow-rack automated storage and retrieval systems. Int. J. Adv. Manuf. Technol. **25**(9), 979–987 (2005)
29. Sari, Z., Grasman, S.E., Ghouali, N.: Impact of pickup/delivery stations and restoring conveyor locations on retrieval time models of flow-rack automated storage and retrieval systems. Prod. Plan. Control. **18**(2), 105–116 (2007)
30. Van Den Berg, J.P., Gademann, A.J.R.M.: Simulation study of an automated storage/retrieval system. Int. J. Prod. Res. **38**(6), 1339–1356 (2000)

31. Yang, P., Miao, L., Xue, Z., Qin, L.: Optimal storage rack design for a multi-deep compact AS/RS considering the acceleration/deceleration of the storage and retrieval machine. Int. J. Prod. Res. **53**(3), 929–943 (2015)
32. Yang, P., Yang, K., Qi, M., Miao, L., Ye, B.: Designing the optimal multi-deep AS/RS storage rack under full turnover-based storage policy based on non-approximate speed model of S/R machine. Transport. Res. Part E Logist. Transport. Rev. **104**, 113–130 (2017)

Intuitive and Intelligent Solutions for Elderly Care

Neja Samar Brenčič, Marius Dragoi, Irina Mocanu, and Tomasz Winiarski

1 Introduction

Vast demand for some particular, advanced and seamless solutions is spurring from current demographic realities, aging population, and burden of chronic diseases. Changing life-style related illnesses, increased demands of people for new, more sophisticated therapeutic and care methods are stretching the limits of innovations, specifically for the respected field considered in this article, the increase of symp-

This work was supported by a grant of the Romanian National Authority for Scientific Research and Innovation, the AAL Program with co-funding from the Horizon 2020 program projects "IONIS – Improving the quality of life of people with dementia and disabled persons" – AAL2017-AAL-2016-074-IONIS-1 and AAL-2016-074-IONIS-2 and – INCARE – Integrated Solution for Innovative Elderly Care", project number AAL-2017-059-INCARE, by the Slovenia Ministry of Public Administration and by the subsidiary contract "CoRSAr" no. 1226/22.01.2018 for the grant 53/05.09.2016, ID 40270, cod MySMIS: 105976.

N. S. Brenčič (✉)
IZRIIS Institute, Ljubljana, Slovenia
e-mail: neja.samar-brencic@izriis.si

M. Dragoi
IT Center for Science and Technology, Bucharest, Romania

I. Mocanu
Computer Science Department, University Politehnica of Bucharest, Bucharest, Romania
e-mail: irina.mocanu@upb.ro

T. Winiarski
Institute of Control and Computation Engineering, Warsaw University of Technology, Warszawa, Poland
e-mail: tomasz.winiarski@pw.edu.pl

L. Chaari (ed.), *Digital Health in Focus of Predictive, Preventive and Personalised Medicine*, Advances in Predictive, Preventive and Personalised Medicine 12,
https://doi.org/10.1007/978-3-030-49815-3_12

toms and consequences related to older age, (like Alzheimer's disease, Dementia and Cognitive impairment). The European Commission in light of the challenge that also concerns stakeholders worldwide is encouraging many streams of endeavors. One of them being innovation in introducing solutions based on new models of services and state-of-the-art technology. Health services and home care services at a distance are the future for the aging population in many countries of the world. They present the possibility for building a sustainable health care system and contribution to a better life for older adults.

In this context, the current work is focusing on two Active and Assisted Living (AAL) projects which are developing information and communications technology (ICT) based platforms to support elderly persons and their caregivers. Both AAL IONIS [12] and AAL INCARE [11] projects originate from the very successful NITICS project [13, 17, 18]. In addition, contributions from the CoRSAr project (Platforma de Programare si Configurare a Robotilor Sociali si Asistivi) which is focusing on robotic based functionalities are also included in this research. IONIS exploits the innovation in NITICS and extends the platform with new technologies and upgraded services dedicated to persons suffering from mild cognitive impairment or incipient dementia and to their caregivers. It offers a fully integrated and validated solution at an affordable cost and with a high degree of personalization. IONIS is developed by exploiting location based services, sleep quality monitoring, communication services and the NITICS functionalities in order to offer continuous support at home (indoor area) and outside (outdoor area). A user-centered design involves extensive trials and piloting employed to both develop and validate the IONIS solution. The INCARE platform is extending NITICS with robotic features following a similar path as the CoRSAr project which can offer active support to the end-users, as exemplified further in this work. All presented projects implement functionalities specific for predictive (health, mobility and sleep patterns), preventive (medication compliance, hazard detection and enhanced activity) and personalized (e.g. robotic platforms).

2 Results and Discussions

2.1 End-User Involvement

A user-centered design was implemented in both IONIS and INCARE by involving elderly and caregivers during the whole development process. User input was also gathered in CoRSAr focusing on the perception of robotic platfomrs. Some important findings of the IONIS multinational survey and conjoint analysis are presented next.

A multinational survey The survey was carried out in four countries: Hungary, Poland, Romania and Slovenia. A total number of 121 primary (elderly) and 103 secondary (caregivers) users filled the dedicated questionnaires. The primary users

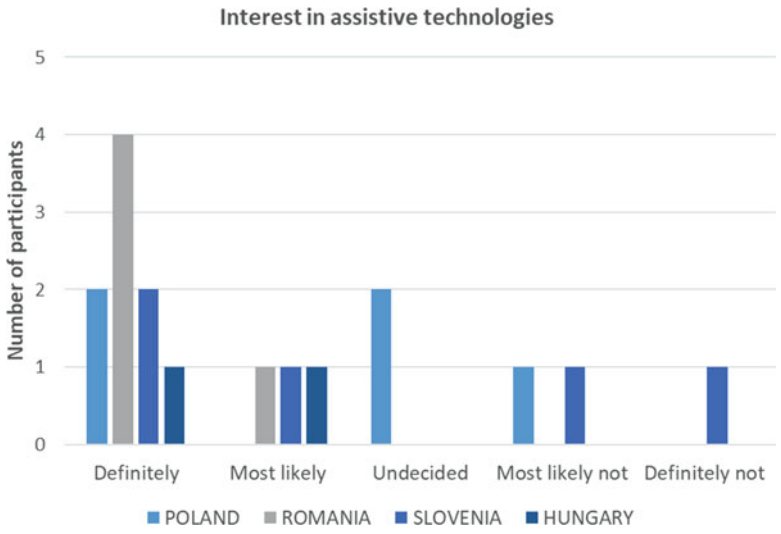

Fig. 1 Interest in using Assistive Technologies among the survey participants

were selected based on their score in the Mini-Mental State Examination (MMSE) test, the eligibility criterion being the presence of mild cognitive impairment or mild dementia signs (MMSE score 19–27 points).

The questionnaires focused on data useful for services design, implementation and testing, such as the living conditions, caregiving status and technology experience. Additional data covered the socialization activities of the primary users, their health status and acceptance [15] of the proposed IONIS services and their financial costs, memory impairment, sleep problems and independence in everyday tasks performed home and outdoors. The processed data was exploited in order to elaborate the Persona Cards and to generate reliable and realistic representations of potential elderly users. The survey results have shown that, although the primary users are generally not acquainted with the ICT solutions, the majority of them perceives the proposed services as useful (see Fig. 1). Most of the participants (70%) would definitely or most likely use Assistive Technology to help them in the activities of daily living. 15% of participants are not interested in Assistive Technologies and would most likely or definitely not use it. About 53% of included participants would definitely use Assistive Technology, 17.6% would most likely use it, about 16% of included participants would most likely or definitely not use it and 11.8% are undecided.

Conjoint analysis The goal of performing a conjoint analysis was to order the users' preferences towards the IONIS functionalities and their possible implementation. A thorough conjoint user preference analysis was designed and implemented at this stage involving 61 total end-users (representing assisted persons and caregivers) from the same four end-user countries. Elderly and their informal caregivers expressed almost similar preferences, with a very small difference for the reminders

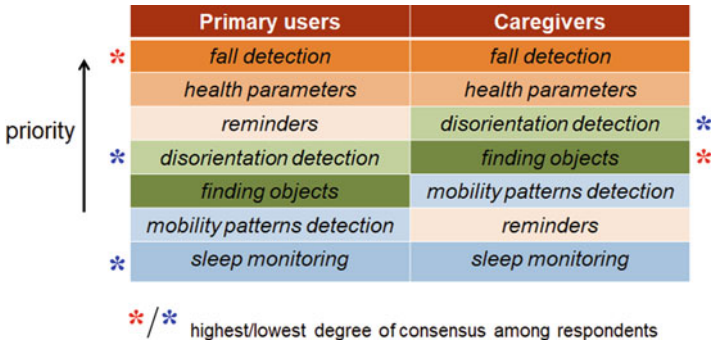

Fig. 2 End-user preferences for the identified services/functionalities

functionality. This scored much higher (3rd) for the elderly than for the caregivers (5th), trumping both the disorientation detection and finding objects (see Fig. 2). The main conclusion regarding the reminders functionality is that both the elderly and the caregivers appraised the email alternative as the least useful with almost the same levels of consensus. Also, both groups valued visual messages with approximately the same 'strength', but the persons in need found the voice messages as being the most useful.

2.2 Novel ICT Approaches in IONIS and INCARE

Both IONIS and INCARE projects follow an intelligent and innovative approach regarding the technologies considered in their integration. Particularly, INCARE aims to integrate robotic platforms as service robots. Additionally, distributed AI approaches are considered for privacy compliance purposes. In this section, we present an overview the end-user needs identified in elderly-robot interaction experiments, a laboratory environment example to be tested within INCARE and recent trends in federated learning.

Elderly-robot interaction For a successful integration in elderly care environments, robots must be carefully designed such that their appearance and functionality match the needs and expectations of both elderly and caregivers [8, 16]. The human necessities and reception of robots within an elderly care environment are usually identified through the use of questionnaires, focus groups and live sessions. The quality evaluation of human-robot interaction in the context of elderly care is focused on the quality of life impact for the caregivers and caretakers [8], but also on psychological and behavioral effects on the elderly, such as decreases in their level of stress and loneliness and improvements in their predisposition to engage in communication activities and overall mood [4]. A review on the robot acceptance identifies age, gender, experience with technology and cultural background as human factors, while appearance, human resemblance and dimensions, gender and

personality are the robot characteristics of high importance [3]. Concern is also directed towards personal data confidentiality and the assessment of the risks and benefits [1]. According to multiple studies, robots resembling human beings usually receive a negative feedback, the robots with a more machine-like appearance being preferred [1, 3, 16, 24].

In general, the preexisting attitudes towards robots proved to be a major factor in their acceptance [20]. In [2], the previous perception of robots and the quality of experience in a setup examining the feelings of the patients during blood pressure and heart rate readings performed by a robot assistant and by a medical student showed a high correlation. The patients were able to identify multiple benefits of the healthcare robots, such as workload balancing for the caregivers, daily routine scheduling and compensating for staff shortages, indicating that low human comfort around robots due to lack of exposure might be a principal negative factor in their acceptance. Several areas of improvement for elderly-robot interaction include empathy emulation, behavior adaptability [21] and unpredictability, as the capacity to generate actions that are not necessarily reactions to user input [10].

Scenario in laboratory environment Various scenarios are intended to be tested within INCARE and CoRSAr, where a robot interacts with elderly and their formal and informal caregivers. The development of cloud services [6] and map creation methods [22] substantially support the effectiveness of not only robot navigation, but also both speech recognition and speech synthesis. Hence, this type of communication was chosen for being both effective and intuitive.

The first scenario covers the need for delivery of small items (e.g. drinks) ordered by the elderly, where the robot substitutes the staff of e.g. elderly facility and the staff can concentrate on more complicated activities. It is assumed that the older person stays in one room, while the staff operates in the other room – i.e. kitchen. The robot will perform its delivery task while also detecting hazards [5, 7] and informing about them. The robot considered for the scenarios is the TIAGo [14, 23] by PAL robotics. The scenario consists of the following, subsequent steps: (1) An elderly person calls for a robot; (2) The robot approaches the elderly person; (3) The robot asks for orders; (4) The elderly person requests for a drink, e.g. tea; (5) The robot confirms an order; (6) The robot goes to the kitchen; (7) The robot approaches the staff in the kitchen and asks for the particular drink to be put on it; (8) The staff confirms that the delivery is ready and placed on the robot; (9) The robot informs that it starts to go back to deliver the order; (10) The robot approaches the elderly person and informs that it has the delivery; (11) The robot asks the elderly person to take the drink; (12) The older person takes the drink and confirms the action.

Federated learning in AI In the past few years, machine learning has led to major breakthroughs in various areas, such as computer vision. Much of this success has been based on collecting huge amounts of data. Machine learning applications need to collect data that are privacy-invasive.

Federated Learning is a distributed form of machine learning approach where the training process is distributed among many users using a training data set composed of decentralized data. A server has the role of coordinating everything and most of the work is performed by each device. Steps involved in the federated learning

are: (1) the server initializes the model and each device/client downloads the global model; (2) the model is updated using its own data; (3) each personalised trained model is sent to the server; (4) on the server a federated average function is used to generate a much improved version of the model than the previous one; and (5) the improved version is sent to all the devices.

Federated learning looks similar with distributed machine learning on a technical level. But there are some major differences: (1) huge number of clients; (2) learning data for each user is obtained from different distribution – two similar users might have similar training data, but two randomly users can obtain totally different data; (3) unbalanced number of examples per device and (4) slow and unstable communication.

In 2018, Intel began a collaboration with the Center for Biomedical Image Computing and Analytics at the University of Pennsylvania showing the first proof concept for federated learning applied for real medical images used for semantic segmentation of brain tumors from images. The study demonstrated training of a convolutional neural network (U-Net model) using federated learning with an accuracy of 99% as the same model trained with the traditional methods [19]. Paper [9] uses electronic medical records together with federated learning to predict disease incidence, patient response to treatment, and other healthcare events. A community-based federated machine learning method was proposed. The method clusters patients into similar clinically communities that has similar diagnoses and geographical locations, learning one model for each community. Also, the learning process keeps data locally at hospitals. Evaluation was performed on 50 hospitals, each with 560 patients. Results show that the proposed method outperforms the baseline federated machine learning method.

3 Conclusions

Many professional teams, companies, policy makers and individuals are working in the field of the challenges posed by AAL. All efforts are necessary to make worthwhile changes providing technological and procedural solutions and to bring them closer to the end-users. Understanding their needs and experiences and enhancing the acceptance of solutions being developed are crucial to make AAL solutions widely and fairly available and bring about significant structural change. For this purpose, the presented projects offer predictive, preventive and personalized support through their design and implemented functionalities.

References

1. Broadbent, E., Jayawardena, C., Kerse, N., Stafford, R.Q., MacDonald, B.A.: Human-robot interaction research to improve quality of life in elder care – an approach and issues. In: Workshops at the Twenty-Fifth AAAI Conference on Artificial Intelligence (2011)

2. Broadbent, E., Kuo, I.H., Lee, Y.I., Rabindran, J., Kerse, N., Stafford, R., MacDonald, B.A.: Attitudes and reactions to a healthcare robot. Telemed. e-Health **16**(5), 608–613 (2010)
3. Broadbent, E., Stafford, R., MacDonald, B.: Acceptance of healthcare robots for the older population: review and future directions. Int. J. Soc. Robot. **1**(4), 319 (2009)
4. Broekens, J., Heerink, M., Rosendal, H., et al.: Assistive social robots in elderly care: a review. Gerontechnology **8**(2), 94–103 (2009)
5. Dudek, W., Banachowicz, K., Szynkiewicz, W., Winiarski, T.: Distributed nao robot navigation system in the hazard detection application. In: 2016 21st International Conference on Methods and Models in Automation and Robotics (MMAR), pp. 942–947. IEEE (2016)
6. Dudek, W., Szynkiewicz, W., Winiarski, T.: Cloud computing support for the multi-agent robot navigation system. J. Autom. Mob. Robot. Intell. Syst. **11**, 67–74 (2017)
7. Dudek, W., Wegierek, M., Karwowski, J., Szynkiewicz, W., Winiarski, T.: Task harmonisation for a single–task robot controller. In: Kozłowski, K. (ed.) 12th International Workshop on Robot Motion and Control, pp. 86–91. IEEE (2019)
8. Feil-Seifer, D., Skinner, K., Matarić, M.J.: Benchmarks for evaluating socially assistive robotics. Interact. Stud. **8**(3), 423–439 (2007)
9. Huang, L., Shea, A.L., Qian, H., Masurkar, A., Deng, H., Liu, D.: Patient clustering improves efficiency of federated machine learning to predict mortality and hospital stay time using distributed electronic medical records. J. Biomed. Inform. **99**, 103291 (2019)
10. Hutson, S., Lim, S.L., Bentley, P.J., Bianchi-Berthouze, N., Bowling, A.: Investigating the suitability of social robots for the wellbeing of the elderly. In: International Conference on Affective Computing and Intelligent Interaction, pp. 578–587. Springer (2011)
11. Integrated solution for innovative elderly care (INCARE). http://www.aal-europe.eu/projects/incare/
12. Indoor and outdoor niticsplus solution for dementia challenges (IONIS). http://www.aal-europe.eu/projects/ionis/
13. Networked infrastructure for innovative home care solutions (NITICS). http://www.aal-europe.eu/projects/nitics/
14. Pages, J., Marchionni, L., Ferro, F.: Tiago: the modular robot that adapts to different research needs. In: International Workshop on Robot Modularity (2016)
15. Paraciani, N., Tabozzi, S., Di Pasquale, D., Padula, M., Biocca, L., Lafortuna, C., Maiuri, F., Rudel, D., Fisk, M.: The telescope code. quality standards for telehealth practice across Europe. In: 2017 E-Health and Bioengineering Conference (EHB), pp. 297–300. IEEE (2017)
16. Pino, M., Boulay, M., Jouen, F., Rigaud, A.S.: "Are we ready for robots that care for us?" Attitudes and opinions of older adults toward socially assistive robots. Front. Aging Neurosci. **7**, 141 (2015)
17. Samar-Brencic, N.: Service requirements for supporting daily activities of elderly people living at home – multi-national survey within aal project nitics. In: Information Society IS 2014, Proceedings of the 17th International Multiconference. IJS, Ljubljana (2014)
18. Samar-Brencic, N.: System elements integration and field trial report for AAL project nitics slovenia. In: Proceedings of the 18th International Multiconference. IJS: Ljubljana (2015)
19. Sheller, M.J., Reina, G.A., Edwards, B., Martin, J., Bakas, S.: Multi-institutional deep learning modeling without sharing patient data: a feasibility study on brain tumor segmentation. In: International MICCAI Brainlesion Workshop, pp. 92–104. Springer (2018)
20. Stafford, R., Broadbent, E., Jayawardena, C., Unger, U., Kuo, I.H., Igic, A., Wong, R., Kerse, N., Watson, C., MacDonald, B.A.: Improved robot attitudes and emotions at a retirement home after meeting a robot. In: 19th International Symposium in Robot and Human Interactive Communication, pp. 82–87. IEEE (2010)
21. Tapus, A., Maja, M., Scassellatti, B.: The grand challenges in socially assistive robotics. IEEE Robot. Autom. Mag. **14**(1), 35–42 (2007)
22. Wilkowski, A., Kornuta, T., Stefańczyk, M., Kasprzak, W.: Efficient generation of 3D surfel maps using RGB–D sensors. Int. J. Appl. Math. Comput. Sci. **26**(1), 99–122 (2016)

23. Winiarski, T., Dudek, W., Stefańczyk, M., Zieliński, Ł., Giełdowski, D., Seredyński, D.: An intent-based approach for creating assistive robots' control systems. arXiv preprint arXiv:2005.12106 (2020). http://arxiv.org/abs/2005.12106
24. Wu, Y.H., Fassert, C., Rigaud, A.S.: Designing robots for the elderly: appearance issue and beyond. Arch. Gerontol. Geriatr. **54**(1), 121–126 (2012)

Interactive Data Visualization for eHealth Retrieval System

Nesrine Ksentini, Mohamed Tmar, and Faïez Gargouri

1 Introduction

Data visualization represents the effective presentation of information and involves a multidisciplinary communication approach. Its goal is to communicate a specific message to a user. Indeed, a visual representation of data has a main goal to communicate quantitative and qualitative information clearly and effectively through graphical means which can be static, animated or interactive [1, 2].

Selecting a color schema in data visualization process is also very important. It allows the designer to set the tone of these visualizations and try to keep a consistent representation [1].

Data visualization has been used to tackle several challenges in many disciplines such as economics, medicine, and education. As eHealth is an actual topic for today and extremely important to all practitioners, we highlight in this paper the importance of data visualization in this area. In fact, many opportunities have received attention to date for supporting people to make health document sense and for supporting them in better understanding their own illnesses and their health conditions to manage them more effectively [3, 4].

Indeed, clinical-researchers are confronted today with a huge and complex patient records based on which they must study them to make sure quality control, and discover new diseases [5].

The same applies to people as they are becoming more aware of for their own health. They need to understand their own diagnostics to improve and manage their health and to better communicate with their doctors.

N. Ksentini · M. Tmar (✉) · F. Gargouri
MIRACL Laboratory, City ons Sfax, University of Sfax, Sfax, Tunisia
e-mail: mohamed.tmar@isimsf.rnu.tn; mohamed.tmar@isims.usf.tn; faiez.gargouri@isims.usf.tn

L. Chaari (ed.), *Digital Health in Focus of Predictive, Preventive and Personalised Medicine*, Advances in Predictive, Preventive and Personalised Medicine 12,
https://doi.org/10.1007/978-3-030-49815-3_13

The body of this paper will be as follows, we start with Sect. 2 to highlight earlier works related to data visualization. The Sect. 3 sheds light on our proposed data visualization system based on LSM (Least Squares Method) which is a statistical method arisen in machine learning to find semantic relationships between a set of terms and not only between a pair of terms. The Sect. 4 gives the obtained results followed by conclusions and future works.

2 Medical Visualization Systems

In this section, we review the state of the art of data visualization systems to support users (patients and clinical researchers for example) to understand personal health information. In eHealth topic, data or information visualization is part of an overall visualization field that incorporates both information and scientific visualization, which are defined in the literature separately and considered as different [3].

Scientific visualizations represent scientific concepts such as molecules, parts of the human body, or natural phenomena, mainly in 3D [6]. The goal of these visualizations is essentially the confirmation or rejection of a particular hypothesis. Information visualization is a visualization tool to represent abstract concepts or terms. Author in [7] classifies this kind of visualization as exploratory analysis visualizations, due to their goal, help user's to find a hypothesis. The power of this tool derives from its ability to represent a large information at once, including internal relations.

In our case, we focus on information visualization and through the literature review, we can find several main researches in medical field, which investigate this kind of visualization [3].

In [8] authors proposed $AsbruView$ tool, a visualization tool developed to assist in handling treatment plans in Asbru. $AsbruView$ relies on a graphical metaphor where plans are represented as a running track which the physician 'runs' along while treating the patient [3].

$LifeLines$ proposed by [9] was one of the first tools to be used for the electronic health records representation. It was originally developed as a general-purpose visualization tool to represent personal histories that was then applied for the visualization of patient records. Our aim in this paper, is to develop a visualization tool, integrated in content based retrieval system, that presents semantic relationships between medical terms appeared in patient records and not to present only patient records data. The goal is to help users to make sense of returned documents when they use content based retrieval systems and search their needs.

3 Proposed System

In this section, we present our proposed content based retrieval system that incorporates two main steps. The first step is based on a local automatic documents-analysis to define semantic relationships between query terms and terms of the top *m* returned documents deemed relevant. The second step illustrates how to visualize these relations in a graph to help users making sense of the returned documents. The process of our search system is illustrated in (Fig. 1)

3.1 Semantic Relationships

Measuring similarity and semantic relationships between terms in a set of documents has become a primary task and plays an important role in the natural language processing (NLP) field in order to improve and to interpret search results [10]. It is the backbone of several applications, such as query expansion, disambiguation, automatic creation of thesaurus [11].

Previous approaches that study this latter idea, can be classified into three main categories [12–14]: those based on semantic knowledge (such as ontologies, data dictionaries), those based on content-based methods documents using general statistical methods [15, 16], and hybrid approaches that combine the earlier two categories.

In our case, we will adopt statistical methods to define semantic relationships between documents terms. The choice to adopt this type of method is justified first, by the independence of this process to the used language and secondly, by its ability

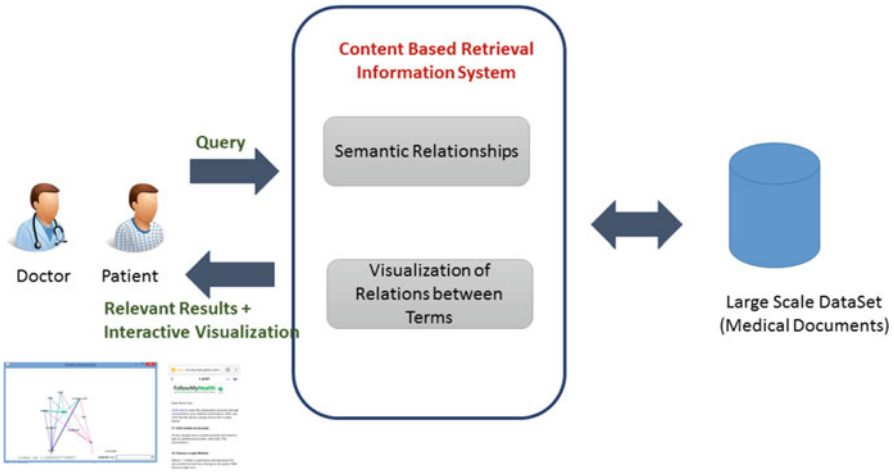

Fig. 1 Proposed content based retrieval system

to define these relations between a set of terms and not only between a pair of terms. We will apply Least Squares Method (LSM) for text analysis [17, 18] which is a method often used to define approximately relationships that may exist between many variables [17, 19–22]. Indeed, this method, known as linear regression, is the most widely used predictive model in the field of machine learning which present a particular approach to artificial intelligence [23].

Indeed, machine learning is a data analysis method which automates analytical model building process. The main idea of this method is to create algorithms that can receive input data and use statistical analysis to predict an output value.

It is an approach of artificial intelligence based on the idea that systems can learn from data and make decisions with little user intervention.

LSM tries to find the connection that may exist between an explained variable (y) and explanatory variables (x). In our case, we take a $term_j$ as an explained variable and the remaining terms in a set of documents as explanatory variables ($term_{1\cdots n}$). The goal is to find the relation between these variables as follows:

$$term_j \approx \sum_{i=1}^{j-1} (\alpha_i term_i) + \sum_{i=j+1}^{n} (\alpha_i term_i) + \epsilon \tag{1}$$

where α represent the real coefficients of the regression model and the weights of relationships between terms. ϵ represents is the associated error.

Explanatory variables are defined from the top m returned documents that meet user's needs. As a result, for each variable which is a term in our case, we will have m measures that represent the $tf-idf$ weights. To minimize calculation complexity, we study as explained variables $term_j$ only the distinctive terms of the user's query (The process of this step is illustrated by Fig. 2).

For example, when a user sends a query with three terms (t_i,t_k,t_l), our content based retrieval system retrieves the top m returned documents which will be treated with a matrix representation. Indeed, we obtain ($terms \times documents$) matrix with ($n * m$) size where n presents the number of terms in the set of returned documents.

For each query term, if it exists in the terms set of returned documents, we calculate then its relationship weight vector $A_{term_j} = (\alpha_1, \cdots, \alpha_n)$ with other n terms. Least Squares Method gives the solution to find this vector in an approximate way:

$$A_{term_j} = \left(X^{jT} \times X^j\right)^{-1} \times X^T[., j] \times T_j \tag{2}$$

Where:

T represent TF-IDF weight vector of $term_j$.
X present the TF-IDF matrix whose columns represent the keyword set and rows represent the m returned documents.
X^j is obtained by removing the column of the term t_j in matrix X.
$X^T[j, .]$ represents the transpose of the weight vector of the term t_j in all documents.

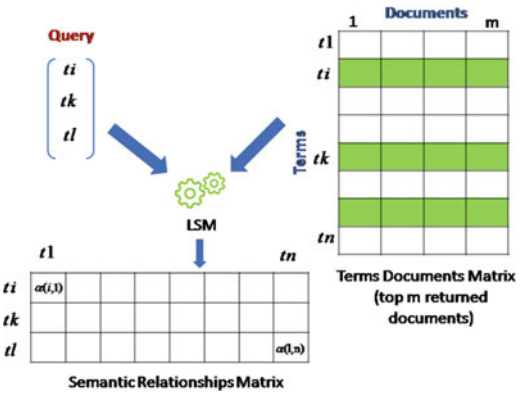

Fig. 2 Process of defining semantic relationships

At the end of this process, we obtain terms by terms matrix (see Fig. 2) (Query-terms $\times$ terms of top m returned documents matrix) which contains the relation values founded for each query term with the remainder terms.

Once the relations are defined, we study them in order to design the graph of semantic relations with the most related terms (for example terms that have positive relations with query terms).

3.2 Data Visualization

Semantic relationships defined in the previous section does not make it possible to interpret the similarity between the terms in an easy way. It is thus preferable to have a comprehensive view of these semantic relationships in order to better assimilate them.

As visualization plays a very important part in the results interpretation, we propose to visualize the defined relations in a graph which will be generated after the search process for each user's query.

The generated visual graph comprises a set of nodes and a set of edges representing respectively terms and semantic relationships between these terms. We have decided to color semantic relationships defined for each query term by a different color because visual sweeping of colors takes less time and effort.

To enhance the importance of defined relations, we have modified the color intensity and the thickness of arcs which will be proportional to the similarity value. Indeed, if the defined relationship between two terms is strong, the arc becomes thicker. In order to help users interpret results, we have used the research option of the tool Prefuse[1] which makes it possible for users to easily find a term searched in the whole graph (for example term *coronari* in Fig. 3).

[1] http://prefuse.org

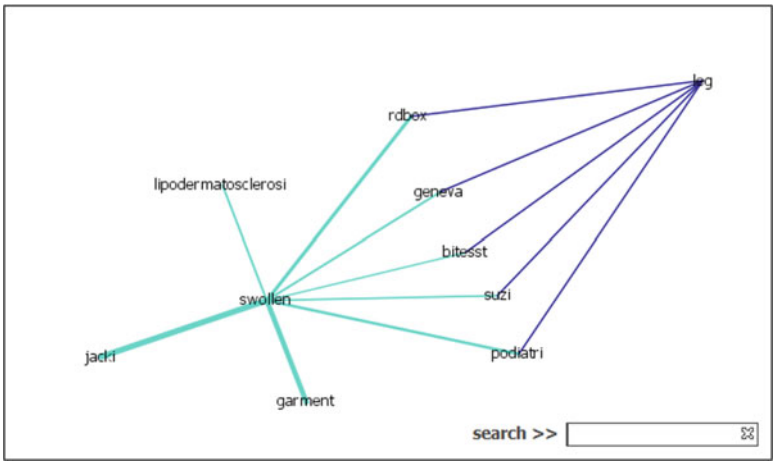

Fig. 3 Graph of Semantic Relationships: query 53 in 2015

4 Results

In order to check the performance of our proposed method, an experimental procedure was set up. This evaluation is performed on a large collection of documents provided from the CLEF company for the two successive years 2014 and 2015 [24–27].

4.1 Document Collection

The document collection is composed of a set of medical documents covering a wide set of medical topics. This collection is around of one million documents provided by the Khresmoi project [24–27] which come from different online sources such as known databases and medical sites (e.g. ClinicalTrial.gov, Genetics Home Reference, the health certified websites).

The test set in 2014 comprises 50 professional and medical queries provided by experts (clinical-researchers for example). These queries present different cases of patient diseases. In 2015, test set has 67 circumlocutory queries provided by patients when they are faced with symptoms and signs of a medical condition.

Table 1 Semantic relationships examples

Base	Query number	Some terms in relation with the query
clef2015	34	**Caviti problem** tooth cari dentistri fluoridepr dentahealth gum
clef2015	53	**Swollen leg** swell clot podiatri garment suzi lipodermatosclerosi
clef2014	1	**Coronari arteri disease** mean myocardi bypass angiograph aortic charlson cholesterol heart-attack translesion revascularis anastomos
clef2014	35	**Peptic ulcer disease** antacid food diagnos recommend gastric oesophag

4.2 LSM Results

Table 1 shows the results of defined semantic relationships for some queries. Terms that are written in bold font represent the original query terms, the other terms represent the most related terms to the original query in their root form. We notice that selected terms usually express the same context of the original query which proves the effectiveness of our proposed method.

For example we take query number 53 in 2015 and we explain some related terms like:

- podiatri: a podiatrist is a health professional who diagnoses and treats disorders of the feet.
- garment: is a pneumatic antishock garment an inflatable garment used to combat shock, stabilize fractures, promote hemostasis and increase peripheral vascular resistance.
- suzi: Extra Roomy Shoes that are cleverly designed to look slim-line but have lots of room for swollen feet.
- lipodermatosclerosi: is a skin and connective tissue disease.

Another example query 35 in 2014, related terms are in strong relation with the original query which talk about peptic ulcer. It is a disease that has long been considered chronic, defined anatomically by a loss of parietal substance not exceeding the submucosa.

4.3 Interactive Data Visualization

Interactive data visualization plays an important role in making sense process. This importance grows when we talk about the eHealth field that is a current topic that draws attention of any person which is today more aware of and take greater responsibility for his health.

The above figures show the illustrations of semantic relationships defined by the statistical method LSM. Each illustration is, as already mentioned, presented as a graph whose nodes represent the terms and the arcs represent relations between these terms.

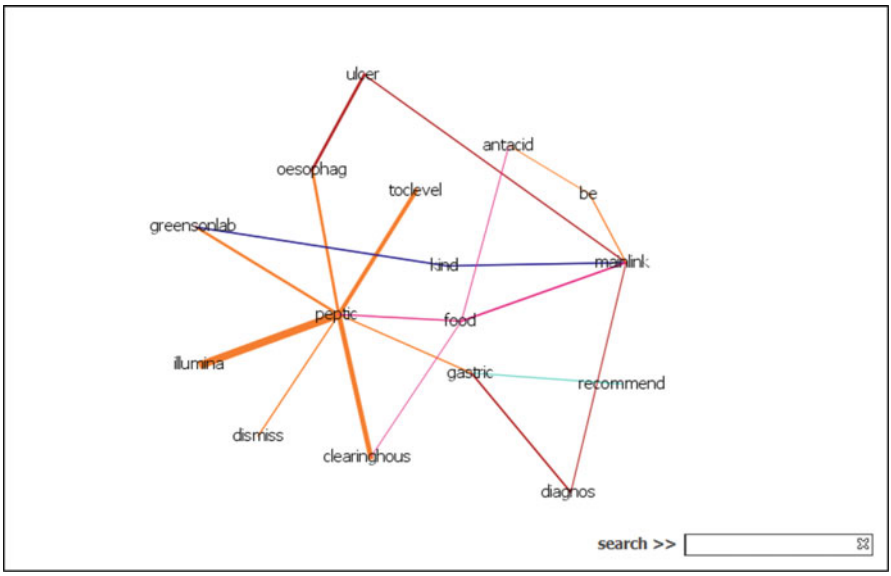

Fig. 4 Graph of Semantic Relationships: query 35 in 2014

These graphs are generated automatically and after each user's query. In fact, these types of graphs help users to understand the general context of the returned documents and to expand the knowledge on the subject later by studying the presented relationships. This study is easy to any user due to the used colors and the difference thickness edges. Indeed, if the edge between two terms is thick, the user can interpret the relation between these two terms is pertinent.

For example, in Fig. 3, edge between terms ($swollen$, $garment$) is very thick, so we conclude the strong relationships between them.

In Fig. 4, we notice the presence of several relations with the term $peptic$ that can expand user's knowledge.

In the case where we end up with a rich graph with many semantic links between the terms, the research option provided by the $Prefuse$ tool makes user's easily find a specific term. Take the example shown in Fig. 5, the user looks for the word $coronari$, our visualization tool try to seek this term, if finded this term will be colored by a pink oval.

5 Conclusion and Future Works

The goal of this work is to help users making-sense when searching medical documents. Our proposed idea is to return with the search results, a graphical representation that illustrates the semantic relationships that may exist between

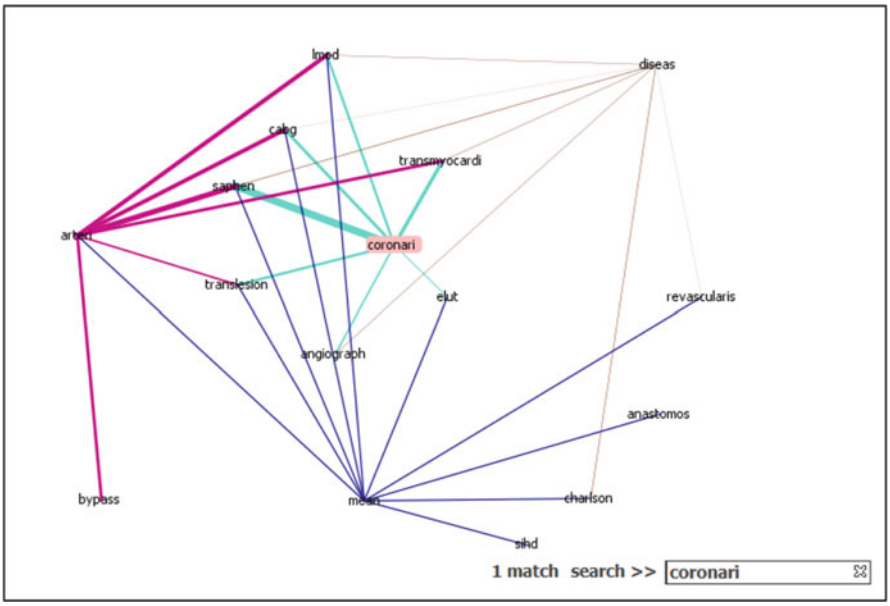

Fig. 5 Graph of Semantic Relationships: query 1 in 2014

terms in the user's query and terms of the returned documents assumed as pertinent, instead of returning only the relevant assumed documents.

Illustrated relationships in the graphs are defined by the statistical method LSM which is the most widely used predictive model in the field of machine learning that present a particular approach to artificial intelligence.

Obtained semantic relationships as well as the obtained graphs show the efficiency of the LSM method which gives significant results that help users to explore more the medical field and to ameliorate their queries with adding appropriate terms.

For future work, we try in the first time, to ask users to explain their needs (queries) based on their interpretation of provided data visualization graph. In the second time, we study the impact of query reformulation process on our content based retrieval system.

References

1. Visocky O'Grady, J., Visocky O'Grady, K.: The information design handbook. How Books, Cincinnati (2008)
2. Ksentini, N., Zarka, M., Ammar, A.B., Alimi, A.M.: Toward an assisted context based collaborative annotation. In: 2012 10th International Workshop on Content-Based Multimedia Indexing (CBMI), pp. 1–6. IEEE (2012).
3. Faisal, S., Blandford, A., Potts, H.W.: Making sense of personal health information: challenges for information visualization. Health Inform. J. **19**(3), 198–217 (2013)

4. Ksentini, N., Tmar, M., Gargouri, F.: Towards automatic improvement of patient queries in health retrieval systems. Appl. Med. Inform. **38**(2), 73–80 (2016)
5. Rind, A., Wang, T.D., Aigner, W., Miksch, S., Wongsuphasawat, K., Plaisant, C., Shneiderman, B.: Interactive information visualization to explore and query electronic health records. Found. Trends®Human-Comput. Interact. **5**(3), 207–298 (2013)
6. Card, S.K., Mackinlay, J.D., Shneiderman, B. (eds.). Readings in Information Visualization: Using Vision to Think. Morgan Kaufmann, San Francisco (1999)
7. Keim, D.A.: Visual exploration of large data sets. Commun. ACM **44**(8), 38–44 (2001)
8. Kosara, R., Miksch, S.: Metaphors of movement: a visualization and user interface for time-oriented, skeletal plans. Artif. Intell. Med. **22**(2), 111–131 (2001)
9. Plaisant, C., Mushlin, R., Snyder, A., Li, J., Heller, D., Shneiderman, B.: LifeLines: using visualization to enhance navigation and analysis of patient records. In: The Craft of Information Visualization, pp. 308–312 (2003)
10. Agirre, E., Alfonseca, E., Hall, K., Kravalova, J., Pasca, M., Soroa, A.: A study on similarity and relatedness using distributional and wordnet-based approaches. In: Proceedings of Human Language Technologies: The 2009 Annual Conference of the North American Chapter of the Association for Computational Linguistics, pp. 19–27. Association for Computational Linguistics (2009)
11. Terra, E., Clarke, C.L.: Frequency estimates for statistical word similarity measures. In: Proceedings of the 2003 Conference of the North American Chapter of the Association for Computational Linguistics on Human Language Technology, vol. 1, pp. 165–172. Association for Computational Linguistics (2003)
12. Agirre, E., Cuadros, M., Rigau, G., Soroa, A.: Exploring knowledge bases for similarity. In: LREC (2010)
13. Hassan, S., Mihalcea, R.: Semantic relatedness using salient semantic analysis. In: AAAI (2011)
14. Santus, E., Chiu, T.S., Lu, Q., Lenci, A., Huang, C.R.: Unsupervised measure of word similarity: how to outperform co-occurrence and vector cosine in VSMs. arXiv preprint:1603.09054 (2016)
15. Sahami, M., Heilman, T.D.: A web-based kernel function for measuring the similarity of short text snippets. In: Proceedings of the 15th International Conference on World Wide Web, pp. 377–386. ACM (2006)
16. Ruiz-Casado, M., Alfonseca, E., Castells, P.: Automatic assignment of wikipedia encyclopedic entries to wordnet synsets. In: International Atlantic Web Intelligence Conference, pp.380–386. Springer, Berlin/Heidelberg (2005)
17. Ksentini, N., Tmar, M., Gargouri, F.: Detection of semantic relationships between terms with a new statistical method. In: WEBIST (2), pp. 340–343 (2014)
18. Ksentini, N., Tmar, M., Gargouri, F.: Towards a contextual and semantic information retrieval system based on non-negative matrix factorization technique. In: International Conference on Intelligent Systems Design and Applications, pp. 892–902. Springer, Cham (2017)
19. Abdi, H.: The method of least squares. In: Salkind, N.J., Rasmussen, K. (eds.) Encyclopedia of Measurement and Statistics. SAGE Publications, Thousand Oaks (2007)
20. Miller, S.J.: The method of least squares. Mathematics Department Brown University, pp. 1–7 (2006)
21. Ksentini, N., Tmar, M., Gargouri, F.: Controlled automatic query expansion based on a new method arisen in machine learning for detection of semantic relationships between terms. In: 2015 15th International Conference on Intelligent Systems Design and Applications (ISDA), pp. 134–139. IEEE (2015)
22. Ksentini, N., Tmar, M., Gargouri, F.: The impact of term statistical relationships on Rocchio's model parameters for pseudo relevance feedback. Int. J. Comput. Inf. Syst. Ind. Manag. Appl. **8**, 135–44 (2016)
23. Huang, G.B., Wang, D.H., Lan, Y.: Extreme learning machines: a survey. Int. J. Mach. Learn. Cybern. **2**(2), 107–122 (2011)

24. Goeuriot, L., Kelly, L., Li, W., Palotti, J., Pecina, P., Zuccon, G., Mueller, H.: Share/clef ehealth evaluation lab 2014, task 3: user-centred health information retrieval. In: Proceedings of CLEF (2014)
25. Ksentini, N., Tmar, M., Gargouri, F.: Miracl at CLEF 2014: eHealth information retrieval task. In: Proceedings of the ShARe/CLEF eHealth Evaluation Lab (2014)
26. Palotti, J.R., Zuccon, G., Goeuriot, L., Kelly, L., Hanbury, A., Jones, G.J., Pecina, P.: CLEF eHealth Evaluation Lab 2015, Task 2: Retrieving information about medical symptoms. In: CLEF (Working Notes) (2015)
27. Ksentini, N., Tmar, M., Boughanem, M., Gargouri, F.: Miracl at Clef 2015: usercentred health information retrieval task. In: CLEF (Working Notes) (2015)

Accuracy Assessment of a Deep-Learning Based Segmentation Tool Over Right Ventricle Short-Axis Slices

Asma Ammari, Ramzi Mahmoudi, Badii Hmida, Rachida Saouli, and Mohamed Hédi Bedoui

1 Introduction

In the cardiac system, both ventricles have the role of pumping blood in the whole body. For the sake of enabling this organized role, the ventricular structure allows its function. Still, each ventricle has its own personalized morphology. Unlike the left ventricle (LV), the right ventricle (RV) has harsher trabeculae with a fibrous

A. Ammari (✉)
The National Engineering School L'ENIS, Sfax, Tunisia

Faculty of Medicine of Monastir, Medical Imaging Technology Lab - LTIM-LR12ES06, University of Monastir, Monastir, Tunisia

Department of computer science, Laboratory of Intelligent Computing (LINFI), Mohamed Khaider University, RP, Biskra, Algeria
e-mail: asma.ammari@enis.tn

R. Mahmoudi
Faculty of Medicine of Monastir, Medical Imaging Technology Lab - LTIM-LR12ES06, University of Monastir, Monastir, Tunisia

Gaspard-Monge Computer-Science Laboratory, Paris-Est University, Paris, France

B. Hmida
Radiology Service, UR12SP40 CHU Fattouma Bourguiba, Monastir, tunisia

R. Saouli
Department of computer science, Laboratory of Intelligent Computing (LINFI), Mohamed Khaider University, RP, Biskra, Algeria

Gaspard-Monge Computer-Science Laboratory, Paris-Est University, Paris, France

M. H. Bedoui
Faculty of Medicine of Monastir, Medical Imaging Technology Lab - LTIM-LR12ES06, University of Monastir, Monastir, Tunisia

L. Chaari (ed.), *Digital Health in Focus of Predictive, Preventive and Personalised Medicine*, Advances in Predictive, Preventive and Personalised Medicine 12,
https://doi.org/10.1007/978-3-030-49815-3_14

discontinuity between valves. The RV provides a thin wall and a crescent shape which makes it difficult to be modelled geometrically [1]. The assessment of the LV is widely handled using many segmentation techniques, even at the clinical practices, they segment and quantify its function automatically [2–4]. However, the RV is routinely assessed manually by expert radiologists to delineate its boundaries through the short axis several slices which are a fastidious, laborious, and time-consuming task. Therefore, automated assessment is crucial especially with the RV importance increasing for numerous pathological diagnosis. Irrefutably, its complex structure makes the segmentation task very challenging. Although many approaches have been proposed to handle those issues [5], still the problem of images variability and shape deformation from base to apex influence the accuracy of the proposed methods. In this paper, our goal is to study the impact of the RV MRI short-axis different slices on the segmentation accuracy using a commercially available cardiac MRI analysis software (CVi42, version 5.5.1, Circle Cardiovascular Imaging Inc., Calgary, Canada) [6]. Thus, we use two MRI exams of sick and healthy patients to experiment segmentation using the tool mentioned above. Based on the ground truth drawn by the expert, we compute the accuracy, the dice score metric, and other functional parameters related to the RV itself. The rest of this paper is organized as follow: We start by the state of the art in Sect. 2 followed by a description of the used image data and the experimented platform in Sect. 3. The experimental results are introduced in Sect. 4. Finally, in Sect. 5, discussion and conclusion are given.

2 State of the Art

The existing attempts to overcome the challenges related to the RV segmentation make use of many medical imaging segmentation techniques [5]. Based on prior information, in [7, 8], multi-atlas based approaches are exploited. Since atlas-based methods depend at the first stage on the database used, its results may fail to provide high accuracy when the segmented cardiac images present different structures from those used in the first place. Deformable models are also used for RV segmentation such in [9] and [10]. These methods are based on the shape information of the right ventricular. On the other hand, other works make use of graph cuts-based methods hybridized with several imaging techniques aiming thus to segment the right ventricular boundaries [11], [12]. Recently with the appearance and the augmented use of deep learning techniques to solve several imaging problems. In [12–14], deep learning methods are used for right ventricular segmentation. These methods depend on used architecture to train the model as well on the amount and the variation of used training sets. In this paper, we attempt to highlight the main issues that might hold back the adaptation of the promising deep-learning solutions for the RV challenging case considering at the first place the RV contour variation from base to apex. For that interest, we investigate the Cvi42 segmentation results, as it is based on a deep-learning approach using a fully conventional neural network trained on thousands of CMRI subjects acquired from the UK Biobank.

3 Image Data and Experiment Platform

To allow the Cvi42 cardiac segmentation tool assessment, the image data used encompasses a short-axis cine cardiac MR DICOM images which belong to two patients gathered from Fattouma Bourguiba Monastir Hospital in Tunisia. One patient presents a normal case while the other suffers from dysplasia in which the RV surface appears dilated. The manual RV delineation for both patients' sequences performed by the expert, based on the 4-chambers and the long-axis slices, is shown in Fig. 1 which is to be used as a referential segmentation. The experiment is done using a 5.10 version of Cvi42 upon an i7 ASUS platform (2.4 GHz CPU, 8GB RAM, Nvidia GeForce 920_M graphical card). The evaluation metrics are computed using MATLAB R2016a.

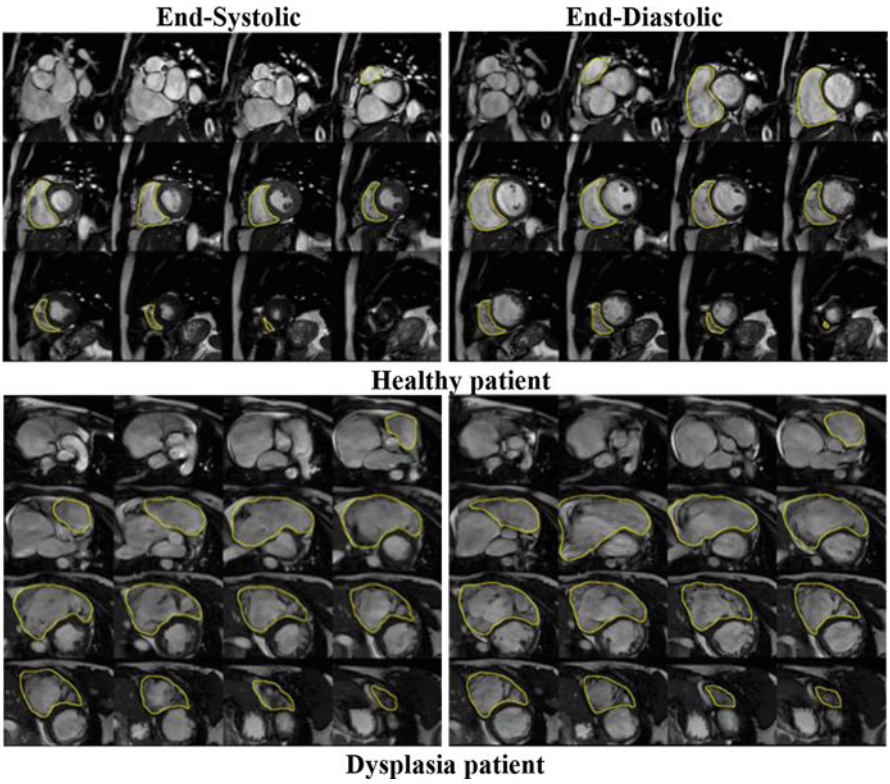

Fig. 1 Expert's manual RV endocardium delineation in end-systole and end-diastole for both healthy and diseased patient. (For interpretation of segmentation yellow color in this figure, the reader is referred to the web version of this article)

4 Experimental Results

In this section, the obtained RV boundaries automatic delineation, as well as the precession evaluation, are presented.

4.1 Segmentation Results

Figure 2 shows the segmentation results of the automated segmentation tool, in which the yellow line is the result of endocardium delineation. Compared to manual segmentation, we notice that the software has failed to detect the first basal and the last apical slices in the case of the healthy patient. However, in the case of dysplasia patient, most of the apical slices were missed out as well as some basal slices. Furthermore, the precession of contouring is clearly over and underestimated

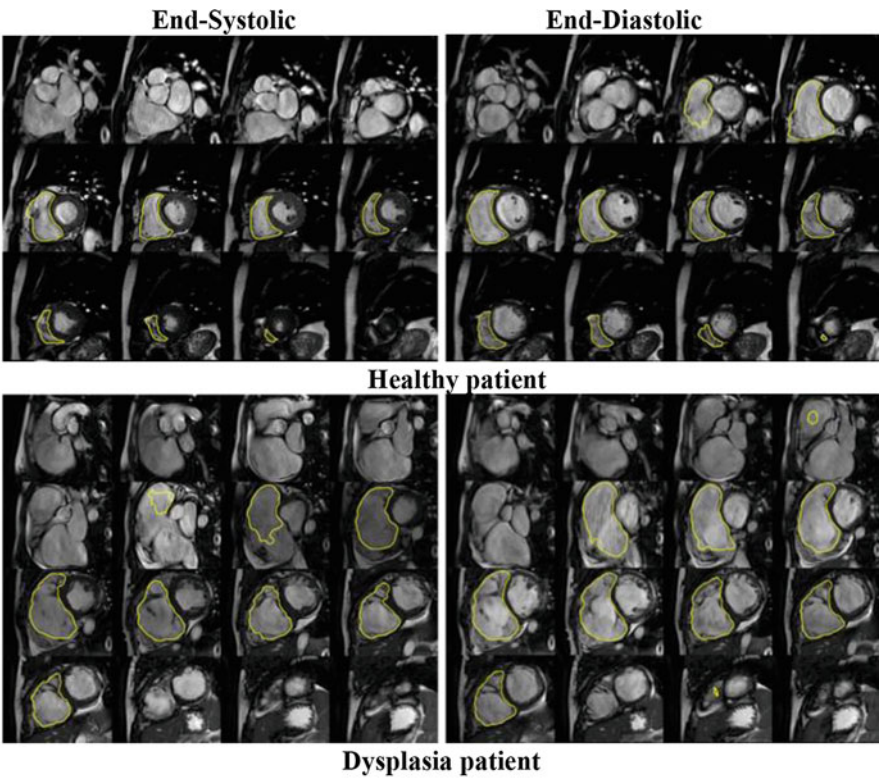

Fig. 2 Automatic Cvi42 RV endocardium delineation in end-systole and end-diastole for both healthy and diseased patient. (For interpretation of segmentation yellow color in this figure, the reader is referred to the web version of this article)

especially for the diseased case. The exact metrical evaluation of these delineation results is assessed in the following sub-section.

4.2 *Empirical Evaluation*

In this paper, we compute the Dice metric (DM) and the accuracy for the sake of evaluating the performance of the RV automatic segmentation offered by the tool (Cvi42). The DM is the overlap between the automatic segmentation result and the manual segmentation result computed following the Eq. (1) [5], and the accuracy computed based on true positives, true negatives, false positives and false negatives as it is described in the Eq. (2). Graphics in Figs. 3 and 4 show respectively the obtained results for the Accuracy and the DM.

$$\mathrm{DM}\,(U, V) = 2\frac{UV}{U+V} \tag{1}$$

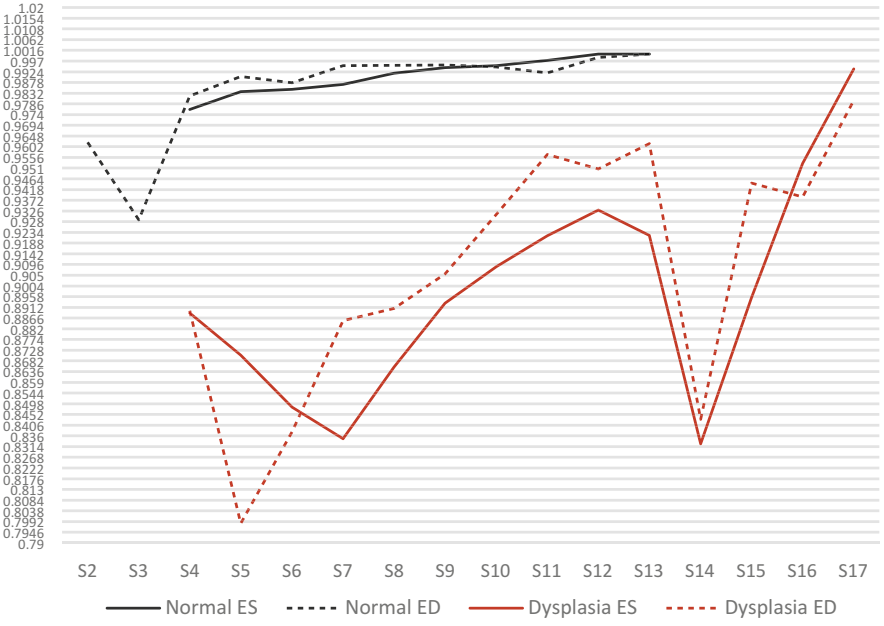

Fig. 3 Accuracy evaluation of Short-Axis Slices from (S2➔S17) for both End-Systolic and End-Diastolic phases considering both normal and diseased patients

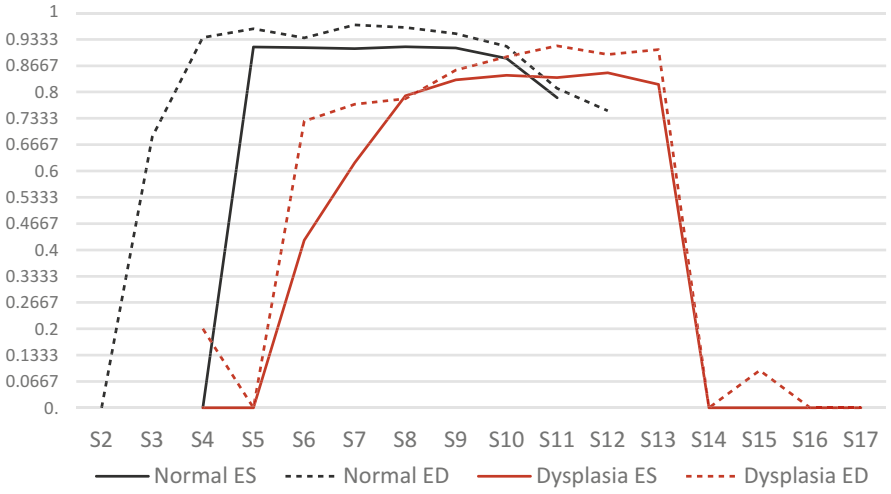

Fig. 4 Dice score metric evaluation of Short-Axis Slices from (S2➔S17) for both End-Systolic and End-Diastolic phases considering both normal and diseased patients

Table 1 Right ventricular functional parameters. (RVESV): RV End Systolic Volume, (RVEDV): RV End Diastolic Volume, RVEF): RV Ejection Fraction

	Healthy patient	Diseased patient
Ground truth	RVEDV: 75.4 ml/m^2	RVEDV: 491 ml
	RVESV: 32.2 ml/m^2	RVESV: 410 ml
	RVEF: 57%	RVEF: 6%
Automatic	RVEDV: 209.52 ml	RVEDV: 401.04 ml
	RVESV: 114.45 ml	RVESV: 276.12 ml
	RVEF: 45.37%	RVEF: 31.15%

$$\text{Accuracy} = \frac{TP + TN}{TP + TN + FP + FN} \tag{2}$$

Table 1 shows some functional parameters such as RV End-systolic Volume, RV End-Diastolic Volume, and the ejection fraction of the assessed cases. The presented values obtained by the expert and the segmentation tool might be computed according to the Eqs. (3, 4 and 5).

$$RVESV = \min_t [V(t)] \tag{3}$$

$$RVEDV = \max_t \Big[V(t)\Big] \tag{4}$$

$$RVEF\,(\%) = \frac{RVEDV - RVESV}{RVEDV} \times 100 \tag{5}$$

Considering both the RV-end-systolic-volume and the RV-end-diastolic-volume, the values obtained by the segmentation tool seem to be higher compared to the values obtained by the expert for the case of the healthy patient. However, in the case of the diseased patient, we find that the automatically obtained volumes show lower values than those obtained by the expert. Consequently, the resulting ejection fraction obtained by the automatic segmentation is lower for the case of the healthy patient and higher for the diseased one compared to the expert' referential results. Indeed, as the main goal of the RV boundaries segmentation is to allow accurate functional parameters computing. Thus, any under or over-estimated contours even at the basal or apical slices might influence the obtained parametrical results especially for the case of pathological patients where neither the size nor the end-systolic and the end-diastolic phases are normal.

5 Conclusion and Discussion

In this paper, a deep-learning-based cardiac segmentation tool is considered for evaluating the impact of CMRI slice from base to the apex on the effectiveness of the segmentation. The metrical presented results in Fig. 3 and Fig. 4 show respectively the computed Accuracy and Dice metric values for each short-axis slice from base to apex (S2, S3 . . . S17). The very first basal slice is excluded as it doesn't belong to the RV space. For the healthy patient, the included slices are S2, S3 . . . S12. However, the pathological patient covers the whole 16 slices as the RV is dilated. For both patients, the very first basal and the very last epical slices associate low accuracy and DM. Besides, the accuracy and the DM results are low for the entire pathological patient' slices compared to the healthy slices. Thus, the segmentation results show that from central to basal and apical slices the effectiveness of the delineation decreases. Also, the case of dysplasia illustrates how widely the effectiveness decreases and how do the diseased cases influence the accuracy of segmentation. As a perspective, we attempt to tackle the basal and apical segmentation issues as well as the pathological problem toward a better effective segmentation process based on deep-learning approaches.

References

1. Sheehan, F., Redington, A.: The right ventricle: anatomy, physiology and clinical imaging. Heart. **94**, 1510–1515 (2008). https://doi.org/10.1136/hrt.2007.132779
2. Irshad, M., Sharif, M., Khan, M.Y.: A survey on left ventricle segmentation techniques in Cardiac Short Axis MRI, https://doi.org/10.2174/1573405613666170117124934, Last accessed 2019/06/12

3. Sami, S.M., Elfawal, S.K., Abdelgawad, M.S., Zidan, M.A., Zaki, A.M., Mowaki, A.F.: MDCT in the study of left ventricular function compared with MRI in patients with myocardial ischemia. Egypt. J. Radiol. Nucl. Med. **49**, 29–41 (2018). https://doi.org/10.1016/j.ejrnm.2017.11.004
4. Epstein, F.H.: MRI of left ventricular function. J. Nucl. Cardiol. Off. Publ. Am. Soc. Nucl. Cardiol. **14**, 729–744 (2007). https://doi.org/10.1016/j.nuclcard.2007.07.006
5. Petitjean, C., Zuluaga, M.A., Bai, W., Dacher, J.-N., Grosgeorge, D., Caudron, J., Ruan, S., Ayed, I.B., Cardoso, M.J., Chen, H.-C., Jimenez-Carretero, D., Ledesma-Carbayo, M.J., Davatzikos, C., Doshi, J., Erus, G., Maier, O.M.O., Nambakhsh, C.M.S., Ou, Y., Ourselin, S., Peng, C.-W., Peters, N.S., Peters, T.M., Rajchl, M., Rueckert, D., Santos, A., Shi, W., Wang, C.-W., Wang, H., Yuan, J.: Right ventricle segmentation from cardiac MRI: a collation study. Med. Image Anal. **19**, 187–202 (2015). https://doi.org/10.1016/j.media.2014.10.004
6. Cardiac MRI and CT Software – Circle Cardiovascular Imaging – Cardiac MRI, https://www.circlecvi.com/cvi42/cardiac-mri/. Last accessed 17 Oct 2019
7. Ou, Y., Doshi, J., Erus, G., Davatzikos, C.: Multi-Atlas segmentation of the Cardiac MR right ventricle. Presented at the (2012)
8. Bai, W., Shi, W., Wang, H., Peters, N.S., Rueckert, D.: Multi-atlas based segmentation with local label fusion for right ventricle MR images. Presented at the (2012)
9. Sun, H., Frangi, A.F., Wang, H., Sukno, F.M., Tobon-Gomez, C., Yushkevich, P.A.: Automatic cardiac MRI segmentation using a biventricular deformable medial model. In: Jiang, T., Navab, N., Pluim, J.P.W., Viergever, M.A. (eds.) Medical Image Computing and Computer-Assisted Intervention – MICCAI 2010, pp. 468–475. Springer, Berlin/Heidelberg (2010)
10. Yang, X., Yeo, S.Y., Su, Y., Lim, C., Wan, M., Zhong, L., Tan, R.S.: Right ventricle segmentation by temporal information constrained gradient vector flow. In: 2013 IEEE International Conference on Systems, Man, and Cybernetics, pp. 2551–2555 (2013). https://doi.org/10.1109/SMC.2013.435
11. Maier, O.M.O., Jiménez, D., Santos, A., Ledesma-Carbayo, M.J.: Segmentation of RV in 4D cardiac MR volumes using region-merging graph cuts. In: 2012 Computing in Cardiology, pp. 697–700 (2012)
12. Quispe, A.M., Petitjean, C.: Shape prior based image segmentation using manifold learning. In: 2015 International Conference on Image Processing Theory, Tools and Applications (IPTA). pp. 137–142. (2015). https://doi.org/10.1109/IPTA.2015.7367113
13. Zotti, C., Luo, Z., Lalande, A., Jodoin, P.-M.: Convolutional neural network with shape prior applied to cardiac MRI segmentation. IEEE J. Biomed. Health Inform. (2018). https://doi.org/10.1109/JBHI.2018.2865450
14. Jang, Y., Hong, Y., Ha, S., Kim, S., Chang, H.-J.: Automatic segmentation of LV and RV in cardiac MRI. In: Pop, M., Sermesant, M., Jodoin, P.-M., Lalande, A., Zhuang, X., Yang, G., Young, A., Bernard, O. (eds.) Statistical Atlases and Computational Models of the Heart. ACDC and MMWHS Challenges, pp. 161–169. Springer (2018)

Big Data Analytics in Healthcare

Wayne Matengo, Ezekiel Otsieno, and Kelvin Wanjiru

1 Introduction

Personalised, Preventive, Predictive and Participatory (P4) medicine is on the rise due to the following factors: (1) increasing capacities and capabilities of systems biology and systems medicine, (2) digital revolution and (3) changing consumer demands in healthcare. The increasing capabilities of systems biology has seen clinical medicine shift from a reductionist approach to a more holistic approach where the human body is seen as an interconnection of different systems all together. On the other hand, the increasing levels of technological advancements has amplified the possibilities for collecting, integrating, storing, analysing and communicating data and information, including conventional medical histories, clinical tests and the results of the tools of systems medicine [4, 5]. Lastly, consumers are increasingly becoming more and more cognizant of their healthcare status and interested in managing their own health.

Since the advent of P4 medicine, various research has shown that the healthcare environment will undergo a paradigm shift under which the industry will be driven by technological buzzwords such as 'big data', 'genomics', 'digital health' and 'personalised medicine' [3, 14]. For this paper, we pay attention to the digital revolution in the healthcare industry and the limitless scope for promoting P4 medicine using Wearable technology. The first section looks at the current craze of big data, followed the trends in the healthcare industry. We further look at the various research publications around big data and wearable technology at large which helps us develop our methodology and analysis procedures and lastly, we present a call to action for the implementation of P4 medicine.

W. Matengo · E. Otsieno (✉) · K. Wanjiru
Strathmore University, Nairobi, Kenya

L. Chaari (ed.), *Digital Health in Focus of Predictive, Preventive and Personalised Medicine*, Advances in Predictive, Preventive and Personalised Medicine 12,
https://doi.org/10.1007/978-3-030-49815-3_15

2 Big Data

Big data refers to data, which is large in volume, high in velocity and in different varieties that can be computationally analysed for insights that lead to better decisions, predictions and strategic business moves. It is used by industry analysts, business users and executives who ask the right questions, recognise patterns, make informed assumptions and predict behaviour. The idea of big data was first embraced by online start-up firms such as Google, eBay, LinkedIn and Facebook. It has grown rapidly, permeating almost every sector. Notably, big data is applied widely in psychographics. This is a qualitative methodology used to describe individuals based on psychological attributes, which is then useful in targeted engagement such as politics, marketing, advertising and now to be used in medicine. It is also applied in weather observatory by repurposing sensors in mobile devices such as android mobile phones to map special readings. Finally, it has applications in sports. For example, in football, sports data analytics Sci-Sports has developed a camera called Ball James to capture big data from all players in the field who don't have the ball. This generates player data such as precision, direction and speed of the passing, sprinting strength and jumping strength. This could be used by football managers to make substitution decisions. These are just but a few of the numerous applications.

With the increasing interest in big data analytics around the world, the big data market is equally booming. According to Forbes, the big data market which was estimated at $ 42 billion in 2018 is expected to grow to $103 billion by 2027. Statista on the other hand estimates that the market will grow to $ 70 billion by 2022. These projections on growth prospects underscore how the use of big data is expected to take a centre stage in decision making across many spheres. If fully adopted in the healthcare industry, the growth in its market size may outrun the current projections.

Big data in healthcare refers to these various large and complex data that includes physician notes, lab reports, X-ray reports and case history, used to capture essential information about a patient for complete insights useful in health management and patient engagement [1]. This data is often difficult to analyse and manage with traditional software or hardware. Big data analytics covers integration of heterogeneous data, data quality control, analysis, modelling, interpretation and validation. Application of big data analytics provides comprehensive knowledge discovering from the available huge amount of data. Particularly, big data analytics in medicine and healthcare enables individual analysis of the large datasets from thousands of patients, identifying clusters and correlation between datasets, as well as developing predictive models using data mining techniques. This integrates the analysis of several scientific areas such as bioinformatics, medical imaging, sensor informatics, medical informatics and health informatics. A survey of big data cases in healthcare institutions is given in [1]. The authors acknowledge the reliance of healthcare institutions on big data technology to improve care coordination and develop outcome-based reimbursement models. The new knowledge discovered by big data analytics techniques should provide comprehensive benefits to the patients, clinicians and health policy makers.

In healthcare, big data's strength is in finding the associations and not showing whether these associations have meanings. Therefore, the intervention of medical practitioners is required to attach meaning to such associations derived from data analytics. While doing so, care must be taken to avoid spurious results. Otherwise, "Big Error" may lead to inaccurate and hence inappropriate decisions [9].

3 Healthcare Trends

In the recent times, the increasing prevalence of non-communicable diseases together with aging population in different parts of the world has led to increased mortality as well as rising costs of healthcare provision. Non-communicable diseases such as cardiovascular diseases (CVDs), cancer, diabetes mellitus and respiratory diseases are now identified as among the world's leading cause of death, disability, diminished quality of life and a key contributor to the rising costs of healthcare. In response to this, traditional reactive approaches to medicine are now being shunned and instead replaced with a proactive approach which encompasses predictive, preventive, personalised and participatory (P4) medicine [13] Aided with advancement in technologies and digitization of medicine, electronic health records (EHRs) are gaining momentum. This is geared towards helping physicians and healthcare providers at large to be able to detect potential diseases early enough and intervene in good time, as well as monitoring the health of a patient.

Since the majority of these diseases are preventable or can be delayed to a significantly later stage in life, notable focus has to be placed on monitoring the lifestyle of individuals by obtaining actionable data about some important health metrics of the individuals. To collect such data continuously and in real-time, adoption of wearable technology in medicine provides a good opportunity to improve disease monitoring, provided that big data analytics are performed on the enormous amount of data stored to derive actionable insights for prediction and timely intervention to prevent the diseases [10].

4 Related Literature

With the rise in popularity of Internet of Things (IoT), big data analytics has found its demand in healthcare as providers seek to analyse unstructured data and recognise trends and patterns that can inform decision making [11]. It stands to improve health by providing insights into the causes and outcomes of disease, better drug targets for precision in medicine, and enhanced disease prediction and prevention [7] Moreover, citizen-scientists will increasingly use this information to promote their own health and wellness. This supports P4 medicine, whose premise is to transform the approach of medicine from being largely reactive and population

based practice to an individual-based approach focused on wellness. If wellness can be quantified, diseases can be demystified.

In healthcare, the use of smart wearable devices has gained traction to the extent that an estimated 245 million units of wearable devices will be sold by the end of 2019 (CCS Insight's Forecast on wearable devices). These devices are used to continuously record useful individual health metrics in real-time which facilitates continuous out-of-clinic health monitoring as well as in-home disease management through lifestyle monitoring. The enormous amounts of data recorded is storable on google cloud and can be analysed using certain algorithms to give predictions of diseases. Medical researchers note that diseases are usually a result of perturbed networks in the body cells and that there are usually early signals that can be tracked even before any symptoms are manifested. Thus, it is the early prediction of such diseases through careful analysis of health metrics data from individuals that will lead to appropriate preventive measures being undertaken. For instance, Sagner et al. [12] reports that monitoring and maintaining of normal values for key health metrics such as blood pressure and blood glucose play a primary role in reducing chronic disease risk.

Whereas the use of smart wearables to record data on health vitals of individuals is novel, there are a few challenges faced. Notably, data privacy and security issues remain the biggest question that could slacken their adoption. These devices are feared as being likely to lead to identity fraud, especially when the manufacturers of the devices (who are deemed to be owning the data) sell it to third parties who are likely to abuse it. Similarly, some researchers argue that sophisticated algorithms have the ability to reveal user identity from anonymous data. We believe that data protection rules will be made in different territories and regions to prevent abuse of personal data [8].

5 Methodology

The study was conducted to examine the wearable devices, their systems architecture, and the data they collect and to investigate any emerging patterns and predictive insights. The main source of the data used for this project is Kaggle website.

Our goal was to observe the risk of Cardiovascular Disease (CVD). Research from the Framingham Heart Study indicate that healthcare officials can use the Framingham Risk Score algorithm to estimate the 10-year Cardiovascular Disease risk of an individual. The key risk factors under CVD include: Gender, Age, Total Cholesterol, Systolic Blood Pressure, Smoking, Family History and Diabetes [6].

Such tools address the need for preventive, predictive, personalised and participatory (P4) medicine. The underlying foundation of P4 Medicine lies in the presence of big data. Wearable biometric monitoring devices (BMDs) allow for remote, high frequency and high-resolution monitoring for patients' health outside the hospital. Coupled with progressive advancements in artificial intelligence (AI), the data collected from wearables will help in informing diagnosis, predicting patient

outcomes and helping care professionals elect the best treatment for their patients. As one of the constituent pillars of P4 medicine, wearable devices heavily contribute to personalized medicine. Individual health status can be uniquely monitored using the continuous key health metrics that these devices are able to record, which can be tracked over the long term to identify any patterns. This is important to aid detection of any deviation from the norm and thus take a remedial action. The devices should not be shared among individuals at any time so that data which is only attributable to one individual can be measured, recorded and accumulated over time. This is crucial in addressing the different health needs of various individuals. Finally, wearables can promote primary prevention measures that aim for reducing the probability or risk of CVD. Secondary prevention measures are also applicable to help reduce the impact of the presence of CVD in an individual.

6 Data Analysis and Results

The examination of wearable data on the first phase only represented a single subject. The data collected had the following parameters:

1. Date time
2. Steps
3. Distance covered
4. Calories
5. Minutes per Activity
6. Weight
7. BMI
8. Fat level

The results were based on various parameters of observations and visualized using ggplot2 library in R-Studio (Fig. 1).

The figure below shows that the user did not take any steps within the years 2013–2014. This could be attributed to various reasons such as: the user might have lost their Fitbit watch, the user might have not worn their watch for that period for various reasons, the user could have actually not been moving around (this is too abnormal though).

To take a new look at the steps of the user, we further analysed the steps taken per day, every year. The figure is shown below (Fig. 2).

This gives us a look into the days in which the patient is taking more steps than average, against the days that the user is taking less steps than average. A further visualisation was made in order to get more sense from the daily steps made and what interventions can be put in place to ensure that the user takes the minimum required steps each day (Fig. 3).

To dig deeper into the steps taken by the user, the fat levels and BMI levels were evaluated with regards to the steps.

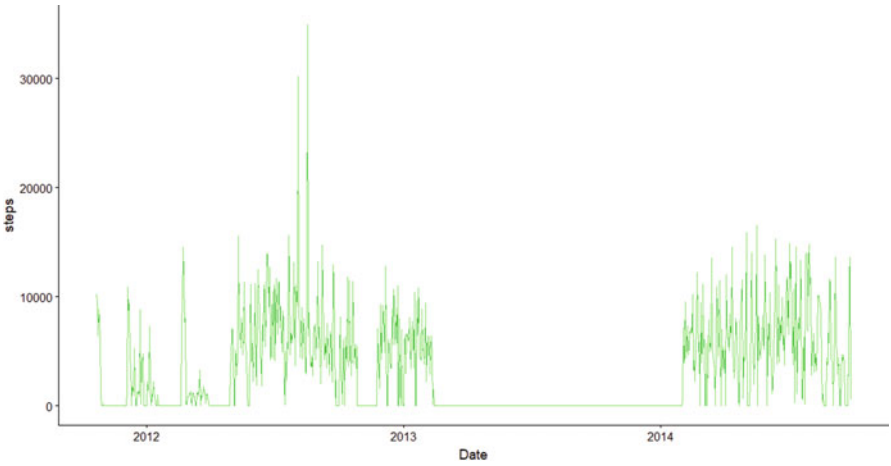

Fig. 1 Variation of Steps taken by the user over a timeline

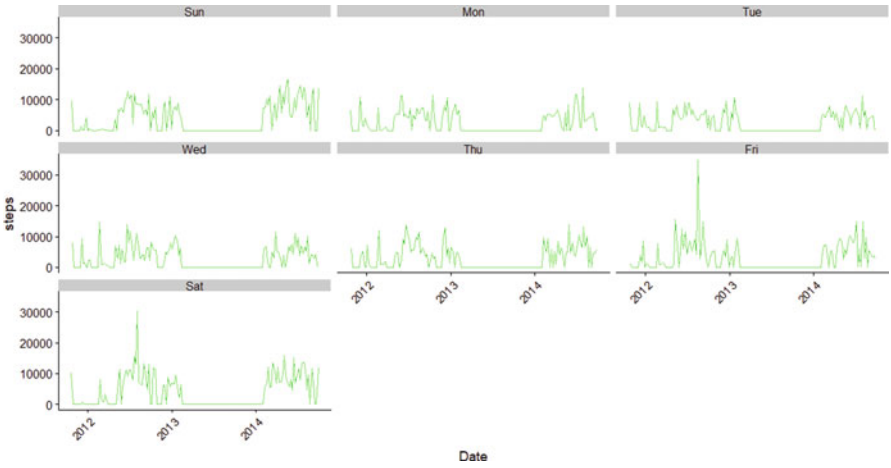

Fig. 2 Variation of steps taken by the user on each day of the week over the time period

It is observed that the fat level and BMI level show almost equal levels of variations over the time period. It is however worth noting that during the period 2013–2014 where there was no record on the number of steps taken, there was an increase in the levels of BMI and Fat, as shown in the figure below (Fig. 4).

These insights, when coupled up with the various electronic health records (EHRs); such as the Blood Pressure of the specific user, would really mean a lot to the health and care professionals. They would be able to predict diseases before they actually come and therefore provide preventive interventions to the user.

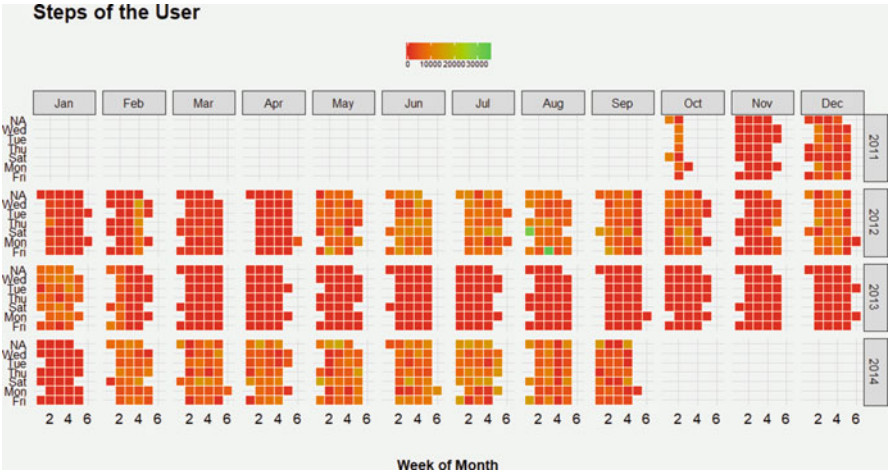

Fig. 3 Analysis of the daily steps taken by the user over the time period

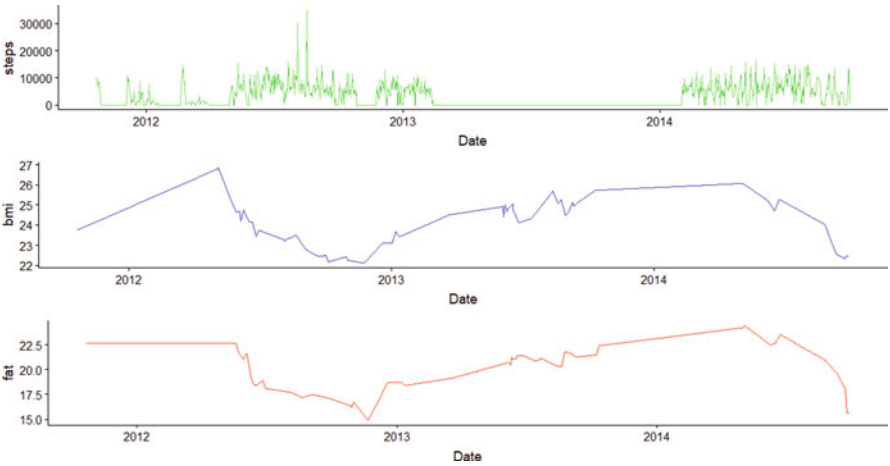

Fig. 4 Fat and BMI Levels against the number of steps of the user

Onto the second phase of our analysis, the examination of the Fitbit data was based on various number of subjects. It was a collective dataset representing the records for various individuals.

We first visualised the correlation between the different variables in the dataset, and came up with the correlation matrix below (Fig. 5).

This informs us that the variables – Heart, Calories and Steps are strongly positively correlated to each other. Also, the presence of Age, Gender, Weight, and Height also indicate a strong correlation.

Having this in mind, we developed a Logistic Regression model to predict the probability of an individual within the dataset contracting heart disease (also known

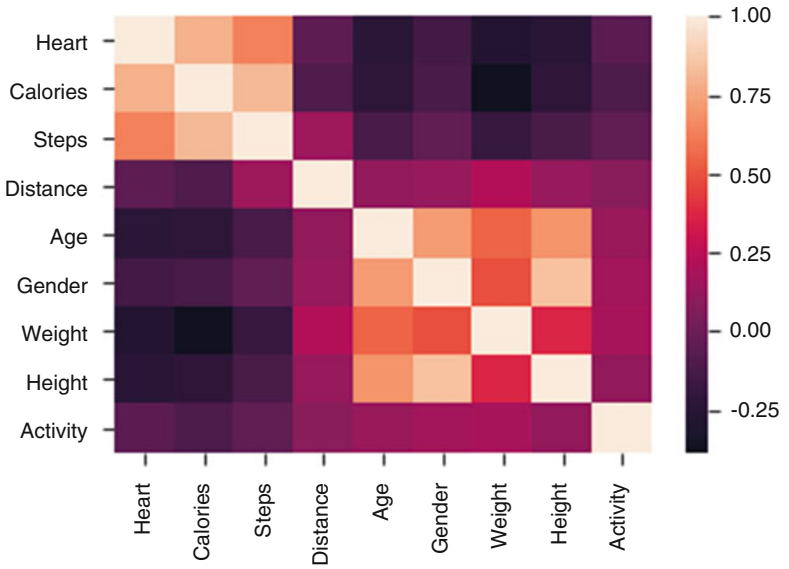

Fig. 5 Correlation Matrix of the Collective Data

as Cardiovascular Disease). First, we came up with a new variable and defined it as BMI; where:

$$BMI = \frac{Weight\ in\ Kilograms}{Height\ in\ Meters\ squared}$$

Various research has indicated the use of BMI as a better indicator of Cardiac Risk Factors [2]. Once BMI was calculated, we categorised it in a binary format as follows:

- BMI between 18.5 to 29.9 = 0
- BMI above 29.9 = 1

Our classification was such that a person is either obese or not, hence the classification format as stated above. However, the conventional way of classifying BMI is as follows:

- BMI <18.5 = Underweight
- BMI 18.5–24.9 = Normal Weight
- BMI 25.0–29.9 = Overweight
- BMI 30–34.9 = Class I Obesity
- BMI 35–39.9 = Class II Obesity
- BMI > 40 = Class III Obesity

Logit Regression Results

Dep. Variable:	bmi_pred	No. Observations:	21489
Model:	Logit	Df Residuals:	21478
Method:	MLE	Df Model:	10
Date:	Sun, 09 Jun 2019	Pseudo R-squ.:	1.000
Time:	20:53:46	Log-Likelihood:	-0.00016464
converged:	False	LL-Null:	-14325.
		LLR p-value:	0.000

	coef	std err	z	P>|z|	[0.025	0.975]
const	812.9701	nan	nan	nan	nan	nan
Heart	-0.0528	6.074	-0.009	0.993	-11.958	11.853
Calories	0.0702	64.068	0.001	0.999	-125.501	125.642
Steps	-0.0011	3.969	-0.000	1.000	-7.780	7.778
Distance	0.0165	10.093	0.002	0.999	-19.766	19.799
Age	-13.0688	nan	nan	nan	nan	nan
Gender	-19.0417	nan	nan	nan	nan	nan
Weight	11.3264	nan	nan	nan	nan	nan
Height	-619.0515	nan	nan	nan	nan	nan
Activity	-0.2843	142.304	-0.002	0.998	-279.195	278.627
BMI	-10.4263	nan	nan	nan	nan	nan

Fig. 6 Logistic Regression Results

Our predictor variable was therefore a binary type with the 0's and 1's. We run the model using Sci-Py library in Python 3.6 environment. The results are as shown above (Fig. 6):

The results indicate that the variables: Heart, Calories, Steps, Distance and Activity are significant in determining the changes in BMI, which would ultimately impact the probability of one getting CVD. We went ahead to split the dataset into testing dataset and training dataset and the model achieved an accuracy score of 69%.

7 Conclusion

Apart from the rapidly advancing genomics, metabolomics, single-cell analysis, phenotyping, micro-fluids and imaging technologies used for early detection of chronic illnesses, wearable technology is a change agent in the entire healthcare industry. The data gotten from wearables present tremendous opportunities for healthcare practitioners to promote a proactive approach to preventing and treating such diseases. The capabilities behind big data tracking and system analytics will ultimately result in personalised actionable health insights. However, it is worth noting that these devices should undergo proper tests and validation to ensure that the data used for the clinical operations is of good quality. Various measures should be put into place to ascertain the levels of data privacy too [8].

P4 medicine presents a myriad of opportunities for research and development. This has been accelerated due to the technological advancements that has led to the explosion of massive amounts of data. The shift from traditional reactive medicine to P4 medicine will only be possible when various stakeholders from the healthcare and other industries form strategic partnerships to work together towards the common goal of attaining sustainable healthcare.

References

1. Archenaa, J., Mary Anita, E. A.: A Survey of Big Data Analytics in Healthcare and Government. International Symposium on Big Data and Cloud Computing (ISBCC'15). (2015)
2. Debnath, S.: BMI is a better indicator of cardiac risk factors, as against elevated blood pressure in apparently healthy females and young adult students: Results from a cross-sectional study in Tripura. Indian J. Community Med. **41**, 292 (2016)
3. ESF: Personalised Medicine for the European Citizen—Towards more Precise Medicine for the Diagnosis, Treatment and Prevention of Disease. European Science Foundation, Strasbourg (2012)
4. Flores, M., Glusman, G., Brogaard, K., Price, N.D., Hood, L.: P4 medicine: how systems medicine will transform the healthcare sector and society. Pers. Med. 565–576 (2013)
5. Hood, L.: Systems biology and P4 medicine: past, present, and future. Rambam Maimonides Med. J. (2013)
6. Jia, X., Baig, M. M., Mirza, F., Gholam Hosseini, H.: A cox-based risk prediction model for early detection of cardiovascular disease: identification of key risk factors for the development of a 10-Year CVD risk prediction. Advances in Preventive Medicine. (2019)
7. Khoury, M.J., loannidis, J.P.: Big data meets public health. PubMed Central. 1054–1055 (2014)
8. Lymberis A.: Smart wearables for remote health monitoring, from prevention to rehabilitation: current R&D, future challenges. Proceedings of the 4th Annual IEEE Conference on Information Technology Applications in Biomedicine, UK (2003)
9. Raghupathi, W., Raghupathi, V.: Big data analytics in healthcare: promise and potential. Health Info. Sci. Syst. **2**, 3 (2014)
10. Ristevski, B., Chen, M.: Big data analytics in medicine and healthcare. J. Integr. Bioinform.. De Gruyter (2018)
11. Rodriguez C., Barrow A., Dangore S., Pathak U., Talledo J.: Applying Data Analytics to Big Data Obtained from Wearable Devices. In Proceedings of Student-Faculty Research Day, CSIS, Pace University, Pleavantville, New York (2018)
12. Sagner et al.: The P4 Spectrum – a predictive, preventive and personalised and participatory continuum for promoting Healthspan. Progress in Preventive Medicine. (2017)
13. Tian, Q., Hood, L.: Systems Cancer Medicine: Towards Realization of Predictive, Preventive, Personalized and Participatory (P4) Medicine. Journal of Internal Medicine, Seattle (2011)
14. Topol, E.J.: The Creative Destruction of Medicine: how the Digital Revolution Will Create Better Health Care. Basic Books, New York (2012)
15. Vogt, H., Hofmann, B., Getz, L.: The new holism: P4 systems medicine and the medicalization of health and life itself. Med. Healthcare Philos. 307–323 (2016)

Towards an Oversampling Method to Improve Hepatocellular Carcinoma Early Prediction

Mahbouba Hattab, Ahmed Maalel, and Henda Hajjami Ben Ghezala

1 Introduction

Knowledge discovery in medical databases has become an attractive and crucial complement for clinical research. Survival and disease prediction are of a highly important task addressed by the medical research communities due to its direct effect on doctor's decisions [1]. Using KDD (Knowledge Discovery in Databases), efficient and important knowledge can be extracted from these data sets. The principal steps in the KDD process are as follows: (1) Data selection, (2) Data management and pretreatment, (3) Transformation, (4) Data mining, and (5) Assessment and interpretation. Ideally, from a computer science perspective, data mining is one of the ultimate steps in the KDD process. Indeed, Data Mining is a discipline resulting from combining statistics and computer science such as Machine Learning algorithms. Data mining aims to extract new and useful knowledge from a large amount of data (i.e.: applied to have an effective and preferment predictive model [2]). However, each of the aforementioned domains has its specifics, therefore it is

M. Hattab (✉)
Higher Institute of Applied Sciences and Technology of Sousse, University of Sousse, Sousse, Tunisia

A. Maalel
Higher Institute of Applied Sciences and Technology of Sousse, University of Sousse, Sousse, Tunisia

National School of Computer Sciences, RIADI Laboratory, University of Manouba, Manouba, Tunisia
e-mail: ahmed.maalel@ensi.rnu.tn

H. H. B. Ghezala
National School of Computer Sciences, RIADI Laboratory, University of Manouba, Manouba, Tunisia

L. Chaari (ed.), *Digital Health in Focus of Predictive, Preventive and Personalised Medicine*, Advances in Predictive, Preventive and Personalised Medicine 12,
https://doi.org/10.1007/978-3-030-49815-3_16

important to wisely choose the best data optimization and pre-treatment algorithm to achieve state-of-the-art classification accuracy.

Due to the abundance of data in the biomedical domain, this latter has a high potential in improving the well being of humankind. Nevertheless, it is very complex to process and analyze such data by traditional methods [1]. As a result, the interest of data mining and machine learning is increasing considerably with a wide range of medical applications. They become useful instruments in bioinformatics thanks to their capability to convert this vast resource into information and knowledge that helps achieve better decision making in several disease areas including cardiovascular disorders, Parkinson's, Alzheimer's, etc. [3].

Cancer is a generic term for a large variety of diseases that can affect any person and any part of the body and it represents one of the leading causes of morbidity and mortality worldwide after heart diseases [4, 15]. Globally, according to the World Health Organisation (WHO) [4], one in six deaths are due to cancer. Relatable to cancer, Hepatocellular carcinoma (HCC) also referred to as malignant hepatoma [3] is a malignant tumor, and represent the sixth most common type of cancer and the third leading cause of cancer-related deaths globally according to [5].

2 Related Works and Motivation

Over the past years, several research works have been conducted on HCC and liver-related diseases. For instance, **Santos et al. (2015)** [5] studied HCC data set using a new cluster-based oversampling algorithm. The proposed methodology is based on the data pre-treatment process considering appropriate distance metrics for both heterogeneous and missing data by applying the Heterogeneous Euclidean-Overlap Metric (HEOM) distance. Then Kmeans clustering algorithm is applied for the first sampling step within the HCC database and SMOTE oversampling algorithm to build a representative balanced data set and use it for Leave-One-Out cross Validation (LOO-CV) assessment with different machine learning algorithms such as logistic regression (LR) and neural networks (NN) classifiers. The results indicated that the proposed approach can achieve efficient results.

In another work, **Sawhney et al.** (2018) [6] explored the performance of the firefly algorithm by adding a penalty function to the existing fitness function. Afterward, they modify the existing wrapper feature to reduce the feature set to an optimal subset. Furthermore, the influence of the method is proved on the classification accuracy as well as feature reduction using a Random Forest classifier for the Hepatocellular Carcinoma dataset in comparison to other contemporary methods such as Deep Learning methods and Information Gain. However, the above-mentioned works, are of a highly computationally expensive and require a large amount of data in order to generate a satisfying model. Moreover, real-world data tends to be incomplete, noisy, and inconsistent and the important task is to fill in missing values, smooth out noise and correct inconsistencies. To address these issues, previous works have relied on applying feature selection [7] to eliminate the

redundant and inconsistent data and thus improve the capacity of the classifier. Other studies used multiple scaling methods such as normalization and standardization to improve the classification model [5, 6]. Despite the good *theoretical* approach of these methods, the delivered results can be tremendously inconsistent as each of the feature selection or the normalization/standardization methods can deliver a different result and thus selecting the best approach is a time consuming and exhausting process. Another important issue that could be found which is:

- outliers: "*Observation which deviates so much from other observations as to arouse suspicion it was generated by a different mechanism"* Hawkins(1980)

In Data Science, an Outlier is an observation point that is distant from other observations on data that diverges from an overall pattern on a sample. They may indicate variability in measurement, experimental errors or a novelty. The quality and the prediction speed of classifier depend on the input data set for the training thus, the more outliers existing in the training set is, the less accurate the prediction is [7, 8]. In fact the most common causes of outliers on a data set are: (1) Incorrect data entry, (2) Data processing errors: application of inappropriate missing values methods in a dataset, (3) Outliers case did not come from the intended sample and (4) Not an outlier, just a novelty in data.

Instance selection is a recommended technique that was developed to overcome the limitations related to noise and outliers. The aim behind using instance selection is to improve the prediction accuracy of the classifier. To achieve that goal these algorithms are designed to remove outliers and noisy instances. The ensemble learning has become one of the most promising machine learning approaches during the last decade. It takes advantage of combining several models, which when grouped together, can outperform each method with only a linear increase in computational complexity [8]. Several states of the art were included in these groups of algorithms. We include, in the first one, an ensemble of C different models trained on the same training set of data T vote for the output of the instance being classified t. In another state of the art, an extension of the voting approach is presented; where c independent models of different types are trained on the same data set T, then all models outputs are combined for an extra model for the final prediction. Also, a third approach consists of c models of the same type, where each of them is trained on the data set T* that is obtained from T by sampling. The final prediction is obtained by voting. Finally, a similar approach to the previous, but the probability of selecting an instance from T depends on a classification error of the previous models so that an instance that was incorrectly classified by the current models is more likely to be selected.this method called Boosting [8].

For small data sets, noise filtering can be used as a step in the pre-processing of training data; on the other hand, the sampling process which selects a subset of the training set may include or followed by noise and outliers filtering.

In machine learning, Data clustering is frequently used in many fields, such as sampling of data (Stratified sampling) [9]. The mechanism of dividing a set of data to a particular set of groups is termed as clustering, and one such prominent methodology is the k-means clustering. Due to the nature of our available data, its

efficiency and its usefulness in several fields of pattern recognition particularly for clustering cancer data, K-means is a well-known unsupervised learning algorithm for data partition with a low computational cost. K-means iteratively reduces the Sum of Squared Error (SSE) from every object to their cluster centroids for every cluster Ck. (SSE) indicates the compactness of the cluster, the lower is, the better is.

Generally, to achieve success ensemble modeling, it recommended ensuring the diversity of the obtained results of each model, which are then combined into a final predictive one. The diversity of the results can be attained in several ways:

– Guarantee diversity of the models: Several different algorithms are used or the same algorithms but with different hyper-parameters or setup.
– Guarantee diversity of the data: we keep the same model, and each subset of the data used for training generates diversity.

In this paper, we address the issue of existing of outliers and noise in small datasets, so that data sampling, the instance selection and data oversampling are combined to ensemble methods and the diversity is obtained by manipulating different algorithms such as K-mean clustering and SMOTE. Our goal is that the ensemble of instance selection algorithm and the Oversampling technique allow us to manipulate the trade-off between the problem of small data sets and prediction accuracy. Moreover, improve both which grouped can outperform each method without an increase of computational complexity. This paper is organized as follows: the next section describes the basic algorithms used in the experiments. The following section describes the testing environment and presents numerical experiments. The last section summarizes the results and presents their interpretation.

3 Model Description

In the presented section, the different stages that compose the followed methodology to construct our approach, as well as the approach itself, are described.

First of all Fig. 1 represent the methodology applied in this work: Data imputation, Data partitioning, Clustering and finally classification. The main aspects of each stage are briefly described.

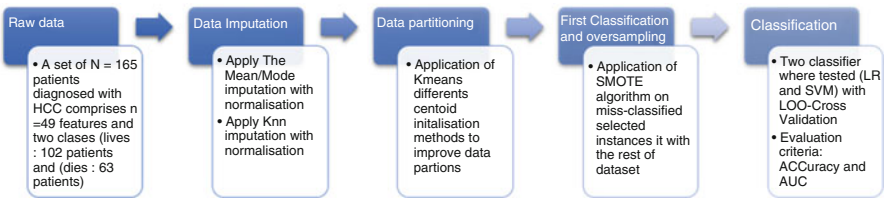

Fig. 1 Followed methodology

We used a HCC dataset composed of N = 165 patients diagnosed comprises n = 49 features provided by UCI machine learning repository.[1] The dataset's class distribution presents 63 cases labeled as 0 (dead) and the remaining 102 cases as 1 (alive) [5]. In the Data Imputation phase, two well-known imputation techniques (Mean/mode and K nearest neighbor) are used to handle missing values with Normalization. According to [10] Cross-validation is a common way of avoiding over-training. Nonetheless, the fundamental problem with this method is the proper partition of data. Simple random sampling is used for most applications. However, a variety of sophisticated methods of statistical sampling suitable for different types of datasets are available. The stratified sampling is one of these methods. The fundamental idea is to investigate the internal structure and distribution of the T dataset and to split T into relatively homogeneous sample groups. The samples were selected from each cluster separately [9]. Various clustering algorithms can be used to divide dataset T into clusters including K-means. For instance, The data sampling phase, in this work, aims to partition the initial data set into a set of tow different partitions by applying classification via clustering method with K-means algorithm for different seed values and three different centroid initialization methods (Random; Kmeans++; Canopy and Farthest first) to ensure diversity of the data. After the data partitioning phase, different resulting partitions are presented and the selection process was based mainly on the SSE that indicates how compact a cluster is: The lower the value, the better. then a manual review is applied to the chosen partitions: correctly labeled instances are kept to learn the classifier, then miss-labeled are used as a supplied test set for the next phase. Once final samples are produced, Our proposed method for selecting the outliers, which is based on the classification error of the previously built model, is performed and the resulting set is oversampled With the SMOTE algorithm. Thus, the oversampled partition is added to the initial dataset and duplicates instances are removed. The final phase consists of fit the classifier with the new augmented dataset. tow classifiers were engaged in this step, which are Logistic regression [11] and Support Vector Machine [12].

Our proposed approach is presented in Fig. 2. It starts by loading the data, then the data imputation is applied on missing values followed by Normalization for features scaling. After the pre-treatment phase, the stratified sampling with k-means is processed with different centroid initialization methods to find better subsets. For the following, and for rigorous scalability, reproducibility, and generalizability, the rest of the process was wrapped by the leave one out cross-validation for underlying subsets selection and the prediction process. It's important to note that the cross-validation strategy guarantees the best performance of the model [13] Step (C) is repeated several times in order to refine the resulting subset. Since the data set is relatively small, each instance is important for the prediction task.

[1] UCI Machine learning Repository, URL: https://archive.ics.uci.edu.

4 Experimental Results and Discussion

Considering the description presented above we have decided to conduct the experiments, which empirically verify the influence of the ensemble learning method on the quality of the instance selection. In the experiments we examine the influence of different parameters on the compression of the training data and the accuracy of the final prediction model.

In our study, we used the Waikato Environment for Knowledge Analysis (WEKA) software V3.8.2 [14] to construct and evaluate the different models. The Weka machine learning workbench offers a general-purpose framework for automated classification, regression, clustering, and selection of features that represents common bioinformatics research data mining issues. This provides a comprehensive collection of machine learning algorithms and data pre-processing methods accompanied by graphical user interfaces for software exploration and practical comparison of various machine learning techniques on the same problem.

For the ensemble of the different used algorithms, basic hyper-parameters were fixed based on several previous tests, such as Number of Nearest neighbor for KNN Imputation $n = 1$, Number of clusters for the classification via clustering with K-means $k = 2$ and with different seed numbers (1 to 10); number of iterations of Step (c) in the approach was fixed to $t = 5$, so each time a new model is created with LOO-CV, then tested with the selected supplied test subset. As shown in Fig. 2; for each iteration of (C): correctly classified subjects are extracted from the test subset and added to the training subset then the process is repeated. For the SMOTE algorithm that based on the similarity between the available minority samples and represents the most popular and applied oversampling procedure, generates synthetic minority

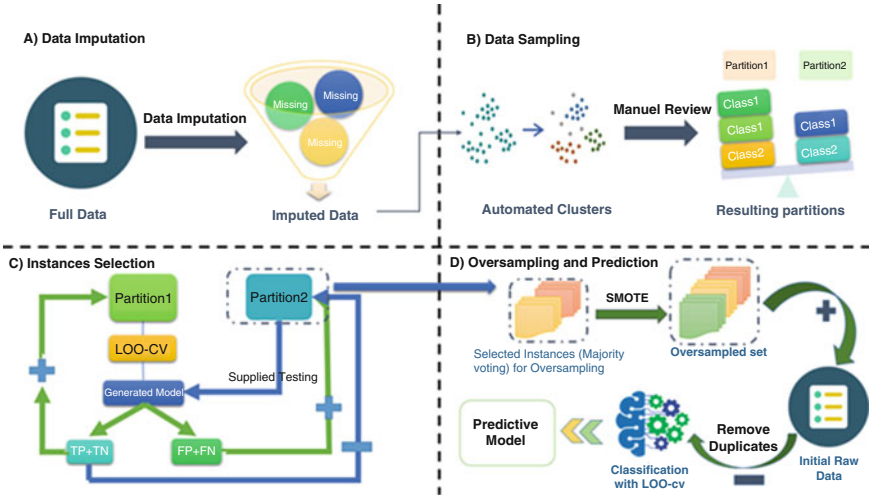

Fig. 2 Schematic representation of the proposed approach

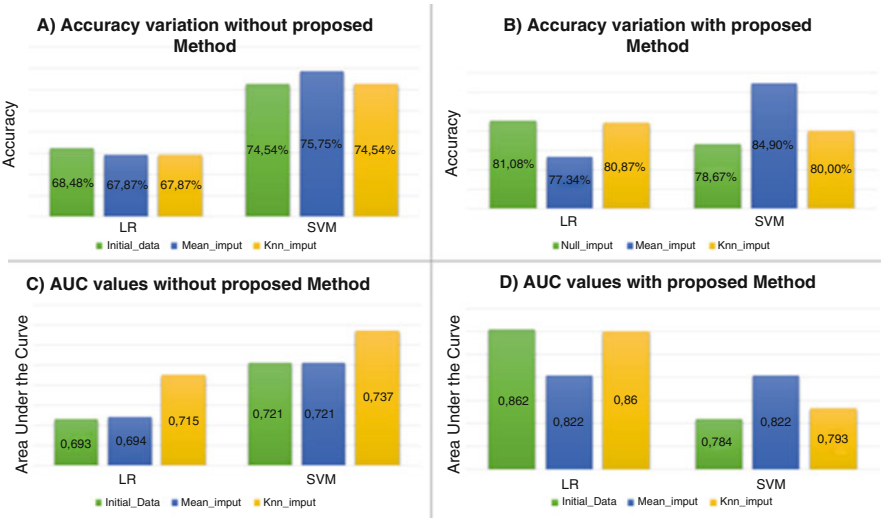

Fig. 3 Comparison the accuracy and AUC of the proposed approach achieved by the instances manipulation for different data imputation and K-means centoid Initialization

samples considering K-nearest neighbors. Thus, different nearest-neighbor values were tested nn = [1,2,3]. Logistic Regression model with ridge estimator = 1.0E-4. Support vector machine model with polynomial kernel and C = 1.0.

All of the experiments were performed on a HCC dataset composed of N = 16 patients diagnosed comprises n = 49 features [4]. Both of the tested algorithms; LR and SVM were tested independently and the results are presented using the Accuracy-Classifier plot and AUC-classifier plot to simplify the interpretation.The obtained results are presented in Figs. 3, 4, and 5. An excellent model with an AUC near to 1, means that it has a good measure of separability. Contrariwise, a poor model with an AUC near to 0 means incapability of separability between classes. When AUC equals to 0.5, it means that the model has no class separation capacity whatsoever.

Hence, in this study, several data mining and machine learning technique were applied; therefore, results were evaluated according to these applied technique. The obtained results show that our approach achieves good results coupled with imputed datasets. In several essays, data imputation didn't ameliorate the model accuracy Fig. 3a with the LR model, instead of the AUC that shows a good response to the imputation with Knn method Fig. 3c. Moreover, the SVM algorithm was sensitive for the applied imputations in terms of ACC and AUC Fig. 3a. The algorithm behaves differently when applying the proposed approach Fig. 3b, d; the accuracy increases remarkably.

Different situations were observed for the LR and SVM algorithms due to the data imputation, the centroid initialization for K-means clustering and SMOTE

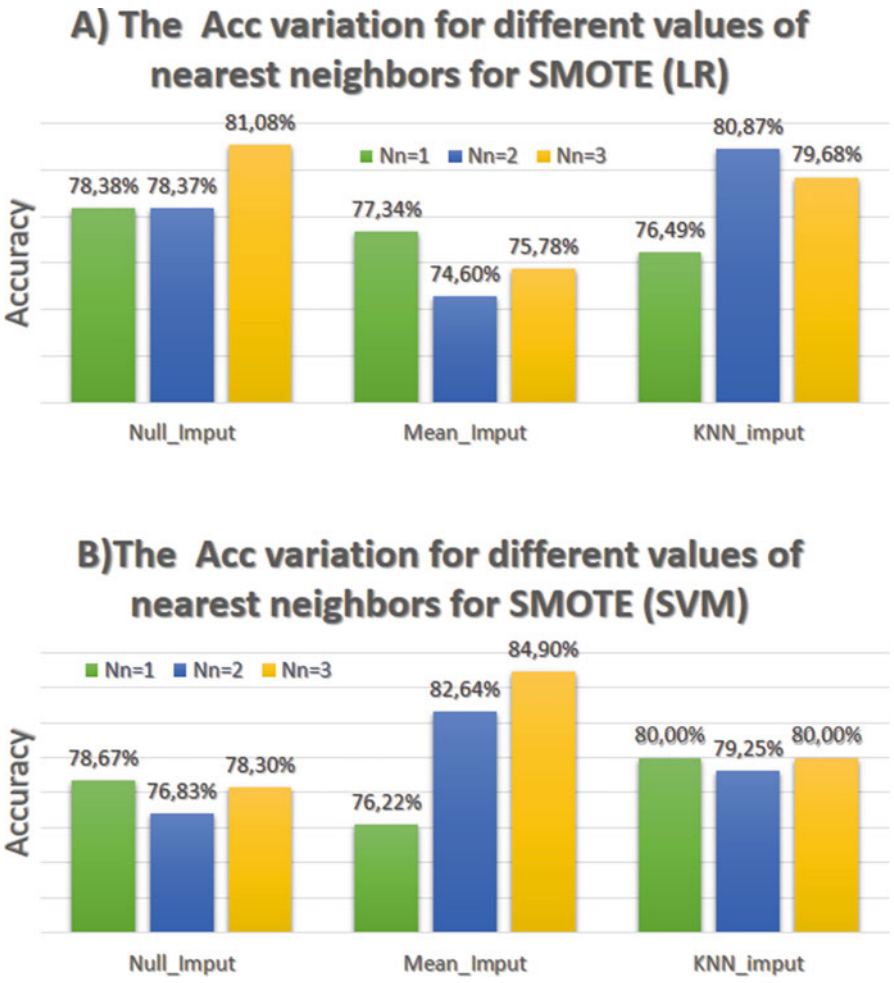

Fig. 4 Comparison the accuracy and AUC of the proposed approach achieved by the instances manipulation for different SMOTE nearest neighbor values

nearest neighbor number Fig. 4; that led to an important diversity of selected instances, hence, conducting to improve the final accuracy.

It can be seen from Fig. 4 that, our method obtained much better performance in the Accuracy and the AUC than the other methods used in [4, 5]. For different parameters of the models, we can improve the accuracy up to 84,90% without any loss of instance or features numbers. It is not possible to define a universal and optimal set of parameters. They must be chosen in each case independently, and based on several experimentation to avoid the wrong choice that cause a significant deterioration in the performance of the model. The advantages of the proposed method are as follows:

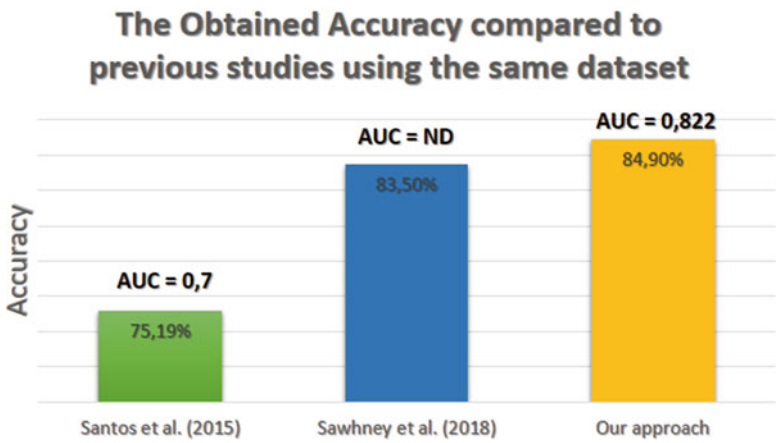

Fig. 5 The Accuracy and AUC achieved by the proposed approach other studies working on the same data set

- Obtained the highest performance (accuracy and AUC).
- Proposed method is robust and accurate as we have employed LOO-CV cross-validation twice (for the Instance selection and the prediction)
- Easy to implement and with a low computational cost.
- Instances selection was used for outliers detection and data oversampling instead of data compression.

5 Conclusion

Nowadays new possibilities open for the use of instance selection methods, in particular in limited and small data sets. These types of applications have two objectives: to improve or maintain the accuracy of the prediction model created on the selected data and to achieve the compression as high as possible. This study aimed to analyze the possibility of using ensemble learning methods to improve the efficiency of instance selection without reducing the size of data. Different data pre-processing techniques associated with learning models were used for this objective. The empirical experiments were performed with the proposed approach, which was based on instances management. The results indicate that it is possible to improve the Accuracy and the AUC while maintaining the initial data size. The approach was able to achieve preforming results compared to other approaches using the same data set.

References

1. El Houby, E.M.F.: A survey on applying machine learning techniques for management of diseases. J. Appl. Biomed. **16**, 165–74 (2018)
2. Maalel, A., Hattab, M.: 'Literature review: overview of cancer treatment and prediction approaches based on machine learning'. In: Smart Systems for E-Health, Advanced Information and Knowledge Processing, p. 324. Springer (2019). ISBN: 978-3-030-14938-3
3. Wu, C.F., Wu, Y.J., Liang, P.C., Wu, C.H., Peng, S.F., Chiu, H.W.: Disease free survival assessment by artificial neural networks for hepatocellular carcinoma patients after radiofrequency ablation. J. Formos. Med. Assoc. **116**, 765–773 (2017)
4. World Health Organization.: Hepatitis C. [online] [cit. 2017-10-15]. Available from: http://www.who.int/mediacentre/factsheets/fs164/en/ (2017)
5. Santos, M.S., Abreu, P.H., García-Laencina, P.J., Simão, A., Carvalho, A.: A new cluster-based oversampling method for improving survival prediction of hepatocellular carcinoma patients. J. Biomed. Inform. **58**, 49–59 (2015)
6. Sawhney, R., Mathur, P., Shankar, R.: A firefly algorithm based wrapper-penalty feature selection method for cancer diagnosis. In: International Conference on Computational Science and Its Applications, pp. 438–449. Springer, Cham (2018)
7. Gamberger D., Lavrač, N.: Filtering noisy instances and outliers. In: Liu, H., Motoda, H. (eds.) Instance Selection and Construction for Data Mining. The Springer International Series in Engineering and Computer Science, vol. 608. Springer, Boston (2001)
8. Blachnik, M.: Ensembles of instance selection methods based on feature subset. Proc. Comput. Sci. **35**, 388–396 (2014)
9. Reitermanova, Z.: Data splitting. In: WDS, pp. 31–36 (2010)
10. Korjus, K., Hebart, M.N., Vicente, R.: An efficient data partitioning to improve classification performance while keeping parameters interpretable. PloS one **11**(8), e0161788 (2016)
11. Kourou, K., Exarchos, T.P., Exarchos, K.P., Karamouzis, M.V., Fotiadis, D.I.: Machine learning applications in cancer prognosis and prediction. Comput. Struct. Biotechnol. J. **13**, 8–17 (2015). https://doi.org/10.1016/j.csbj.2014.11.005
12. Chang, C-C., Lin, C-J.: LIBSVM: a library for support vector machines. ACM Trans. Intell. Syst. Technol. **2**(3), 27 (2011). Article 27. https://doi.org/10.1145/1961189.1961199
13. Nebli, A., Rekik, I.: Gender differences in cortical morphological networks. Brain Imaging Behav. (2019). https://doi.org/10.1007/s11682-019-00123-6
14. Han, J., Kamber, M., Pei, J.: Data Mining: Concepts and Techniques, 3rd edn. Morgan Kaufmann Publishers Inc., San Francisco (2011)
15. Schutte, A.E.: Global, regional, and national age-sex specific mortality for 264 causes of death, 1980–2016: a systematic analysis for the Global Burden of Disease Study (2017)

Towards a Chatbot Based Smart Pervasive Healthcare Medical Emergency Cases

Nourchène Ouerhani, Ahmed Maalel, and Henda Ben Ghézela

1 Introduction

The rise of chatbots inspired many researches to adopt chatbots into healthcare to avail of their multiple advantages. One of the oldest examples includes Eliza [10]. However, to the best of our knowledge, very few works [1–3] use them to manage medical emergencies. In fact, when facing a medical emergency case and human lives are on the line, there is a need of performing an immediate treatment to the victim. Unfortunately,the current prehospital emergency process [6] shows that the emergency medical staff would take a lot of time to locate the emergency incident spot [6]. Even worse, people who are present in the emergency spot may not interfere because most of them have no skills in first aid. Even more severe, there are persons who take advantage of such situations to share it on social media. Given the previously outlined circumstances, a chatbot based smart pervasive healthcare is proposed in this paper in order to save time during medical emergencies and to provide care starting immediately to the victim or his companions. The remainder

N. Ouerhani (✉)
Higher Institute of Applied Sciences and Technology, University of Sousse, Sousse, Tunisia

A. Maalel
Higher Institute of Applied Sciences and Technology, University of Sousse, Sousse, Tunisia

National School of Computer Sciences, RIADI Laboratory, University of Manouba, Manouba, Tunisia
e-mail: ahmed.maalel@ensi.rnu.tn

H. B. Ghézela
National School of Computer Sciences, RIADI Laboratory, University of Manouba, Manouba, Tunisia
e-mail: henda.benghezala@ensi.rnu.tn

L. Chaari (ed.), *Digital Health in Focus of Predictive, Preventive and Personalised Medicine*, Advances in Predictive, Preventive and Personalised Medicine 12,
https://doi.org/10.1007/978-3-030-49815-3_17

of the paper is organized as follows: First, we explain our approach in Sect. 2. Then, we evaluate our work by a test case in Sect. 3. And finally in Sect. 4, we conclude the work and give some future works for interesting research directions.

2 Proposed Approach

The proposed chatbot is designed to be able to help victims or companion perform first aid work properly.

Our proposed chatbot's architecture is depicted in Fig. 1. It is divided into several modules as follows: Input Pre-processor module (IPM), Natural Language Pipeline, Storage module (SM) and Response Engine (RE).

When the chatbot receives a message (text/voice) that will be pre-processed by the IPM to bring out a text whatever is its initial form. In case of a voice input, IPM should convert the speech to text through the speech recognition [4].

Then, the Natural Language Pipeline's main task is to convert the natural language text received form the IPM into a structured format consisting of intents and entities. Thus, to properly realize the natural language processing (NLP), it is required to transform the text to the vector domain which is referred as word embedding [5, 7]. Our solution is to simply train the pre-trained model GloVe [5] on our domain specific medical data. Since the embeddings are already trained and entities are extracted [9], our intent classifier [8] requires only little training to make confident intent predictions that are relative to the ongoing emergency case.

In order to be more efficient our chatbot is able to store all information the user provided once he/she starts communicating with the platform such as location, as well as information gathered during the ongoing discussion in order to influence

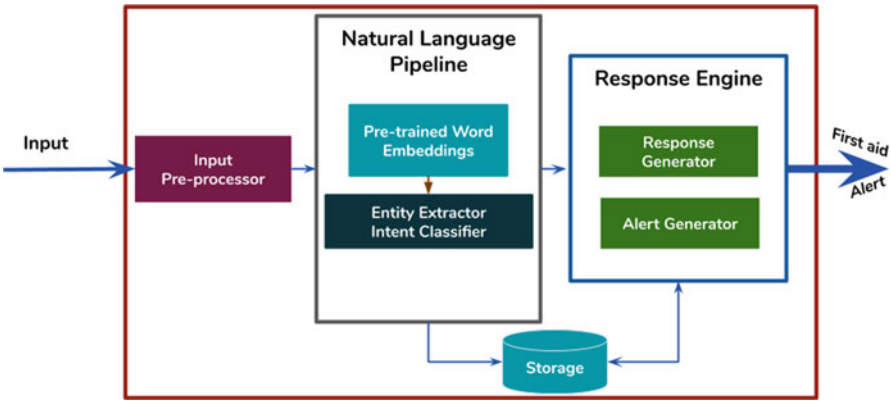

Fig. 1 Architecture of the chatbot based smart pervasive healthcare

how the dialogue progresses. All these data will be consulted later on by the RE in order to respond to the user, or request more information if required.

The RE's task is formulated as a classification problem, over a predefined list of actions for each emergency case. The generated answers are based on the information stored in the SM. An immediately response is generated once there are sufficient information describing the emergency situation, otherwise, if there are some missing information which are crucial for the bot better understand the situation, it will keep requesting information from the user according to the St John DRSABCD action plan[1] that we learnt before having a first aid certification from the civil protection in our Tunisian government. This process will be repeated until the bot has enough knowledge of the emergency victim's state to generate helpful first aid tips. More over, the chatbot is able to send a real time alert to the emergency medical service when the situation presents high risk to the victim and individuals on the scene.

3 Experimental Set Up: Application Development and Deployment

We have developed two separate but inter-dependent applications: The mobile application that will be used by the user and the chatbot back-end. However, the implementation of health information management via mobile devices poses many problems, such as storage and data management so we used the cloud, where each of the proposed modules is written as web services which are exposed as REST API micro services on the cloud, as shown in Fig. 2.

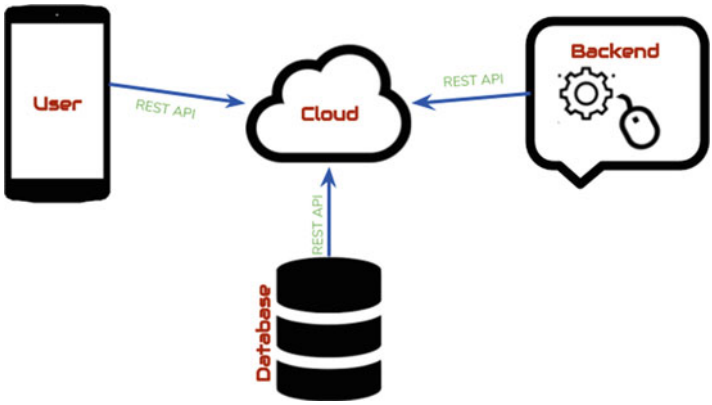

Fig. 2 Implementation of chatbot based smart pervasive healthcare

[1] https://www.stjohnnsw.com.au/drsabcd-action-plan/

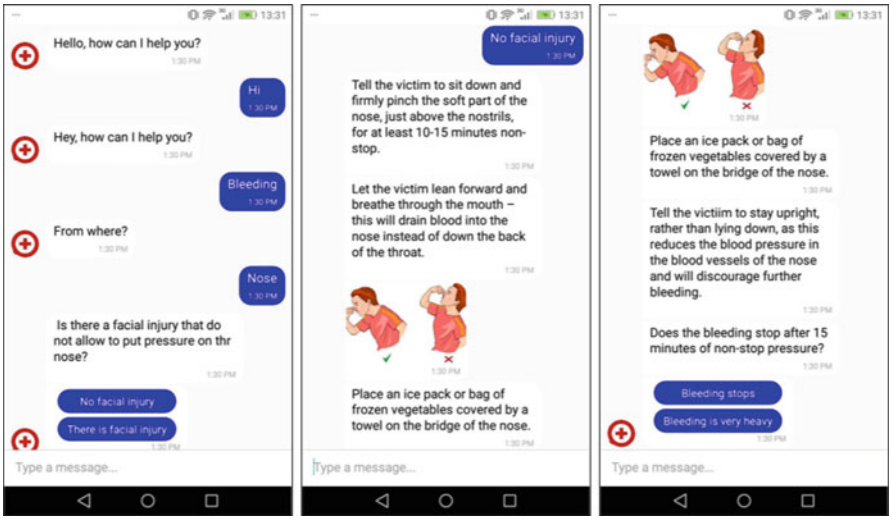

Fig. 3 Responses of Chatbot based Smart Pervasive healthcare amongst a victim suffers from epistaxis (nosebleed)

The chatbot asks specific questions to understand the victim's condition. The user is free whether to write his own answer or to choose one of the answers suggested by the chatbot, this method allows a faster response time from the user. Once the chatbot understands the victim's situation, first aid is performed before aid arrives. The implemented process is shown in Fig. 3.

4 Conclusions and Future Works

We proposed to develop a chatbot based smart pervasive healthcare, which is designed to help people react well in medical emergency cases. The pervasiveness of our chatbot is clear since it is available anytime and is accessible from everywhere and for every body including experts or normal people and it's context-aware since its response differs on the medical emergency case and the user supplies information. We introduced the chatbot architecture by proposing the notion of its several modules. The current system has foundations in each domain including a response engine and other natural language processing tool-kits. We used GloVe to solve the NLP problem in our case because it works well according to our evaluation experiments. The work is still under implementation and much further work is needed to improve our chatbot's capability to manage more emergency cases.

References

1. Tsai, M-H., Chen, J.Y., Kang, S-C.: Ask Diana: a keyword-based chatbot system for water-related disaster management. Water **11** (2019). https://doi.org/10.3390/w11020234, http://www.mdpi.com/2073-4441/11/2/234
2. Chung, K., Park, R.: Chatbot-based heathcare service with a knowledge base for cloud computing. Clust. Comput. (2018). https://doi.org/10.1007/s10586-018-2334-5
3. Srivastava, M., Suvarna, S., Srivastava, A., Bharathiraja, S.: Automated emergency paramedical response system. Health Inf. Sci. Syst. **6**, 22 (2018). https://doi.org/10.1007/s13755-018-0061-1
4. Mohammed, M., Badruddin Khan, M., Bashier, E.: Machine learning: algorithms and applications. Mach. Learn. Algorithms Appl. (2016). https://doi.org/10.1201/9781315371658
5. Pennington, J., Socher, R., Manning, C.: Glove: global vectors for word representation. In: Proceedings of the 2014 Conference on Empirical Methods in Natural Language Processing (EMNLP), pp. 1532–1543, Association for Computational Linguistics, Doha (2014). https://doi.org/10.3115/v1/D14-1162, http://aclweb.org/anthology/D14-1162
6. Söderström, E., van Laere, J., Backlund, P., Maurin Söderholm, H.: Combining Work Process Models to Identify Training Needs in the Prehospital Care Process. In: Johansson, B., Andersson, B., Holmberg, N. (eds.) Perspectives in Business Informatics Research, pp. 375–389. Springer International Publishing, Cham (2014)
7. Mikolov, T., Chen, K., Corrado, G., Dean, J.: Efficient estimation of word representations in vector space, CoRR, abs/1301.3781 (2013). http://arxiv.org/abs/1301.3781
8. Chang, C-C., Lin, C-J.: LIBSVM: a library for support vector machines. ACM TIST **2**, 27:1–27:27 (2011)
9. Lafferty, J.D., McCallum, A., Pereira, F.C.N.: Conditional random fields: probabilistic models for segmenting and labeling sequence data. In: Proceedings of the Eighteenth International Conference on Machine Learning, pp. 282–289. Morgan Kaufmann Publishers Inc., San Francisco (2001). http://dl.acm.org/citation.cfm?id=645530.655813
10. Weizenbaum, J.: ELIZA & Mdash; a computer program for the study of natural language communication between man and machine. Commun. ACM **9**, 36–45 (1966). ACM, New York. http://doi.acm.org/10.1145/365153.365168

A Tool for Multi-scale Modeling of Software Architectures: Application to the Smart Home for Telemonitoring Elderly People at Home

Ilhem Khlif, Mohamed Hadj Kacem, Khalil Drira, and Ahmed Hadj Kacem

1 Introduction

The design of a software architecture is a complex task. On the one hand, we have to describe the system with enough details for understanding without ambiguity and implementing in conformance with architects requirements and users expectations. On the other hand, we have to master the complexity induced by the increasing model details both at the human and automated processing levels. So, there is a need for a new approach that automates the construction of the design architecture and guarantees its correctness. An iterative modeling process that helps architects to elaborate complex but yet tractable and appropriate architectural models and specifications can be implemented by successive refinements. Providing Rules for formalizing and conducting such a process is our objective, which we implemented in visual modeling notations. For this purpose, we propose to consider different architecture descriptions with different levels of modeling details called **"the scales"**. We define a step-wise iterative process starting from a coarse-grained description and leading to a fine-grained description. We propose a modeling solution to describe software architectures using a visual notation based on the UML graphic language [1]. UML is a standard modeling language defined by the OMG. These diagrams are submitted to vertical and horizontal transformations. The intermediate models provide a description with a given abstraction that

I. Khlif · M. H. Kacem (✉) · A. H. Kacem
University of Sfax, ReDCAD Research Laboratory, Sfax, Tunisia
e-mail: ilhem.khlif@redcad.org; mohamed.hadjkacem@isimsf.usf.tn; ahmed.hadjkacem@fsegs.rnu.tn

K. Drira
LAAS-CNRS, Université de Toulouse, Toulouse, France
e-mail: khalil.drira@laas.fr

L. Chaari (ed.), *Digital Health in Focus of Predictive, Preventive and Personalised Medicine*, Advances in Predictive, Preventive and Personalised Medicine 12,
https://doi.org/10.1007/978-3-030-49815-3_18

allow the validation to be conducted significantly while remaining tractable w.r.t. complexity. The validation scope can involve intrinsic properties ensuring the model correctness w.r.t. the UML description. To ensure model consistency, our approach supports model transformation and validation of UML models with OCL constraints. In order to experiment our approach, we tested it with a predictive and preventive system dedicated to the smart home application for maintaining personalized medicine at home. This system is helpful for people with loss of autonomy, exposed to risks of accidents or needing a precise daily medical follow-up. The remainder of the paper is organized as follows. In Sect. 2, we describe the multi-scale approach in Sect. 2. Section 3 presents the e-health application dedicated to the smart home for the homecare of elderly people. We conclude and outline some perspectives in Sect. 4.

2 Approach in a Nutshell

We propose a multi-scale modeling approach for software architectures [2, 5]. The proposed design approach is founded on UML notations and uses component diagrams. The diagrams are submitted to vertical and horizontal transformations for refinement; this is done to reach a fine-grain description that contains necessary details. The model transformation ensures the correctness of UML description, and the correctness of the modeled system. UML provides a formal language, the Object Constraint Language (OCL), to define constraints on model elements. Our approach supports model transformation and validation of UML models with OCL constraints [4].

The approach supports the modeling of multi-scale architectures using the semi-formal language UML. We propose a modeling solution to describe software architectures using a visual notation based on the UML graphic language. UML is a standard modeling language defined by the OMG [6]. The UML diagrams make it possible to present the structural properties as well as the behavioral properties of the multi-scale architecture. These diagrams are submitted to vertical and horizontal transformations. The intermediate models provide a description with a given abstraction that allow the validation to be conducted significantly while remaining tractable w.r.t. complexity. The validation scope can involve intrinsic properties ensuring the model correctness w.r.t. the UML description. To achieve this, we propose a set of model transformation rules. The rules manage the refinement and abstraction process (vertical and horizontal) as a model transformation from a coarse-grain description to a fine-grain description. To ensure model consistency, our approach supports model transformation and validation of UML models with OCL constraints. The choice of using OCL is motivated by its wide adoption in the MDE approach and the fact that it is a standard formal language supported by OMG. The second phase ensures validation of the model with the OCL language. Consequently, we have defined constraints on the elements of the model using OCL language. Tools are used to check and validate OCL constraints such as the

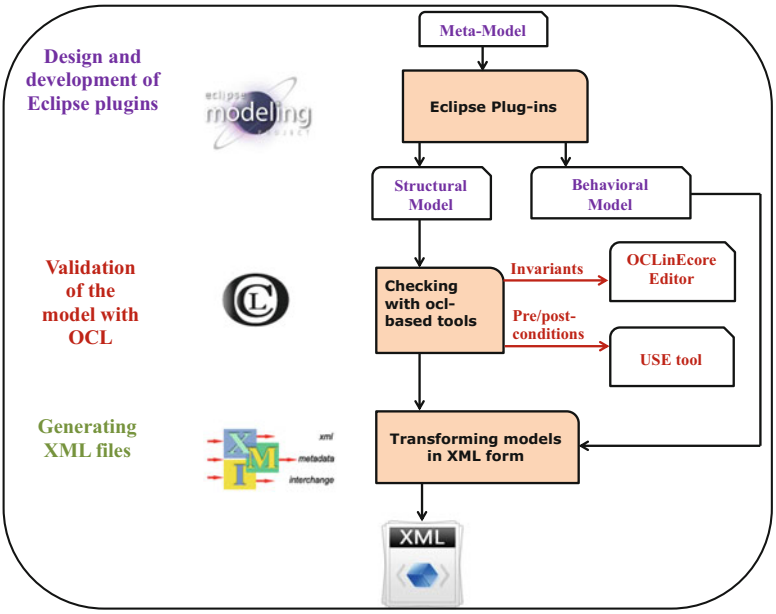

Fig. 1 Description of used tools for multi-scale modeling

OCLinEcore Editor to validate the invariants and the USE tool to validate the pre/post conditions. The third phase allows XML files to be generated using XMI, which transforms the models into XML. So we can get the XML file of the templates that we created. Figure 1 shows the different used tools during the design process.

2.1 Multi-scale Modeling

We present the multi-scale approach by a two-dimensional array describing vertical and horizontal scales [3]. The top-down scale transformation process, much like regular refinement, begins with a high level description of a system which we describe as a whole. Then, scale changes are applied to obtain a more detailed description, by describing components and connections. An iterative modeling allows to refine software systems descriptions. The vertical scales add the architecture decomposition details to obtain a more detail on the internal architecture of previously defined components. The horizontal scales describe or give details on the interconnections between components and their interfaces. We iterate on the architecture until reaching the details necessary to verify the associated architectural properties. The first scale Sv_0 begins with specifying the application requirements. It defines the whole application by its name. Two horizontal refinements called horizontal scales are associated with the first scale Sv_1. The first horizontal scale

shows all components that compose the application. The second one describes the links between those components. Four horizontal refinements are associated with the second scale Sv_2. The first scale presents subcomponents for components, and enumerates all the roles that each component can take. The second one identifies the list of communication ports for each component, and refines those roles. The third one shows the list of interfaces for communication ports. The last one is obtained by successive refinements while adding the list of connections established between components and subcomponents. This scale allows us to define the architectural style. With a graphical modeling language like UML, we are not able to express all the information required to convey the exact information of the domain in the diagram. We propose to use OCL to define constraints on models to define the well-formedness rules of our iterative design process.

3 Application to the Smart Home System

This section focuses on modeling the smart home system for the homecare monitoring of elderly and disabled persons. The smart home constituent elements are largely distributed in the house area. The main issue is to ensure efficient management of the optimized comfort, and the safety of the elderly and disabled person at home. We specify the essential information architecture and we illustrate, in (Fig. 2), the constituent elements of the smart home System. The monitoring center is

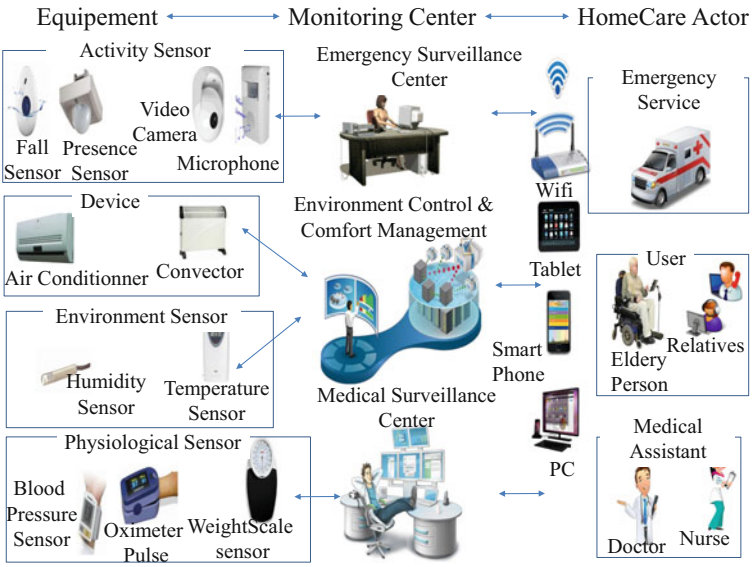

Fig. 2 Smart home system

composed of three systems:the Environment Control and Comfort Management, the Emergency Surveillance Center, and the Medical Surveillance Center. Thus, the actors selected who interact with other entities of the system are: The Home Care Actor, who interacts with the monitoring center, by setting medical or emergency conditions. The Equipment, that includes sensors and house devices. The emergency surveillance center controls critical situations using the activity sensors. In order to track the presence, activity sensors can be installed in each room. Activity sensors include fall sensors, presence sensors, video camera and microphone. The sensors send urgent signals to the center which treats immediately the received information. Once the signal is correct and the situation is critical, the center call the Emergency Medical Service to react and help the person. The medical surveillance center monitors physiological sensors. To track the medical information, physiological sensors can be installed in the bed, the chair, and on the body to detect the O2 level, the blood pressure, and the weight. The functions are achieved by the Oximeter, the Pressure Sensor, and the Weight Scale Sensor, classified as physiological sensors. While there are problems, the center requires the medical assistant intervention (the doctor, the nurse). The comfort management and the environment control system guarantees a comfort life for the users which are the elderly person and his relatives. This center enables communications between users, control the environment sensors (Humidity and Temperature Sensors), and commands the house devices (Convectors, Air conditioners). We are interested in studying the smart home system established for the home monitoring of elderly and disabled persons at home.

3.1 Structural Features

We experiment our approach by applying successive iterations to the smart home SoS. We illustrate the implemented iterative process applied to the smart home system. We obtained then the following results: In $S_{0.0}$, we define the application named "*SmartHome*". The constituent systems of the smart home are described (in $S_{1.1}$): *HomeCare-Actor*, *Equipment*, and *MonitoringCenter*. Those systems communicate with each other via the monitoring center. Those participants communicate with each other via the monitoring center. Those relationships are represented (in $S_{1.2}$) as links. UML associations. We also illustrate instances obtained in the next scale. We apply successive model transformation operations to add the following composites: *MedicalAssistant, EmergencyService, User, Physiological-Sensor, Activity-Sensor, Environment-Sensor, House-Device, MedicalSurveillance-Center, EmergencySurveillanceSystem, and EnvironementControlAndComfortManagement*. The *MonitoringCenter* plays the role of an "*EventDispatcher*". The *HomeCare-Actor* and *Equipement* play roles of "*Producer-Consumer*" in the application. $S_{2.1}$ allows to add the list of the ports for each component. We briefly describe the list of required/provided services of the *HomeCare-Actor* component. The *MedicalAssistant* receives information about the patient's situa-

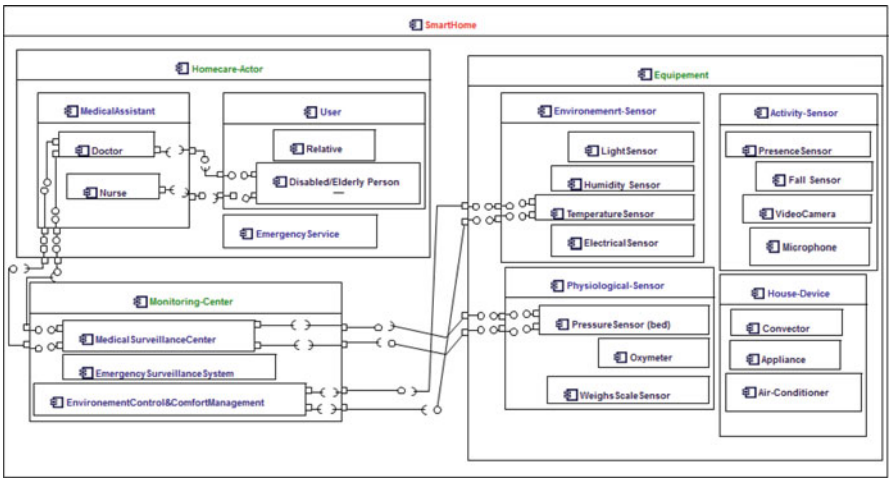

Fig. 3 Structural modeling applied to the smart home (Scale Sv_3/Sh_3)

tion from the *MedicalSurveillanceCenter*, he manages the patient's medical care (provides) and return a report after the care. The *EmergencyService* receives information about a critical situation *EmergencySurveillanceCenter*, reacts to save the patient (provides), and return a report after the intervention. The *User* receives not only emergency and medical services but also comfort services like online communication or house device command provided by the *EnvironementControl And ComfortManagement* component. $S_{2.2}$ assigns to each port an interface of the type provided or required according to the type of service. Finally, we indicate at the scale $S_{2.3}$ connections established according to the used topology and we define the "*Publish-Subscribe*" style. We implemented Eclipse plugins that allow multi-scale modeling of a software architecture based on the component diagram and the sequence diagram. We have checked and validated the OCL constraints under Eclipse (the structural part) and with the USE tool (the dynamic part). Finally, we have presented the level of instances of our case study using the Eclipse plugins (Fig. 3).

4 Conclusion

In this paper, we applied the multi-scale modeling approach on a case study for a predictive and preventive system dedicated to the smart home application for maintaining personalised medicine at home. This system is helpful for people with loss of autonomy, exposed to risks of accidents or needing a precise daily medical follow-up. We have experimented and evaluated the functional and the performance aspect of our approach as well as the functional aspect of our developed tool

supporting the multi-scale modeling approach for software architectures. In our future work, we expect to apply the multiscale modeling approach to other complex use cases for e-health applications for public health.

References

1. Khlif, I., Hadj Kacem, M., Hadj Kacem, A.: Iterative multi-scale modeling of software-intensive systems of systems architectures. In: Proceedings of the Symposium on Applied Computing, SAC 2017, Marrakech, 3–7 Apr 2017, pp. 1781–1786 (2017)
2. Khlif, I., Hadj Kacem, M., Hadj Kacem, A., Drira, K.: A multi-scale modelling perspective for SoS architectures. In: Proceedings of the 2014 European Conference on Software Architecture Workshops, ECSAW 14. Association for Computing Machinery, New York (2014)
3. Khlif, I., Hadj Kacem, M., Hadj Kacem, A., Drira, K.: A UML-based approach for multi-scale software architectures. In: 17th International Conference on Enterprise Information Systems (ICEIS), pp. 374–381 (2015)
4. Khlif, I., Hadj Kacem, M., Stolf, P., Hadj Kacem, A.: Software architectures: multi-scale refinement. In: 14th IEEE International Conference on Software Engineering Research, Management and Applications, SERA 2016, Towson, 8–10 June 2016, pp. 265–272 (2016)
5. Khlif, I., Tounsi, I., Hadj Kacem, M., Eichler, C., Hadj Kacem, A.: A refinement-based approach for specifying multi-scale software architectures: application to sos. In: Proceedings of the 33rd Annual ACM Symposium on Applied Computing, SAC '18, pp. 1660–1667. ACM, New York (2018)
6. UML, O.M.G.: Unified modelling language: Infrastructure (2011)

Index

L. Chaari (ed.), *Digital Health in Focus of Predictive, Preventive and Personalised Medicine*, Advances in Predictive, Preventive and Personalised Medicine 12,
https://doi.org/10.1007/978-3-030-49815-3